AD 779 527

TECHNICAL REPORT
74-9-AD

DEVELOPMENT OF A TOTAL TRAJECTORY SIMULATION FOR SINGLE RECOVERY PARACHUTE SYSTEMS

Volume I: Analytical Model and Computer Program Design Rationale

by

Helmut G. Heinrich

Robert A. Noreen

and

David P. Saari

University of Minnesota

Minneapolis, Minnesota USA

Approved for public release;
distribution unlimited.

December 1973

UNITED STATES ARMY
NATICK LABORATORIES
Natick, Massachusetts 01760

U.S. ARMY TROOP SUPPORT COMMAND

Airdrop Engineering Laboratory

Approved for public release; distribution unlimited.

Citation of trade names in this report does not constitute an official indorsement or approval of the use of such items.

Destroy this report when no longer needed. Do not return it to the originator.

Unclassified
Security Classification

DOCUMENT CONTROL DATA - R & D

(Security classification of title, body of abstract and indexing annotation must be entered when the overall report is classified)

1. ORIGINATING ACTIVITY *(Corporate author)*

University of Minnesota
Minneapolis, Minn. 55455

2a. REPORT SECURITY CLASSIFICATION

UNCLASSIFIED

2b. GROUP

3. REPORT TITLE

Development of a Total Trajectory Simulation for Single Recovery Parachute Systems. Volume I: Analytical Model and Computer Program Design Rational

4. DESCRIPTIVE NOTES *(Type of report and inclusive dates)*

Final Report Nov 1971 - June 1973

5. AUTHOR(S) *(First name, middle initial, last name)*

Helmut G. Heinrich
Robert A. Noreen, David P. Saari

6. REPORT DATE

7a. TOTAL NO. OF PAGES: 100

7b. NO. OF REFS: 15

8a. CONTRACT OR GRANT NO.

DAAG 17-72-C-0030

b. PROJECT NO.

1F162203AA33

c. Task Area: 04

d. Work Unit Number: 024

9a. ORIGINATOR'S REPORT NUMBER(S)

None

9b. OTHER REPORT NO(S) *(Any other numbers that may be assigned this report)*

74-9-AD

10. DISTRIBUTION STATEMENT

Distribution of this document is unlimited.

11. SUPPLEMENTARY NOTES

12. SPONSORING MILITARY ACTIVITY

Airdrop Engineering Laboratory
US Army Natick Laboratories
Natick, Mass. 01760

13. ABSTRACT

A method of total trajectory simulation was established which is based on the governing equations of the various phases of an aerial delivery or recovery system. In view of these equations, a computer program capable of predicting the performance characteristics of a parachute-load system from the instant of initiation to the moment of landing was established. Calculations were performed for a number of different aerial delivery systems. The calculated results fall well within the broad ranges of expected performance, based upon a familiarity with field test results. The system is ready to be used for overall prediction of parachute performance characteristics and an intensive comparison of calculated and recorded field test results is highly desirable for validation and improvement of the technique of total trajectory simulation.

The report is presented in two volumes. Volume I discusses and shows the development of the phases of the total trajectory simulation, and includes the results of sample calculations from release to ground impact for several cases of parachute-load systems. Volume II presents the computer program and methods for obtaining numerical results in detail

DD FORM 1 NOV 65 1473 REPLACES DD FORM 1473, 1 JAN 64, WHICH IS OBSOLETE FOR ARMY USE.

Security Classification

Security Classification

14. KEY WORDS	LINK A ROLE	LINK A WT	LINK B ROLE	LINK B WT	LINK C ROLE	LINK C WT
Extraction	8					
Cargo	2		9			
Aircraft	1					
Recovery	10		4			
Parachutes	10					
Low Altitute Drop	4					
Airdrop Operations	4		9, 4			
Tests			8			
Equations			8			
Data			8			
Computer Programming			10			
Aerial Delivery			9			
Loads			9			

Security Classification

Distribution of this
document is unlimited

AD_____

TECHNICAL REPORT

74-9-AD

DEVELOPMENT OF A TOTAL TRAJECTORY SIMULATION FOR SINGLE RECOVERY PARACHUTE SYSTEMS

Volume I: Analytical Model and Computer Program Design Rationale

by

Helmut G. Heinrich
Robert A. Noreen
David P. Saari

University of Minnesota
Minneapolis, Minnesota USA

DDC
RECEIVED
MAY

Contract No. DAAG17-72-C-0030

Project Reference:
1F162203AA33

December 1973

Airdrop Engineering Laboratory
U. S. ARMY NATICK LABORATORIES
Natick, Massachusetts 01760

ib

ERRATA

Technical Report 74-9-AD

Development of a Total Trajectory Simulation for Single Recovery Parachute Systems, Volume I: Analytical Model and Computer Program Design Rationale by Helmut G. Heinrich, Robert A. Noreen and David P. Saari, December 1973.

On pages 26, 30 and 35, in Equations (33), (48) and (64) respectively, the

$$+\frac{V}{m_T}\left(\frac{dm_i}{dt}+\frac{dm_a}{dt}\right)$$ term should be $$-\frac{V}{m_T}\left(\frac{dm_i}{dt}+\frac{dm_a}{dt}\right)$$

DDC

FOREWORD

This work was performed under US Army Natick Laboratories Contract No. DAAG 17-72-C-0030 during the period 15 November 1971 and 30 June 1973. The project Number was 1F162203AA33 and the Task Number was 04 entitled "Study of Dynamic Stability Characteristics of Parachute-Load Systems". Mr. Edward J. Giebutowski served as Project Officer.

The objective of the effort was to produce a computerized trajectory simulation which would describe the motion of a single parachute and its cargo from the time of release from the aircraft to the time of impact.

This report describes the analytical modeling and design rationale for the computer simulation of the trajectory and shows typical results obtained from computer solutions of several test cases involving a selected number of parachute configurations as used by the US Army for airdrop of cargo and personnel.

CONTENTS

PAGE

I. Introduction 1

II. Separation and Deployment Systems 4

A. Static Line System 4

B. Static Line Deployed Pilot Chute System . . . 6

C. Extraction Parachute System 6

D. Reefed Main Parachute Extraction System . . . 10

III. Trajectory Simulation Methods 12

A. Atmospheric Density Function 12

B. Two Dimensional Point Mass Trajectory 12

C. Separation from Aircraft 16

1. Load Extraction 16

2. Static Line Extension 17

D. Deployment and Snatch Force 17

1. Static Line Deployment 18

2. Deployment by Pilot or Extraction Parachute 18

a. Suspension Line and Riser Deployment 20

b. Snatch Force 21

c. Main Parachute Canopy Unfolding . . . 22

3. Summary of Assumptions for the Deployment Phase 23

E. Inflation of the Main Parachute 24

1. Governing Equations 24

a. Inflation without Reefing 27

b. Reefed Inflation 31

2. Summary of Assumptions for the Inflation Phase 36

PAGE

F. Free Descent 37

1. Governing Equations 38

a. Three Degrees of Freedom 44

b. Six Degrees of Freedom 53

2. Summary of Assumptions for the Free Descent Phase 60

IV. Numerical Trajectory Calculations of Several Parachute-Load Systems 61

A. Steady State Canopy Volume and Geometry . . 61

B. Aerodynamic Coefficients 63

C. Examples of Total Trajectory Simulations . . 67

1. T-10 Parachute with Static Line System . 69

2. G-12D Cargo Parachute with Static Line Deployed Pilot Chute System 70

3. G-11A Cargo Parachute with Extraction Parachute System 75

4. G-11A Cargo Parachute with Reefed Main Parachute Extraction System 78

5. Additional Calculations 78

V. Summary 86

VI. References 88

Appendix 90

ILLUSTRATIONS

Fig No.	Title	Page
1	Static Line System	5
2	Static Line Deployed Pilot Chute System	7
3	Extraction Parachute System	8
4	Extraction Parachute System with Reefed Main Parachute Inflation	9
5	Reefed Main Parachute Extraction System	11
6	Air Density Function	13
7	Definition of Quantities for Two Dimensional Point Mass Trajectory Analysis	15
8	Parachute-Load System During Deployment by Pilot or Extraction Parachute	19
9	Parachute-Load System During Inflation of the Main Parachute	25
10	Time Scale Adjustment for Reefed Inflation Periods	33
11a	Orientation of the Parachute-Load System	39
11b	Euler Angles ψ, θ, φ	40
12	The Parachute-Load System Constrained to Three Degrees of Freedom	45
13	Profile View of Parachute-Load System in the XZ-Plane	50
14	External Forces and Moments Acting on the Parachute-Load System	54
15	Tangent Force Coefficient vs Parachute Angle of Actack, Solid Flat Circular and T-10 Parachutes	65
16	Moment Coefficient vs Parachute Angle of Attack, Solid Flat Circular and T-10 Parachutes	66

ILLUSTRATIONS (CONT.)

Fig No.	Title	Page
17	Normal Force Coefficient vs Parachute Angle of Attack, Solid Flat Circular and T-10 Parachutes .	68
18	Altitude Loss and System Angle for the T-10 Parachute with Static Line System	71
19	Horizontal and Vertical Velocities for the T-10 Parachute with Static Line System	72
20	Altitude Loss and System Angle for the G-12D Cargo Parachute with Static Line Deployed Pilot Chute System	73
21	Horizontal and Vertical Velocities for the G-12D Cargo Parachute with Static Line Deployed Pilot Chute System	74
22	Altitude Loss and System Angle for the Unreefed G-11A Cargo Parachute with Extraction Parachute System	76
23	Horizontal and Vertical Velocities for the Unreefed G-11A Cargo Parachute with Extraction Parachute System	77
24	Altitude Loss and System Angle for the Reefed G-11A Cargo Parachute with Extraction Parachute System	79
25	Horizontal and Vertical Velocities for the Reefed G-11A Cargo Parachute with Extraction Parachute System	80
26	Altitude Loss and System Angle for the G-11A Cargo Parachute with Reefed Main Parachute Extraction System	81
27	Horizontal and Vertical Velocities for the G-11A Cargo Parachute with Reefed Main Parachute Extraction System	82
28	T-10 Parachute with Static Line System	91

ILLUSTRATIONS (CONT.)

Fig No.	Title	Page
29	G-13 Cargo Parachute with Static Line System . . .	93
30	G-12D Cargo Parachute with Static Line Deployed Pilot Chute System	95
31	G-12D Cargo Parachute with Extraction Parachute System	97
32	G-11A Cargo Parachute with Extraction Parachute System	99

TABLES

		Page
I	Parachute-Load Systems and Initial Conditions for the Total Trajectory Simulation Calculations	83
II	Results of the Trajectory Simulation Calculations	84
III	Total Trajectory Simulation Inputs for T-10 Parachute with Static Line System	92
IV	Total Trajectory Simulation Inputs for G-13 Cargo Parachute with Static Line System	94
V	Total Trajectory Simulation Inputs for G-12D Cargo Parachute with Static Line Deployed Pilot Chute System	96
VI	Total Trajectory Simulation Inputs for G-12D Cargo Parachute with Extraction Parachute System	98
VII	Total Trajectory Simulation Inputs for G-11a Cargo Parachute with Extraction Parachute System or Reefed Main Parachute Extraction System	100

SYMBOLS

$\underline{a}$	acceleration
a_{ij}	component of the matrix $\underline{\underline{A}}$, i^{th} row, j^{th} column
A	inverse of effective spring constant of suspension system, Eqn (21)
$\underline{\underline{A}}$	direction cosine matrix, Eqn (71)
B	Eqn (22)
c	effective porosity
C	Eqn (23)
C_{D_o}	drag coefficient of parachute based on nominal area
C_{D_p}	drag coefficient of parachute based on projected area
C_DS	drag area
C_{N_o}	aerodynamic normal force coefficient of parachute
C_{M_o}	aerodynamic moment coefficient of parachute
C_{T_o}	aerodynamic tangent force coefficient of parachute
d	canopy inlet diameter
D	aerodynamic drag
D_o	nominal diameter of parachute
D_p	instantaneous projected diameter of parachute
$D_{p_{max}}$	projected diameter of fully inflated parachute
$\underline{e}$	general vector in space-fixed corrdinate system

$\underline{E}$	general vector in body-fixed coordinate system
$\underline{F}$	force
$\underline{F}_a$	force due to included and apparent mass
F_A	aerodynamic force (during snatch)
F_{max}	opening shock
$\underline{F}_N$	aerodynamic normal force
F_0	instantaneous opening force
g	gravitational acceleration
h	altitude; D_p/D_o
$\underline{H}$	angular momentum
$\underline{\underline{I}}$	inertia tensor of parachute-load system about its mass center
$\underline{\underline{I}}_{CM}$	component tensor of $\underline{\underline{I}}$ due to physical masses of load, parachute, and suspension system
$\underline{\underline{I}}_a$	component tensor of $\underline{\underline{I}}$ due to the effect of included and apparent mass
ℓ	distance between load and secondary body during deployment
ℓ_1	distance from parachute-load system center of mass to load
ℓ_2	distance from parachute-load system center of mass to parachute center of volume
ℓ_3	distance from parachute-load system center of mass to parachute moment center
ℓ_R	reefing line length
L	distance load travels in aircraft, X-component of M, body fixed
L'	length of suspension system and deployed canopy

L_{Br}	length of load bidle in Z-direction
L_E	length of riser extension
L_R	length of risers
L_S	length of suspension lines
L_{static}	length of static line
m	mass
m_a	apparent mass of parachute
m_{Br}	mass of load bridle
m_E	mass of riser extensions
m_i	mass of included air in parachute canopy
m_{L_S}	mass of suspension lines
m_{pb}	mass of pilot or extraction parachute and main parachute deployment bag
m_{rs}	total mass of load and packed recovery system
m_R	mass of risers
m_{ss}	mass of suspension lines, risers, extensions, bridle and links
m_T	total mass = $m_\ell + m_{ss} + m_p + m_i + m_a$
m_I	mass of primary body during deployment of the suspension system = $m_\ell + m_{ss}$
$\underline{M}$	moment acting on parachute-load system
M	Y-component of $\underline{M}$, body fixed
$\underline{M}_A$	aerodynamic moment due to parachute
M_C	control or turning moment
M_I	mass of primary body at snatch = $m_\ell + m_{ss}$

M_{II}	mass of secondary body during deployment of the suspension system = $m_p + \frac{1}{2} m_{ss} + m_{pb}$
n	number of finite steps chosen to approximate inflation
N	Z-component of $\underline{M}$, body fixed
P	X-component of $\underline{\omega}$, body fixed
P_{max}	maximum snatch force
Q	Y-component of $\underline{\omega}$, body fixed; mass ratio, Eqn (26)
$\underline{r}$	position of parachute-load system center of mass
R	reefing ratio, Eqn (57); Z-component of $\underline{\omega}$, body fixed
$\bar{s}$	Eqn (111)
s_1	reference distance from canopy skirt to suspension line center of mass in fully inflated configuration
s_2	reference distance from canopy skirt to riser center of mass in fully inflated configuration
s_3	reference distance from canopy skirt to riser extension center of mass in fully inflated configuration
s_4	reference distance from canopy skirt to load bridle center of mass in fully inflated configuration
s_5	reference distance from canopy skirt to load center of mass in fully inflated configuration
s_c	reference distance from canopy skirt to parachute center of volume in fully inflated configuration
S_p	projected area
S_o	nominal area
t	time
t_{CD}	reefing cutter delay time

t_{ff}	final filling time; measured from end of bag strip to first attainment of hemispherical canopy volume
t_{f_R}	filling time for reefed inflation period
T	dimensionless time scale; aerodynamic tangent force of parachute
T_R	dimensionless time scale for reefed inflation periods
U	X-component of $\underline{v}$, body fixed
$\underline{v}$	general velocity; velocity of parachute-load system mass center
v	general velocity; magnitude of velocity of parachute-load system center of mass
v_{in}	inflow velocity to inflating parachute
v_s	snatch velocity
V	volume; Y-component of $\underline{v}$, body fixed
W	Z-component of $\underline{v}$, body fixed; weight
x	space-fixed coordinate direction; position of parachute-load system center of mass
X	body-fixed coordinate
y	space-fixed coordinate direction; position of parachute-load system center of mass
Y	body-fixed coordinate
z	space-fixed coordinate direction; position of parachute-load system center of mass
Z	body-fixed coordinate
α	angle of attack in XZ-plane
β	angle of attack in YZ-plane
γ	angle between velocity and XZ-plane

δ	angle between velocity and YZ-plane
ϵ_{max}	maximum elongation
θ	Euler angle, system angle for problems constrained to three degrees of freedom
ν	Eqn (40)
ρ	air density
ρ_o	sea level air density
σ	air density ratio ρ/ρ_o
$\underline{\omega}$	angular velocity of parachute-load system
φ	Euler angle
ψ	Euler angle

Subscripts

a	apparent
B	main parachute deployment bag
c	parachute canopy
ex	extraction parachute(s)
i	included
ℓ	load
o	nominal, initial
p	parachute
R	referring to inflation of the main decelerator with reefing
x	component in space-fixed x coordinate direction
X	component in body-fixed X coordinate direction

y	component in space-fixed y coordinate direction
Y	component in body-fixed Y coordinate direction
z	component in space-fixed z coordinate direction
Z	component in body-fixed Z coordinate direction
1	referring to end of reefed inflation stage
I	primary body
II	secondary body
_	indicates vector quantity
=	indicates matrix or tensor quantity

ABSTRACT

A method of total trajectory simulation was established which is based on the governing equations of the various phases of an airdrop or recovery system. In view of these equations, a computer program capable of predicting the performance characteristics of a parachute-load system from the instant of initiation to the moment of landing was established. Calculations were performed for a number of different aerial delivery systems. The calculated results fall well within the broad ranges of expected performance, based upon a familiarity with field test results. The system is ready to be used for overall prediction of parachute performance characteristics and an intensive comparison of calculated and recorded field test results is highly desirable for validation and improvement of the technique of total trajectory simulation.

The report is presented in two volumes. Volume I discusses and shows the development of the phases of the total trajectory simulation, and includes the results of sample calculations from release to ground impact for several cases of parachute-load systems. Volume II presents the computer program and methods for obtaining numerical results in detail.

I. INTRODUCTION

The process of delivering a load from an airplane in flight to the ground--or the recovery of a manned or instrumented capsule, drone airplane, or missile--encompasses a number of dynamic and aerodynamic problems. The various phases of such a process are usually organized in detailed groupings concerning parachute deployment, inflation and descent. In each field intensive investigations have been carried out and generally the basic physical and mathematical models have been established. In many cases the actual processes are so complicated that closed, or semi-closed, solutions can be established only by imposing stringent simplifications and restrictions. In certain phases of the entire operation, for example the parachute deployment and inflation, the assumption that the parachute-load system moves in one plane is quite acceptable. However, during the descent phase, many types of parachutes impose motions upon the system in three dimensions, and neglecting this fact is often an unacceptable simplification.

The availability of large high speed computers makes it possible to pursue numerical solutions which allow the introduction of non-linear performance characteristics and considerations of multiple degrees of freedom. This is particularly important for the analysis of the descent phase of the operation where large deflections of the system from the ideal trajectory occur, and where three dimensional oscillations and coupling between planar oscillations and roll modes of the parachute-load system can exist.

One objective of the following study was then the establishment of a computer program to calculate all performance characteristics and capable of three dimensional calculations

for the descent phase, using established performance parameters and functional relationships with a minimum of numerical simplifications. A further objective was that the program allow the continuous performance calculation of a given parachute-load system from initiation of parachute deployment to landing.

In view of these primary objectives, mechanical and mathematical models for the various phases, whose validity had previously been proven by comparison with experimental results, were selected from the literature and formed the basis for the computer program. A major feature of the program is that it has been arranged so that entire calculation methods can easily be replaced or updated when better methods become available. This can be done simply by replacing major subroutines.

The basic approach to the various phases can be described as follows. The motion of the parachute-load system during the phases of load extraction, when applicable, parachute deployment, and inflation is considered to be two-dimensional. The calculation follows the state-of-the art methods and is coupled with the equations for a two-dimensional trajectory. In the final descent phase, the parachute-load system is treated as a rigid body and a classical mechanics formulation is used to find the equations of motion with six degrees of freedom which provide trajectory data in three dimensions, or with three degrees of freedom for two-dimensional solutions.

Numerical results are obtained using finite-difference methods for the trajectory simulation prior to full inflation, and the Runge-Kutta method is used for numerical integration of the equations of motion for the final descent phase.

The report is presented in two volumes. Volume I discusses and shows the development of the phases of the total

trajectory simulation, and includes the results of sample calculations from release to ground impact for several cases of parachute-load systems. Volume II presents the computer program and methods for obtaining numerical results in detail.

The authors wish to express their gratitude to Mr. Edward J. Giebutowski of the United States Army Natick Laboratories for his cooperation in establishing the composition and physical data of the various airdrop systems and for his many constructive contributions throughout this study.

II. SEPARATION AND DEPLOYMENT SYSTEMS

This section describes the various physical airdrop systems to which the total trajectory simulation applies. The basic phases of functioning for any parachute-load system are: 1) separation from the aircraft, 2) deployment of the parachute, 3) inflation, and 4) free descent. The physics of the last two processes is essentially the same for any parachute type decelerator; however, there are many distinctly different physical processes used to accomplish separation and deployment. This study considers four different systems which represent methods most likely to be used by the United States Army for cargo and personnel airdrop (Ref 1).

The four separation and deployment systems incorporated in the trajectory simulation are: 1) static line, 2) static line deployed pilot chute, 3) extraction parachute, and 4) reefed main parachute extraction. Separation from the aircraft is achieved by the load merely falling away from the aircraft in the first two systems, whereas in the last two systems a parachute is attached to the load to increase the relative velocity between aircraft and load. A detailed description of the four systems follows.

A. Static Line System

Figure 1 shows the static line separation-deployment system used with calculations for the T-10 personnel parachute and the G-13 cargo parachute. The static line is attached to the aircraft while its free end pulls the deployment bag from the parachute after the lines are extended. The canopy is then free to inflate. No distinction is made between

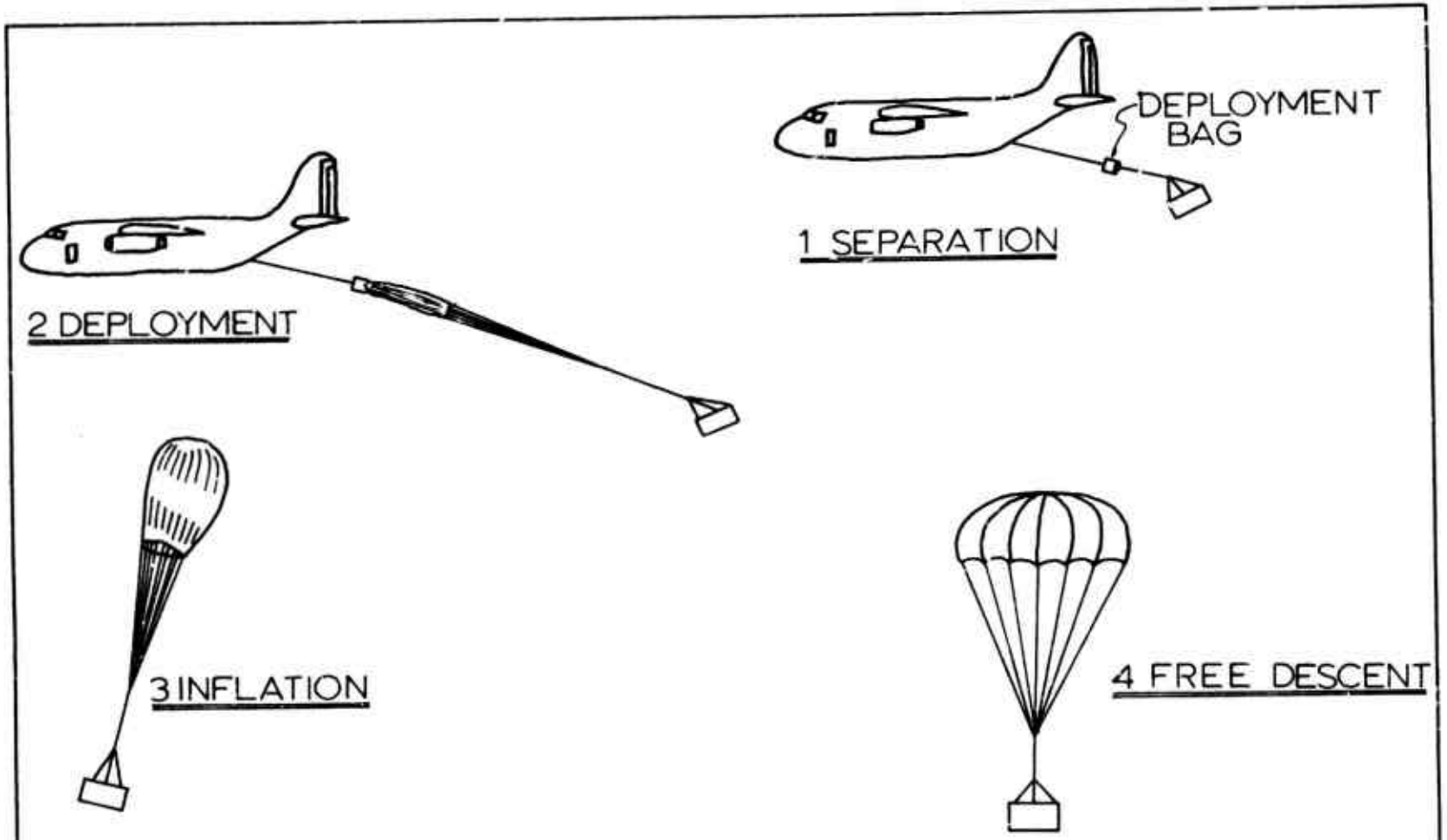

Fig 1 Static Line System

"lines first" and "canopy first" deployments, since the modeling equations apply to either.

B. Static Line Deployed Pilot Chute System

Figure 2 illustrates the use of a static line with a pilot chute, used for separation-deployment of the G-12D cargo parachute. After release of the parachute-load system, the static line deploys the pilot chute from its pack. The pilot chute is then used to deploy the main canopy in a lines-first fashion, and the deployment bag is separated.

C. Extraction Parachute System

Figure 3 illustrates the extraction parachute system, used for separation-deployment of the G-12D and G-11A cargo parachutes. The load is separated from the aircraft by means of the extraction parachute. As the load leaves the aircraft, the extraction parachute force is transferred to the deployment bag of the main parachute, and the canopy is deployed in a lines-first manner. Figure 4 shows a reefing sequence, as used with large parachutes. The extraction parachute again separates the main canopy deployment bag from the load, paying out the risers and suspension lines. But, as the suspension lines tighten, the reefing cutters are armed, and the remainder of the canopy is deployed. After a prescribed delay time, the reefing line is cut, and the parachute is free to inflate fully or to a second reefed stage.

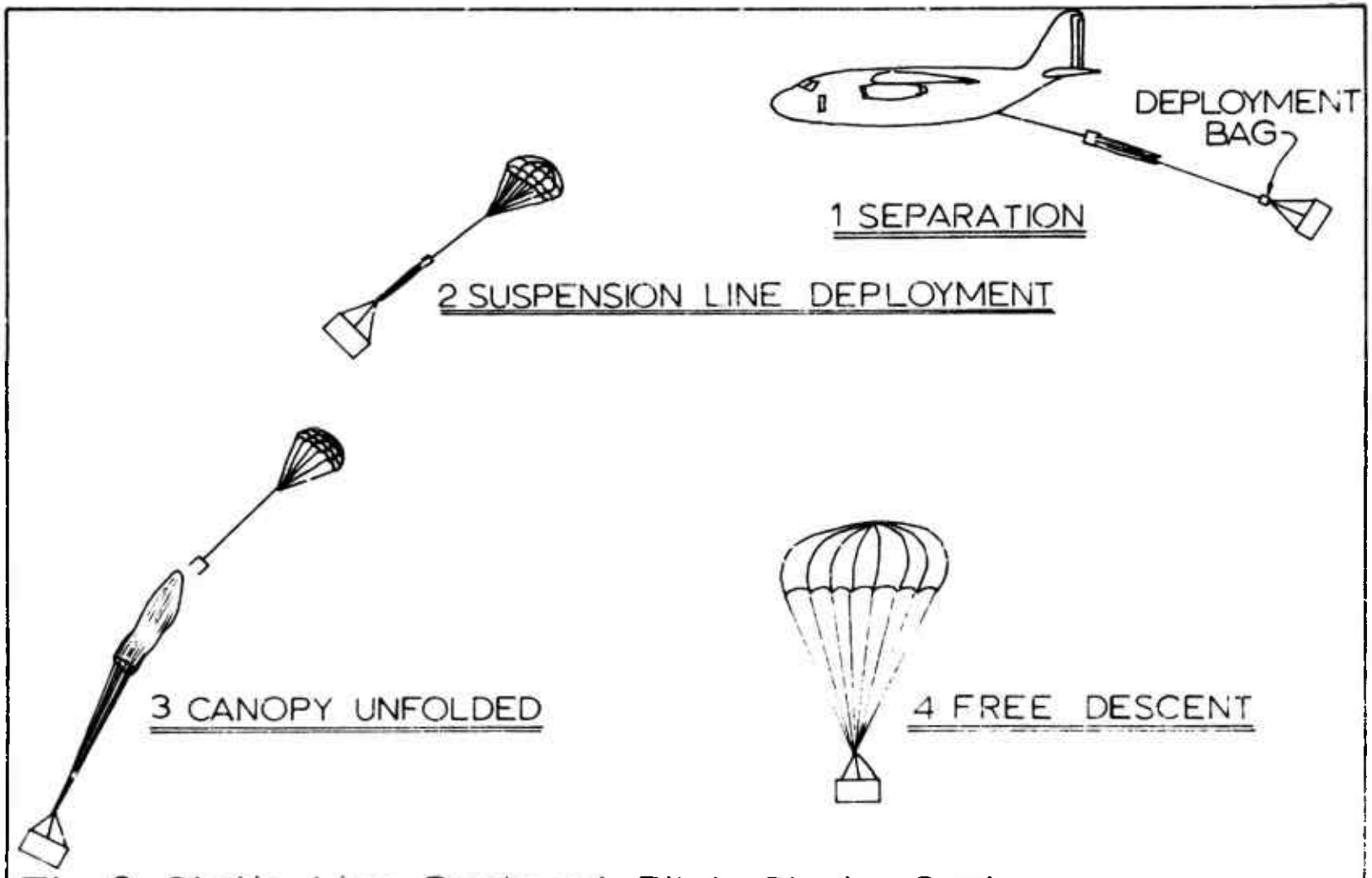

Fig 2 Static Line Deployed Pilot Chute System

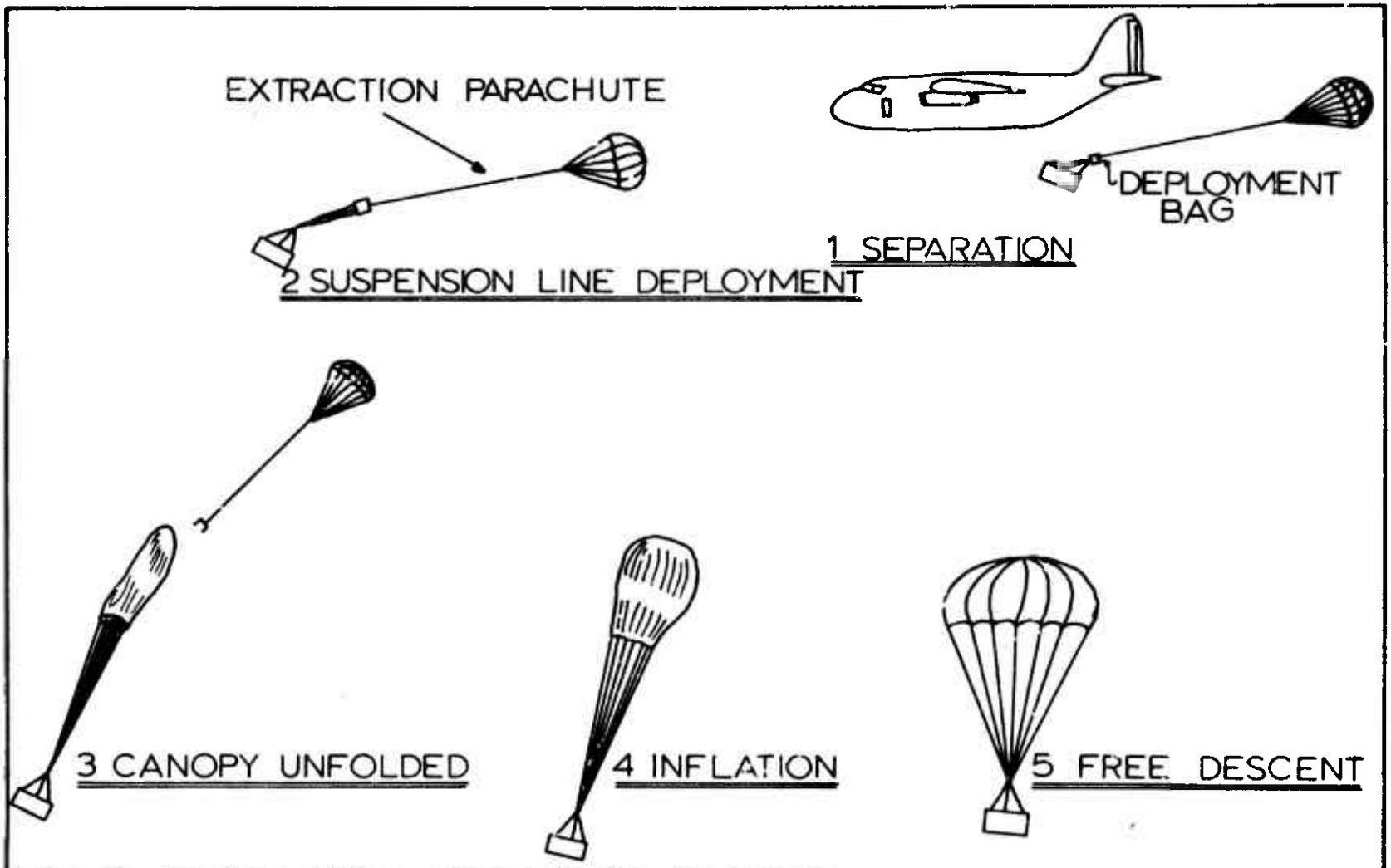

Fig 3 Extraction Parachute System

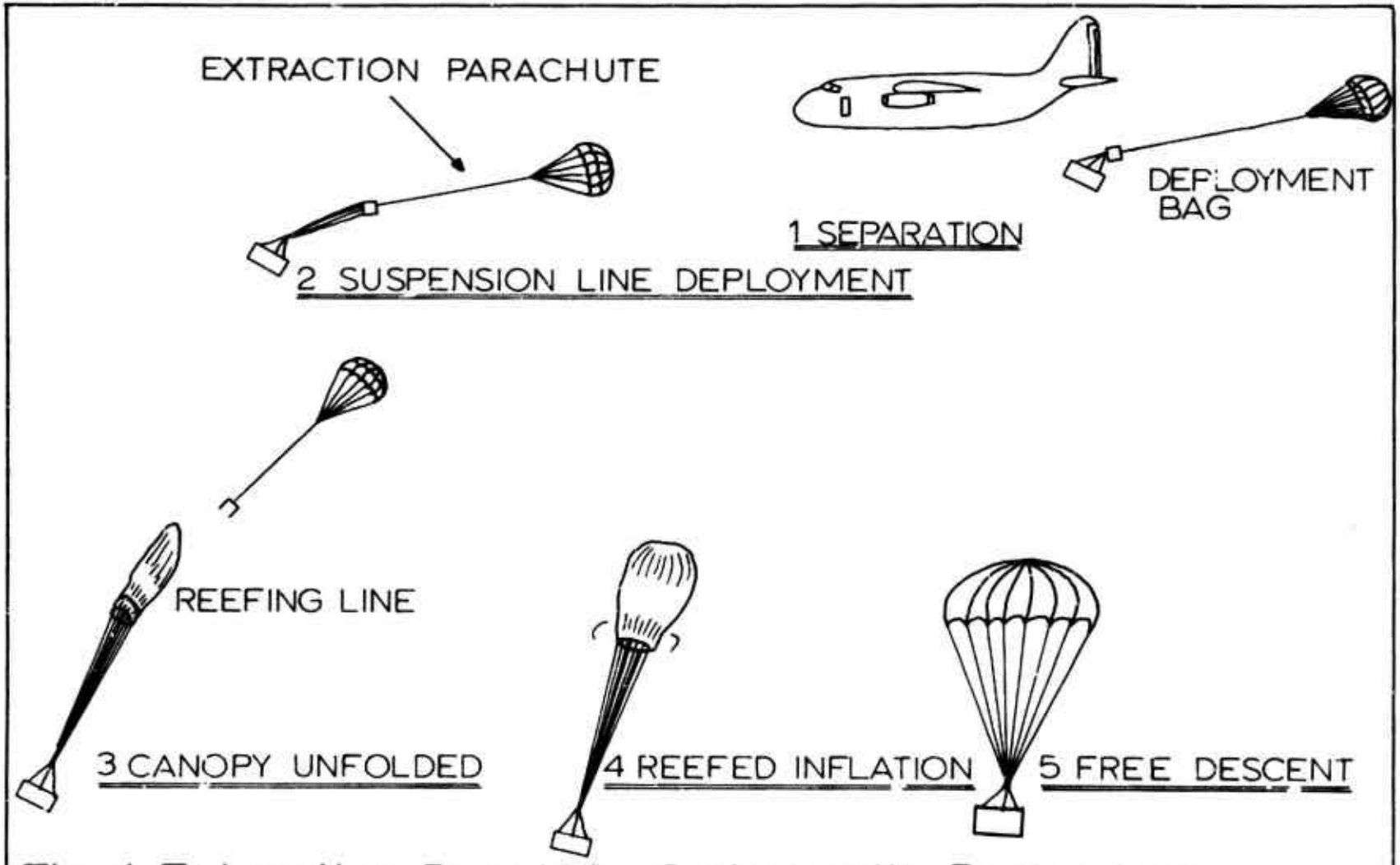

Fig 4 Extraction Parachute System with Reefed Main Parachute Inflation

D. Reefed Main Parachute Extraction System

The fourth system, Fig 5, involves the use of the main canopy in a reefed configuration as the extraction parachute. The load is pulled from the aircraft, and after a prescribed delay the reefing line is severed.

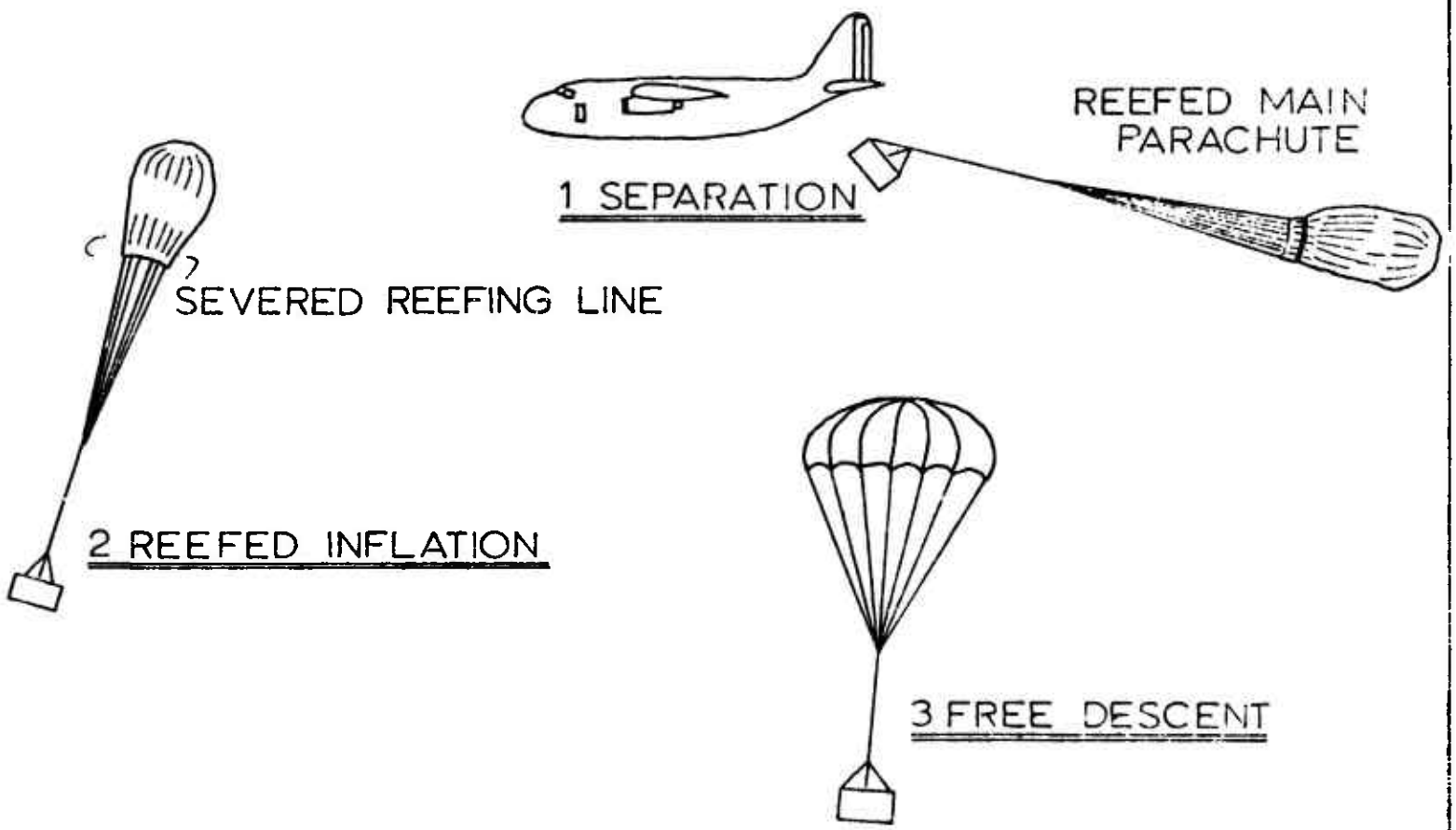

Fig 5 Reefed Main Parachute Extraction System

III. TRAJECTORY SIMULATION METHODS

The total trajectory simulation was divided into phases which represent the significant physical processes of the airdrop and relate to computer program major subroutines, which can be replaced individually. Details of the different phases are described in the following. The first two Subsections, entitled Atmospheric Density Function (III A) and Two Dimensional Point Mass Trajectory Analysis (III B), represent calculations which are made at various points throughout the total trajectory simulation and thus are discussed first.

A. Atmospheric Density Function

During the trajectory simulation, the values for the air density used in the various equations governing the motion throughout the airdrop are determined by the position of the parachute-load system center of mass. The function that is used to describe the air density for a standard day is

$$\rho = \rho_o \, e^{-h/32{,}916} \quad , \; 0 < h \leq 15{,}000 \text{ ft}$$

$$\rho = \rho_o \, (1.07133) \, e^{-h/28{,}953} \quad , \; 15{,}000 \text{ ft} \leq h \leq 35{,}000 \text{ ft} \qquad (1)$$

where $\rho_o = 0.002378$ slug/ft^3. This function was determined by fitting two straight lines to a logarithmic plot of σ vs altitude determined from Ref 2 as shown in Fig 6.

B. Two-Dimensional Point Mass Trajectory Analysis

The motion of the parachute-load system is assumed to

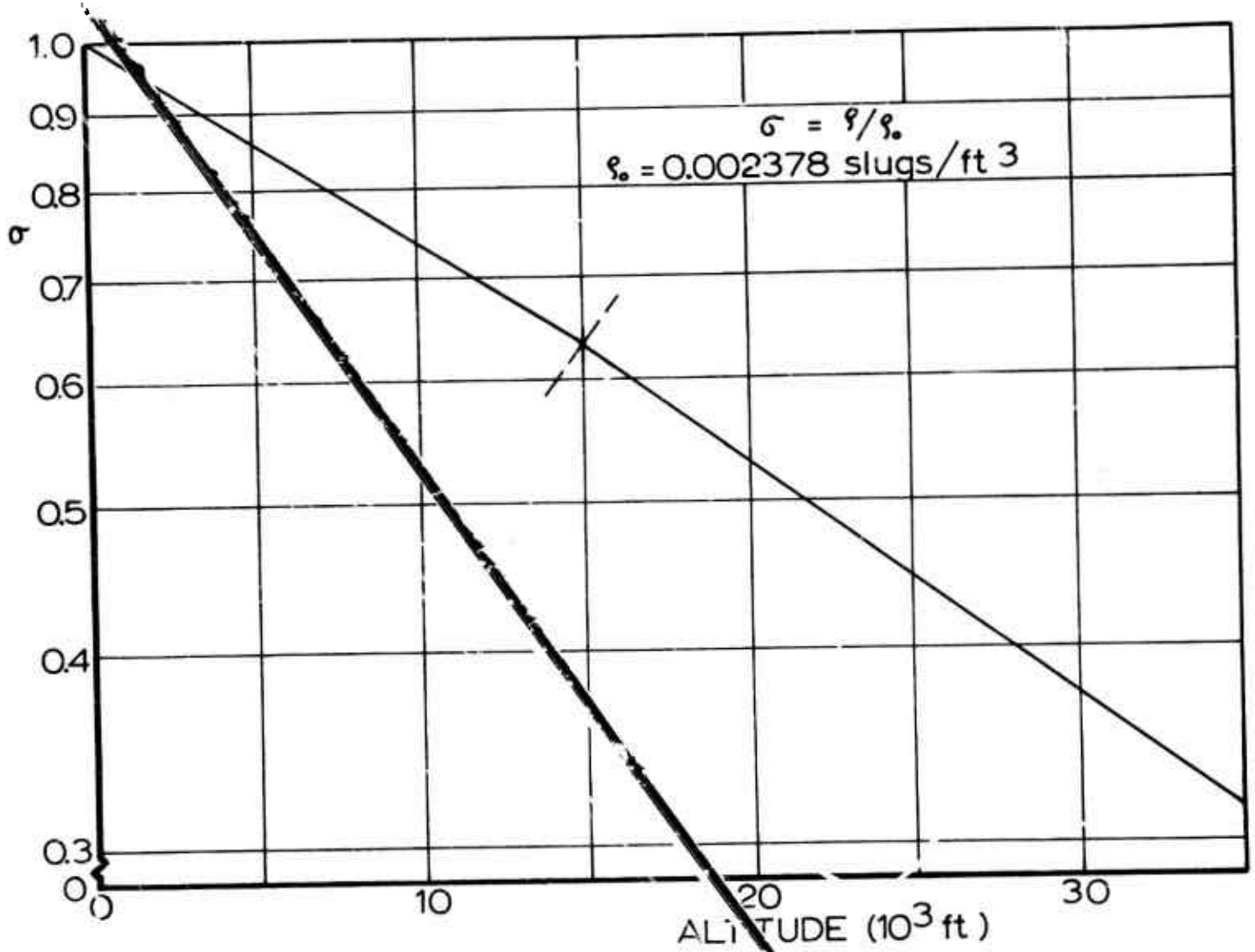

Fig 6 Air Density Funtion

be two-dimensional during the processes of separation, deployment, and inflation, since all forces act in one vertical plane during these processes. For the periods during this two-dimensional portion of the airdrop when the position of the mass center does not change significantly, such as in separation and deployment, the motion of the mass center is approximated by a point mass ballistic trajectory. Equations for the trajectory of the parachute-mass system can then be found by considering the forces acting on a point mass with a given drag area.

Summing forces parallel and perpendicular to the trajectory of a particle of mass m with drag area $C_D S$ (Fig 7) yields the equations

$$m \frac{dv}{dt} = mg \cos\theta - \frac{1}{2}\rho v^2 C_D S \tag{2}$$

$$mv \frac{d\theta}{dt} = -mg \sin\theta \tag{3}$$

The velocity and angle can then be found numerically by expressing Eqns (2) and (3) in finite difference form, and the values of x and z are easily found from $\frac{dx}{dt} = v \sin\theta$ and $\frac{dz}{dt} = v \cos\theta$ expressed in finite difference form. Summarizing, for all processes which can be approximated by point mass trajectories, the governing equations are

$$\Delta v = \left[g \cos\theta - \frac{\rho v^2 C_D S}{2m} \right] \Delta t \tag{4}$$

$$\Delta\theta = -\frac{g \sin\theta}{v} \tag{5}$$

$$\Delta x = v \sin\theta \, \Delta t \tag{6}$$

$$\Delta z = v \cos\theta \, \Delta t \tag{7}$$

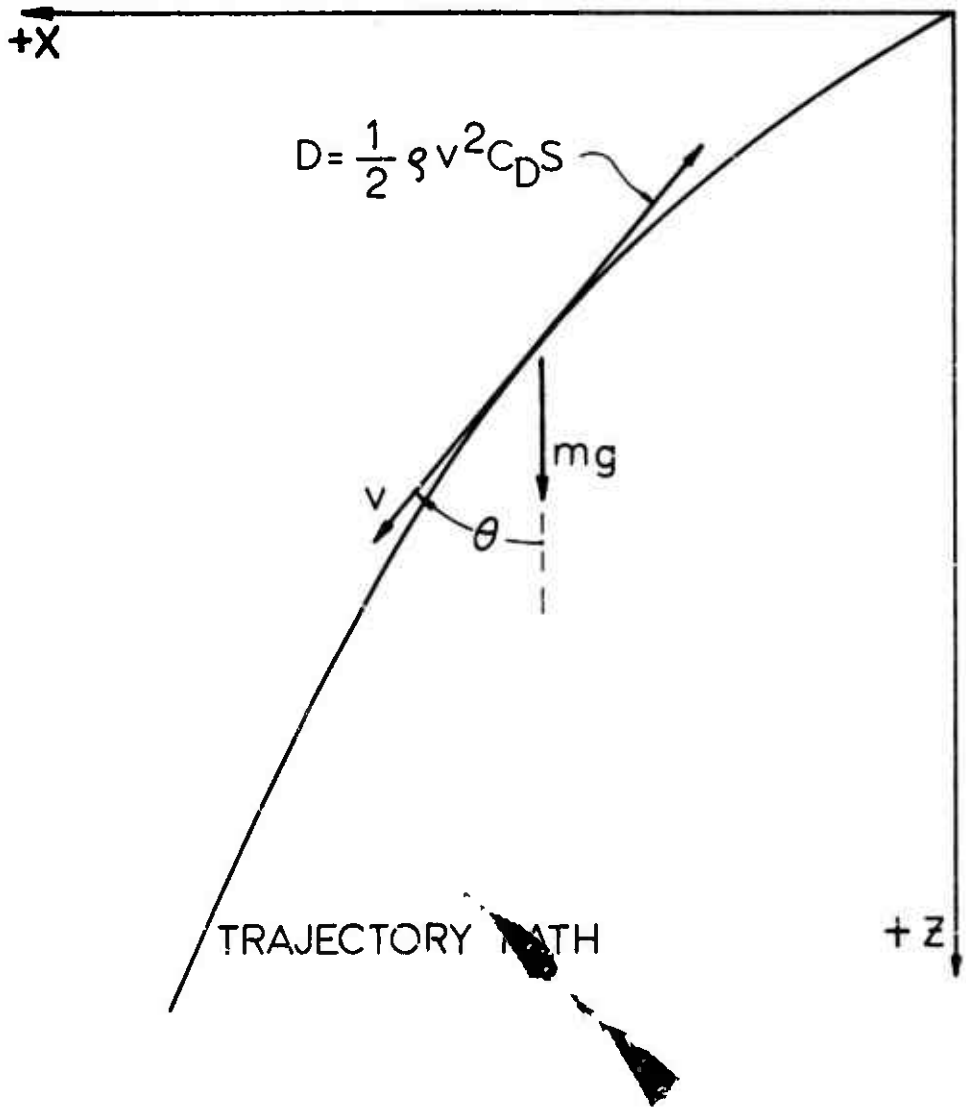

Fig 7 Definition of Quantities for Two Dimensional Point Mass Trajectory Analysis

C. Separation from Aircraft

There are several possible calculation schemes for this phase of performance, depending on the separation-deployment system to be used. This is the first phase of the total trajectory simulation, beginning at the instant the load is released from the aircraft.

1. Load Extraction

If the load is to be extracted with extraction parachutes or by the reefed main parachute, the governing equation is for horizontal deceleration until the load leaves the aircraft, i.e.

$$m \frac{dv}{dt} = -\frac{1}{2} \rho v^2 C_D S \tag{8}$$

The modeling equations incorporated in the total trajectory simulation are then, expressing Eqn (7) in finite difference form,

$$\Delta v = -\frac{\rho v^2 C_D S}{2m} \Delta t \tag{9}$$

$$\Delta x = v \Delta t \tag{10}$$

where m is the mass of the entire recovery system and $C_D S$ is the drag area of the extraction parachute, $(C_D S_{ex})$, or the reefed main parachute, $(C_{D_p} S_p)$. Equations (9) and (10) govern the motion until the load has traveled a specified distance L and leaves the aircraft, i.e., until

$$v_o t - x = L \tag{11}$$

where v_o is the aircraft velocity. Once the conditions are such that (11) is satisfied, the system is then governed by the two-dimensional trajectory Eqns (4) through (7), with the mass remaining the same but increasing the drag area to include the load and main parachute bag which are now exposed to the flow, for a specified time until the extraction main canopy is disreefed or deployment of the main canopy by the extraction parachutes is initiated. The next phase of the simulation is then inflation of the main parachute from its reefed configuration for the former case or deployment and snatch force for the latter.

2. Static Line Extension

When a static line is used, the system is governed by Eqns (4) through (7) using the mass and drag area of the load and the packed recovery system. This is true until the distance between the aircraft and the load equals the length of the static line, plus the suspension system and half the diameter of the pilot parachute, if used. This criterion is

$$\sqrt{(v_o t - x)^2 + z^2} = L_{static} + L' \qquad (12)$$

where L' is the additional length of the suspension system and deployed pilot parachute canopy. If a pilot chute is used, the trajectory can be governed by Eqns (4) through (7) with the drag area increased to include the pilot chute until a specified time is reached.

D. Deployment and Snatch Force

Once the system has separated from the aircraft and

coasted on the extraction or pilot parachutes if desired, i.e., remained unchanged in configuration while following its trajectory for a specified time, the deployment of the main parachute begins. Two methods are considered, static line deployment and deployment by pilot or extraction parachute. It has been assumed that the "snatch force" from a static line deployment can be neglected.

1. Deployment by Static Line

For the case of deployment by static line, the trajectory is governed by the same equations as during the static line separation process. Thus the governing equations are Eqns (4) through (7), and the canopy is deployed when Eqn (12) is satisfied, where L' is the length of the suspension system plus half the diameter of the main canopy. The total trajectory simulation then proceeds to the inflation calculation phase.

2. Deployment by Pilot or Extraction Parachute

The physical process involved in this method begins at the instant that deployment of the main parachute is initiated and includes the deployment of the suspension lines, risers, etc., snatch force, and the deployment of the main parachute canopy.

Certain assumptions concerning the motion of the primary and secondary bodies during this phase of operation must be made. Basically, it is assumed that the primary body alone determines the trajectory that the system follows during the deployment, i.e., that the velocity vector of the secondary body is always aligned with that of the primary body (Fig 8).

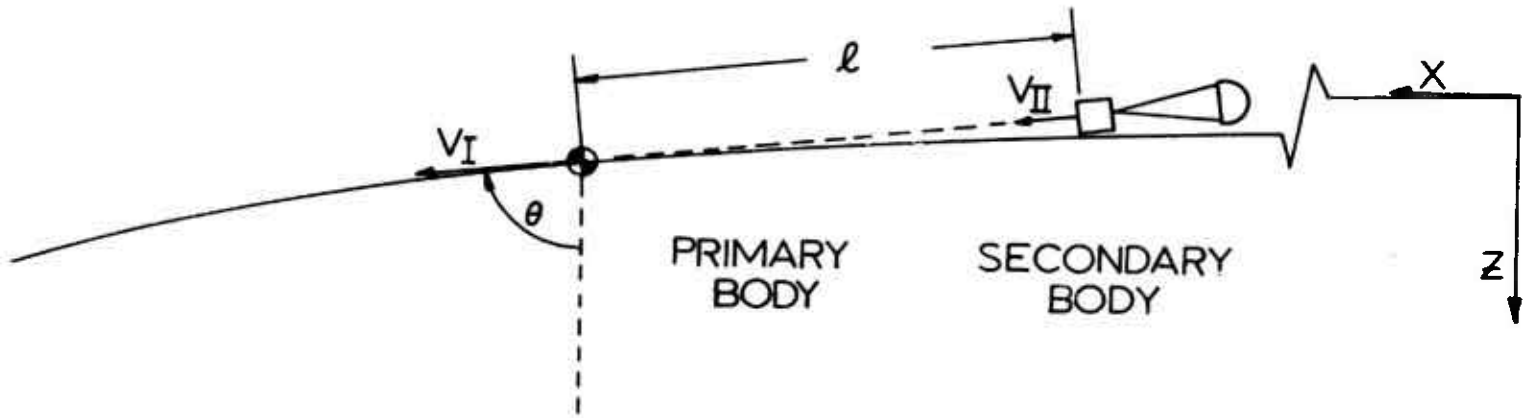

Fig 8 Parachute Load System During Deployment by Pilot or Extraction Parachute

a. Suspension Line and Riser Deployment

The motion during deployment is given by a point mass trajectory analysis of the primary body with the secondary body decelerating at a different rate but in the same direction as the primary body. To simplify the problem of time varying mass as the suspension system is deployed, the primary and secondary body masses are defined in a manner similar to Ref 3 during deployment of the suspension system,

$$m_I = m_\ell + \frac{1}{2} m_{ss} \tag{13}$$

$$M_{II} = m_p + \frac{1}{2} m_{ss} + m_{pb} \tag{14}$$

where m_{ss} is the mass of the suspension lines, risers, extensions, bridle, and links and m_{pb} is the mass of the pilot or extraction parachute and the main parachute bag. In finite difference form, the governing equations during deployment of the suspension system are then

$$\Delta\theta = -\frac{g \sin\theta}{v_I} \Delta t \tag{15}$$

$$\Delta v_I = \left(g \cos\theta - \frac{\rho C_D S_\ell v_I^2}{2 m_I} \right) \Delta t \tag{16}$$

$$\Delta v_{II} = \left(g \cos\theta - \frac{\rho C_D S_\pi v_{II}^2}{2 M_{II}} \right) \Delta t \tag{17}$$

$$\Delta z = v_I \cos\theta \, \Delta t \tag{18}$$

$$\Delta z = v_I \cos\theta \, \Delta t \tag{19}$$

$$\Delta \ell = v_I \Delta t - v_{II} \Delta t \tag{20}$$

where ℓ is the distance between the primary and secondary bodies. $C_D S_{II}$ in Eqn (17) is the drag area of the pilot or extraction parachute and the main parachute bag.

b. Snatch Force

When the value of ℓ, which is initially zero, equals the length of the suspension lines, risers, extensions, and bridle, the line elongation and the development of the line force begins. The force calculation follows the energy conservation method of Ref 3, and the maximum or snatch force is given by

$$P_{max} = -B + \sqrt{B^2 - C/A} \tag{21}$$

where

$$B = F_{A_I}\left[1 + Q + \frac{2v_{II}}{v_s - v_{II}} Q\right] + F_{A_{II}}\left[Q + \frac{2v_{II}}{v_s - v_{II}} Q\right] \tag{22}$$

$$C = M_I \frac{Q-1}{Q}\left[\frac{Q+1}{Q}(v_s - v_{II})^2 + 2v_{II}(v_s - v_{II})\right] + m_p\left[(v_s - v_{II})^2 + 2v_{II}(v_s - v_{II})\right] \tag{23}$$

$$F_{A_I} = \frac{\rho C_D S_I}{4}\left(V_I^2 + V_s^2\right) \tag{24}$$

$$F_{A_{II}} = \frac{\rho C_D S_{II}}{4}\left(V_{II}^2 + V_s^2\right) \tag{25}$$

$$Q = \frac{M_I}{M_I + m_p} \tag{26}$$

$$V_s = \frac{M_I V_I + m_p V_{II}}{M_I + m_p} \tag{27}$$

and A is the inverse of the effective spring constant of the suspension lines, risers, extensions, and bridle. The value M_I is given by $M_I = m_\ell + m_{ss}$, and Eqns (26) and (27) reflect the assumption that the suspension system is moving at the same velocity as the load and only the main parachute canopy is accelerated at snatch. The time increment during which the lines elongate is very short and is neglected in view of the total elapsed time.

c. Main Parachute Canopy Unfolding

After snatch, the main parachute unfurls from the bag. The primary body is now considered to consist of the suspended load, risers, and canopy, and the secondary body consists of the pilot or extraction parachute and the deployment bag. The equations governing the motion during unfolding of the main parachute are similar to Eqns (14) through (19) with the exception that (15) and (16) are replaced by

$$\Delta v_I = \left[g\cos\theta - \frac{\rho(C_D S_\ell + 0.015\, C_{D_0} S_0)\, v_I^2}{2(M_I + m_p)} \right] \Delta t \quad (28)$$

$$\Delta v_{II} = \left(g\cos\theta - \frac{\rho\, C_D S_{II}\, v_{II}^2}{2\, m_{pb}} \right) \Delta t \quad (29)$$

The drag area in Eqn (28) is increased by the addition of 1.5% of the fully inflated drag area of the main parachute. This value represents the drag area of the uninflated main parachute and was taken from Ref 4. The trajectory is calculated with Eqns (15), (28), (29), (18) and (19) and the separation with Eqn (20) until the value of ℓ equals the value at snatch plus half the nominal diameter of the main parachute at which time the canopy is deployed. The next phase is then the inflation phase.

3. Summary of Assumptions for the Deployment Phase

In the following the assumptions on which the preceding calculations were based are summarized. For static line deployment, it is assumed that (1) the static line remains in a straight configuration between the aircraft and the load, and (2) there is no appreciable "snatch force." When the main decelerator is deployed by extraction or pilot parachute several assumptions are made: (1) the trajectory of the parachute-load system during deployment is determined only by the load; (2) the positions of the primary and secondary bodies can be described by point-mass trajectory equations using "average" values for the masses; (3) the occurrence of snatch is instantaneous for elapsed time consideration; (4) the mass of the parachute bag and pilot or extraction

parachute is decelerated relative to the load as the canopy unfurls. The above assumptions are simplifications of actual deployment conditions. The need for a more exact treatment of this phase should be determined in future work.

E. Inflation of the Main Parachute

The inflation of the main parachute begins at the instant the parachute is deployed in a stretched-out configuration with assumed zero projected area, or at some initiation time t_D when the parachute is used in a reefed configuration to extract the load. The total trajectory simulation calculates the motion of the parachute-load system as it inflates to its fully open configuration with or without intermediate reefed configurations.

1. Governing Equations

The basis for the total trajectory simulation during the inflation of the main parachute is a coupling of the calculations of the opening force (Ref 5), and a ballistic trajectory. The opening force calculation assumes that the inflating parachute has the shape of a truncated cone with a hemispherical cap such that the suspension lines extend parallel to the edges of the truncated cone (Fig 9). The trajectory calculation is based on force equations parallel and perpendicular to the trajectory of the mass center of the parachute-load system, and it is assumed that the velocity components of the load and the parachute normal to the systems axis are assumed to be negligible. This assumption may be questionable, especially for large parachutes with long distances between

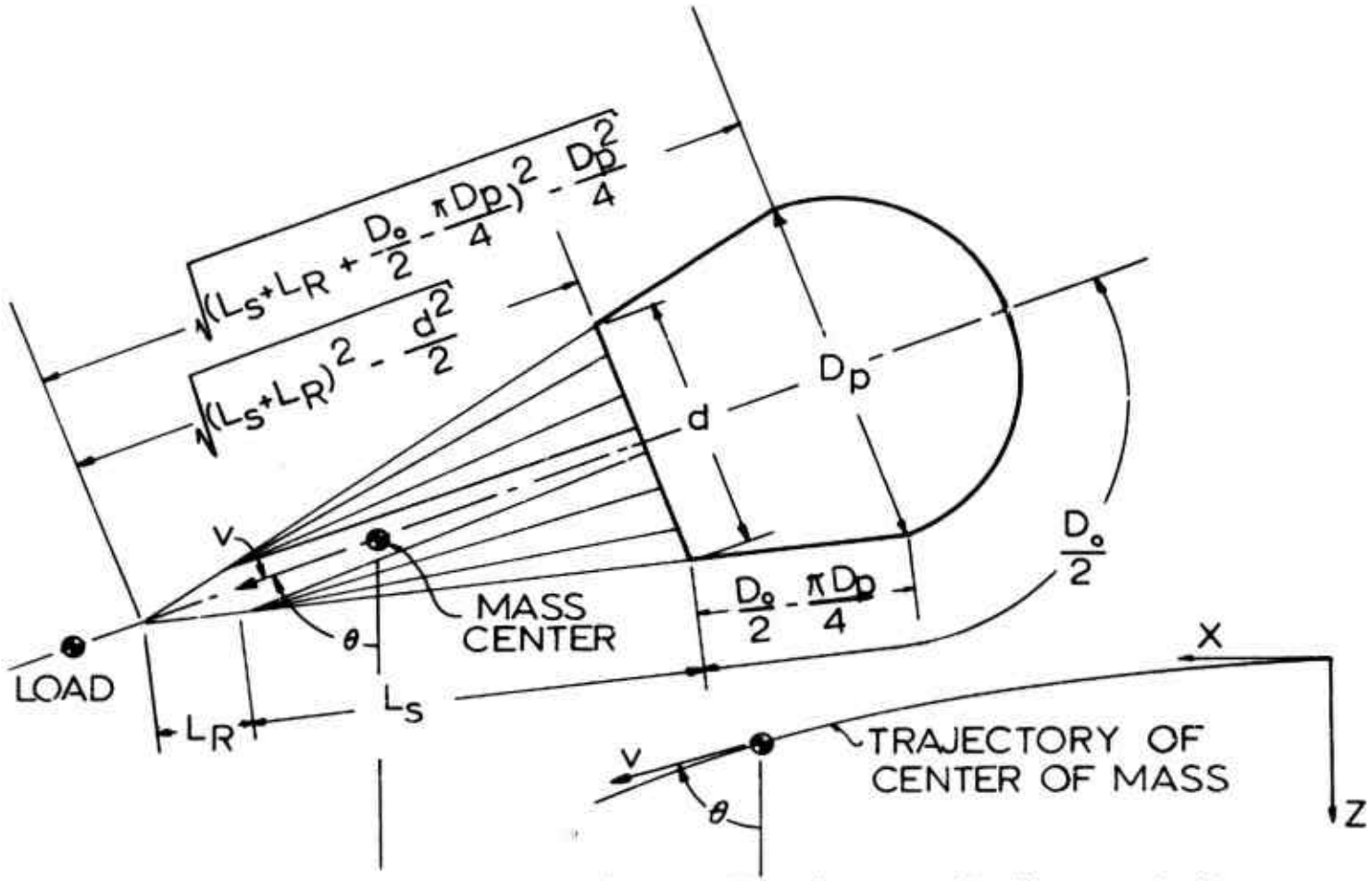

Fig 9 Parachute-Load System During Inflation of the Main Parachute

parachute and load; however, it was felt that such an assumption was a reasonable first approximation. It should be noted that the above velocity components are not neglected in the free descent phase.

Therefore, the parachute-load system is considered to be, in effect, a point mass with varying mass and drag area during the inflation process. The force equations parallel and perpendicular to the trajectory of the mass center are then

$$-\frac{1}{2}\rho v^2\left(C_D S_\ell + C_{D_p}\frac{\pi D_p^2}{4}\right) + (m_\ell + m_{ss} + m_p)\, g\cos\theta - v\frac{d}{dt}(m_i + m_a) - (m_i + m_a)\frac{dv}{dt} = (m_\ell + m_{ss} + m_p)\frac{dv}{dt} \tag{30}$$

and

$$(m_\ell + m_{ss} + m_p)\, g\sin\theta - (m_i + m_a)\, v\frac{d\theta}{dt} = (m_\ell + m_{ss} + m_p) \cdot v\frac{d\theta}{dt} \tag{31}$$

Defining a total mass by

$$m_T = m_\ell + m_{ss} + m_p + m_i + m_a \tag{32}$$

the equations governing the motion can be written in finite difference form as

$$\Delta v = \left\{\left(\frac{m_\ell + m_{ss} + m_p}{m_T}\right) g\cos\theta - \frac{\rho v^2}{2m_T}\left(C_D S_\ell + C_{D_p}\frac{\pi D_p^2}{4}\right) + \frac{v}{m_T}\left(\frac{dm_i}{dt} + \frac{dm_a}{dt}\right)\right\}\Delta t \tag{33}$$

and

$$\Delta\theta = -\left(\frac{m_\ell + m_{ss} + m_p}{m_T}\right)\frac{g\sin\theta}{v}\,\Delta t \tag{34}$$

Thus the motion of the parachute-load system during inflation can be found numerically from Eqns (33) and (34) if the values of m_i, m_a, dm_i/dt, dm_a/dt, and D_p are known throughout the inflation process.

a. Inflation Without Reefing

The basic assumptions of Ref 5 are that the canopy geometry at any time instant during inflation is determined by a linear growth of the projected area and a linear function of the influx versus a dimensionless time $T = (t - t_o)/t_{ff}$. These are commonly used assumptions which are subject to change on the basis of future studies. Certain differences appear between the definitions of filling time used in this report and in other literature, such as Ref 6. The dimensionless time scale T as used in Ref 6 ranges from T = 0 at peak snatch force to T = 1 when the projected area first reaches its steady state value. The dimensionless time scale in this study begins after the main parachute canopy unfolding process has been completed, T = 0, and continues until the steady state volume of the parachute canopy is reached, T = 1. Thus the base of the dimensionless scale is referred to as the final filling time, t_{ff}.

The first assumption provides for the projected diameter the relationship

$$D_p = \frac{2D_o}{\pi} T^{1/2} \tag{35}$$

All other terms in the equations of motion can then be determined from D_p and the assumed geometry. Expressing projected diameter as a function of dimensionless time adds the unknown t_{ff} to the problem. The solution for t_{ff} is accomplished by examining the continuity equation describing

the imbalance of mass flow into and out of the parachute canopy. This equation is, in accordance with Ref 5,

$$\frac{dV}{dT} = \pi t_{ff} v \left[(1+2.2cT-T) \frac{d^2}{4} - \frac{1.1 c D_p^2}{2} \right] \tag{36}$$

which is based on the inflow velocity in the form of

$$\frac{v_{in}}{v} = (1+2.2cT-T) \tag{37}$$

Thus the filling time t_{ff} for inflation without reefing can be found by integration of Eqn (36) as T ranges from 0 to 1. The volume V of the fully inflated parachute is equal to

$$V = \pi t_{ff} \int_0^1 v \left[(1+2.2cT-T) \frac{d^2}{4} - \frac{1.1 c D_p^2}{2} \right] dT \tag{38}$$

The filling time is readily found by a numerical procedure as follows. An initial value must be estimated for the filling time. Equation (38) can then be numerically integrated with Simpson's Rule using a number, n, of equal increments of time ΔT such that T ranges from 0 to 1, yielding a result which depends on the assumed filling time. This numerical integration is expressed as

$$V(t_{ff_i}) = \pi t_{ff_i} \frac{\Delta T}{3} \left[\nu_0 + 4\nu_1 + 2\nu_2 + 4\nu_3 + 2\nu_4 + \cdots + \nu_n \right] \tag{39}$$

where

$$\nu_j = v(T_j) \left\{ (1+2.2cT_j - T_j) \frac{d^2(T_j)}{4} - \frac{1.1 c D_p^2(T_j)}{2} \right\} \tag{40}$$

T_j, j = 1, 2, ..., n, represent the values of the time scale selected for the numerical integration. The numerical value of $D_p(T_j)$ is found from Eqn (35) evaluated at $T = T_j$, and

the corresponding numerical value of $d(T_j)$ is determined by the geometrical relation

$$d = \frac{4(L_s+L_R)\,D_p}{4(L_s+L_R)+2D_0-\pi D_p} \tag{41}$$

The velocity $v(T_j)$, however, must be found from the equations of motion, Eqns (33) and (34) with initial conditions $\theta = \theta_0$ and $v = v_0$ for $T = 0$. The mass terms in the equations of motion based on the assumed geometry and expressed as functions of T and D_p are

$$m_a = \frac{\pi\rho}{32}\,\frac{D_p^5}{(D_{p_{max}})^2} \tag{42}$$

$$m_i = \frac{\pi\rho}{12}\left\{D_p^3 + D_p^2\sqrt{\left(L_s+L_R+\frac{D_0}{2}-\frac{\pi D_p}{4}\right)^2-\frac{D_p^2}{4}} - d^2\sqrt{(L_s+L_R)^2-\frac{d^2}{4}}\right\} \tag{43}$$

$$\frac{dm_a}{dT} = \frac{5\pi\rho}{32\,(D_{p_{max}})^2}\,D_p^4\,\frac{d(D_p)}{dT} \tag{44}$$

$$\frac{dm_i}{dT} = \frac{\pi\rho}{12}\left\{3D_p^2\frac{d(D_p)}{dT} - D_p^2\left[\frac{\left[2(L_s+L_R)+D_0-\frac{\pi D_p}{4}\right]\frac{\pi}{4}\frac{d(D_p)}{dT}}{2\left[\left(L_s+L_R+\frac{D_0}{2}-\frac{\pi D_p}{4}\right)^2-\frac{D_p^2}{4}\right]^{1/2}} + \frac{\frac{D_p}{2}\,d(D_p)/dT}{2\left[\left(L_s+L_R+\frac{D_0}{2}-\frac{\pi D_p}{4}\right)^2-\frac{D_p^2}{4}\right]^{1/2}}\right] + 2D_p\frac{d(D_p)}{dT}\sqrt{(L_s+L_R+\frac{D_0}{2}-\frac{\pi D_p}{4})^2-\frac{D_p^2}{4}} + \frac{d^3}{\left[4(L_s+L_R)^2-\frac{d^2}{4}\right]^{1/2}} - 2d\frac{d(d)}{dT}\sqrt{(L_s+L_R)^2-\frac{d^2}{4}}\right\} \tag{45}$$

where

$$\frac{d(D_p)}{dT} = \frac{D_o}{\pi T^{1/2}} \tag{46}$$

$$\frac{d(d)}{dT} = \frac{\left(L_s + L_R + \frac{D_o}{2} - \frac{\pi D_p}{4}\right)(L_s + L_R)\frac{d(D_p)}{dT}}{\left(L_s + L_R + \frac{D_o}{2} - \frac{\pi D_p}{4}\right)^2} + \frac{(L_s + L_R)\frac{\pi D_p}{4}\frac{d(D_p)}{dT}}{\left(L_s + L_R + \frac{D_o}{2} - \frac{\pi D_p}{4}\right)^2} \tag{47}$$

Eqns (32) and (33) are, in terms of t_{ff} and T,

$$\Delta v = \left\{\left(\frac{m_\ell + m_{ss} + m_p}{m_T}\right) g \cos\theta - \frac{\rho v^2}{2m_T}\left[C_D S_\ell + C_{D_p} \cdot \frac{\pi D_p^2}{4}\right]\right\} t_{ff}\,\Delta T + \frac{V}{m_T}\left(\frac{dm_i}{dT} + \frac{dm_a}{dT}\right)\Delta T \tag{48}$$

$$\Delta\theta = -\left(\frac{m_\ell + m_{ss} + m_p}{m_T}\right)\frac{g \sin\theta}{V}\, t_{ff}\,\Delta T \tag{49}$$

Thus the velocity can be found for any value of T_j by using Eqns (48) and (49) for the particular choice of t_{ffi}, and the numerical integration (39) can be performed.

The value of $V(t_{ffi})$ determined from Eqn (39) is then compared with the known volume of the fully inflated canopy, and a new approximation to the filling time is found from

$$t_{ff_{i+1}} = t_{ff_i} \frac{V}{V(t_{ff_i})} \tag{50}$$

The process outlined above is repeated until $\left|V - V(t_{ff_i})\right|$ is small enough that the filling time can be considered accurate.

It may be mentioned that the method of Ref 5 follows a similar scheme, however, the various functions are simplified by means of curve fitting since a practically closed solution is pursued in Ref 5.

Once the filling time is known, the trajectory of the parachute-load system mass center is determined from Eqns (48) and (49) in conjunction with

$$\Delta x = v \sin\theta \; t_{ff} \, \Delta T \tag{51}$$

$$\Delta z = v \cos\theta \; t_{ff} \, \Delta T \tag{52}$$

and the instantaneous opening force is found from

$$F_0 = m_\ell \left(g\cos\theta - \frac{\Delta v}{t_{ff}\,\Delta T} \right) \tag{53}$$

b. Reefed Inflation

When the inflation process includes intermediate reefed configurations, the trajectory simulation is divided into periods of inflation and periods of coasting in the reefed configuration, if desired. Provision for the coasting periods is made by prescribing a reefing cutter delay from the time of suspension line deployment, or from t = 0 when the load is released in the aircraft for systems extracted by the reefed main parachute.

During the coasting periods, the drag area remains constant, and the motion is described by the two-dimensional ballistic trajectory equations (4) through (7), with the value of the load drag area plus the drag area corresponding to the particular reefed configuration of the parachute, and the mass of the parachute-load system. When the final configuration of an inflation phase is the fully inflated configuration, there is no coasting period, but the trajectory simulation proceeds immediately with the free descent phase.

During each period of inflation, it is assumed that the projected area increases linearly with time (Fig 10). Defining a dimensionless time scale for each period of inflation such that

$$T_R = \frac{t - t_o}{t_{fR}} \tag{54}$$

where t_o is the initial time and t_{fR} is the inflation time for the particular reefed inflation period, enables the problem to be viewed in a manner similar to the approach followed for the unreefed inflation. The projected area growth for each of the inflation periods is given by (Fig 10)

$$\frac{S_p}{S_o} = h_o^2 + (h_1^2 - h_o^2)\, T_R \tag{55}$$

where, with the geometry as used before,

$$h_o = \left.\frac{D_p}{D_o}\right)_{T_R=0} = \frac{4(L_s+L_R)R_o + 2R_o D_o}{4(L_s+L_R) + \pi R_o D_o}$$

and

$$h_1 = \left.\frac{D_p}{D_o}\right)_{T_R=1} = \frac{4(L_s+L_R)R_1 + 2R_1 D_o}{4(L_s+L_R) + \pi R_1 D_o} \tag{56}$$

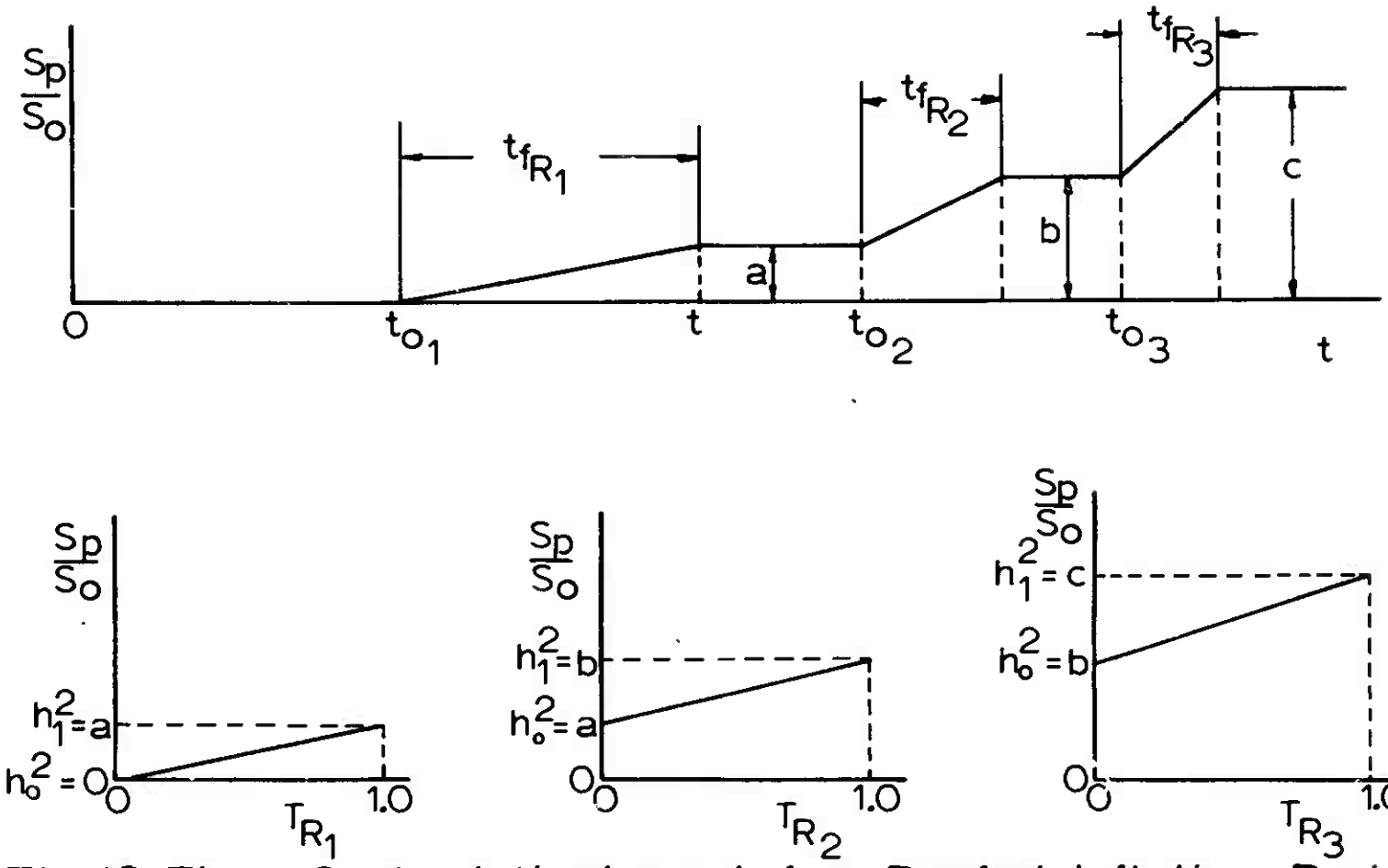

Fig 10 Time Scale Adjustment for Reefed Inflation Periods

In these equations, R_0 and R_1 are the reefing ratios defined by

$$R = \frac{l_R/\pi}{D_0} \tag{57}$$

corresponding to the reefing lines at the beginning and end of the inflation period. The projected diameter is then found from Eqn (55) to be

$$D_p = D_0\sqrt{h_1^2 T_R + h_0^2(1-T_R)} \tag{58}$$

Comparing Eqns (35) and (58), it is evident that one can consider the projected diameter growth during an inflation period to be a function of T, the dimensionless time scale which would exist if the inflation were taking place in one complete step without reefing, i.e., the functions describing the reefed inflation can be considered to be portions of the functions developed for the unreefed case. The values of projected diameter, masses, etc. can then be found for any value of T_R by evaluating the equations presented in Item a at a value of T given by

$$T = \frac{\pi^2}{4}\sqrt{h_1^2 T_R + h_0^2(1-T_R)} \tag{59}$$

which is obtained by equating the right hand sides of Eqns (35) and (58).

The procedure for calculation of the filling time, trajectory, and opening force is similar to that discussed for the unreefed case. The filling time is found from numerical integration, with T_R ranging from 0 to 1, of

$$V_R = \pi t_{4R} \int_0^1 v\left[(1+2.2cT-T)\frac{d^2}{4} - \frac{1.1cD_p^2}{2}\right] dT_R \tag{60}$$

i.e.

$$V_R(t_{fR_i}) = \pi t_{fR_i} \frac{\Delta T_R}{3} \left(\nu_0 + 4\nu_1 + 2\nu_2 + \cdots + \nu_n \right) \tag{61}$$

where ν_j is given by Eqn (40) with T_j evaluated from Eqn (59). The value V_R represents the increase in the volume of the parachute canopy as it inflates from the initial to the final reefed configuration and is given by

$$\begin{aligned} V_R = \frac{\pi}{12} \Bigg\{ & D_0^3 (h_1^3 - h_0^3) + D_0^2 \Bigg[h_1^2 \sqrt{\left(L_s + L_R + \frac{D_0}{2} - \frac{\pi}{4} h_1 D_0\right)^2 - \frac{h_1^2 D_0^2}{4}} \\ & - h_0^2 \sqrt{\left(L_s + L_R + \frac{D_0}{2} - \frac{\pi}{4} h_0 D_0\right)^2 - \frac{h_0^2 D_0^2}{4}} \Bigg] \\ & - D_0^2 \Bigg[R_1^2 \sqrt{(L_s + L_R)^2 - \frac{R_1^2 D_0^2}{4}} - R_0^2 \sqrt{(L_s + L_R)^2 - \frac{R_0^2 D_0^2}{4}} \Bigg] \Bigg\} \end{aligned} \tag{62}$$

Successive values of t_{f_R} are given by

$$t_{fR_{i+1}} = t_{fR_i} \frac{V_R}{V_R(t_{fR_i})} \tag{63}$$

until the value $\left| V(t_{fR_i}) - V_R \right|$ is small enough.

The necessary values for evaluation of Eqn (61) are determined as follows.

The velocity is found from

$$\begin{aligned} \Delta v = & \left[\left(\frac{m_\ell + m_{ss} + m_P}{m_T} \right) g \cos\theta - \frac{\rho v^2}{2 m_T} \left(C_0 S_\ell + C_{D_P} \frac{\pi D_P^2}{4} \right) \right] \cdot \\ & \cdot t_{fR} \, \Delta T_R + \frac{v}{m_T} \left(\frac{dm_i}{dT} + \frac{dm_a}{dT} \right) \Delta T \end{aligned} \tag{64}$$

$$\Delta\theta = -\left(\frac{m_\ell + m_{ss} + m_p}{m_T}\right) \frac{g \sin\theta}{v} t_{fR} \Delta T_R \tag{65}$$

The values of D_p, m_i, m_a, dm_i/dT, and dm_a/dT are found from Eqns (35), (42), (43), (44), and (45) with T from Eqn (59). The increment ΔT is determined from the prescribed increment ΔT_R by

$$\Delta T = \frac{\pi^2}{4}\left(h_1^2 - h_0^2\right) \Delta T \tag{66}$$

The trajectory is described by

$$\Delta x = v \sin\theta \; t_{fR} \Delta T_R \tag{67}$$

$$\Delta z = v \cos\theta \; t_{fR} \Delta T_R \tag{68}$$

and the instantaneous opening force is given by

$$F_0 = m_\ell \left(g \cos\theta - \frac{\Delta v}{t_{fR} \Delta T_R} \right) \tag{69}$$

2. Summary Assumptions for the Inflation Phase

The inflation phase of the trajectory simulation is modeled by the following assumptions. (1) The shape of the parachute is described by a truncated cone with a hemispherical cap and the projected area increases linearly with

time during both reefed and unreefed inflation periods. (2) The motion is confined to a vertical plane. (3) The magnitudes of the components of parachute and load velocities normal to the trajectory of the mass center are assumed negligible. (4) When reefing is used and coasting between the inflation periods is arranged, the path of the center of mass can be approximated by the two-dimensional point mass trajectory equations. (5) The time functions describing the performance of the parachute when inflating without reefing can be used to describe the reefed inflation periods by adjusting the time scale.

F. Free Descent

This phase begins at the instant the parachute is fully inflated and terminates at ground impact.

Two-body trajectory analyses are available, such as Refs 7 and 8, which describe the two-dimensional motion of the separate masses of the parachute and payload when constrained by the elastic connection (risers, slings, and suspension lines) between them. While consideration of elasticity is undoubtedly a more accurate representation of an actual system, it was felt that a reasonable approximation of the free descent phase could be achieved by analyzing the system as a rigid body having realistic distribution of the masses. It should be noted that the systems under consideration are limited to single parachutes with assumed point mass payloads. Further, the requirement for developing three-dimensional equations of motion and computer programs would have been considerably complicated by the assumption of a two-body system.

1. Governing Equations

In the following, a set of orthogonal coordinate axes fixed in the parachute load system is defined (Fig 11a) with respect to which the mass distribution is constant. These body-fixed axes are denoted by XYZ. The Newtonian or space-fixed axes, with respect to which all accelerations must be measured, are chosen to be fixed at the point of release from the drop aircraft. These Newtonian coordinates are the same axes, denoted xyz, used to describe the motion of the system during the previous phases of the trajectory simulation.

The orientation of the parachute-load system is described by Euler angles, ψ, θ, φ, chosen to correspond with the notation of Refs 9 and 10. The Euler angles chosen for the trajectory simulation are three consecutive rotations, beginning with a coordinate system $x_1y_1z_1$ parallel to the space-fixed reference frame (see Fig 11b), defined as follows:

(1) a rotation ψ about axis 0_{z_1}, yielding $x_2y_2z_2$

(2) a rotation θ about axis 0_{y_2}, yielding $x_3y_3z_3$

(3) a rotation φ about axis 0_{x_3}, yielding XYZ.

Vector quantities expressed in the space-fixed axes are then related to quantities expressed in the body-fixed axes by the direction cosine matrix, i.e.

$$\underline{e} = \underline{\underline{A}}\,\underline{E} \tag{70}$$

where $\underline{e}$ and $\underline{E}$ are vectors in the space-fixed and body-fixed coordinate systems, respectively. The direction cosine matrix is the direction cosine matrix of Ref 10 transposed:

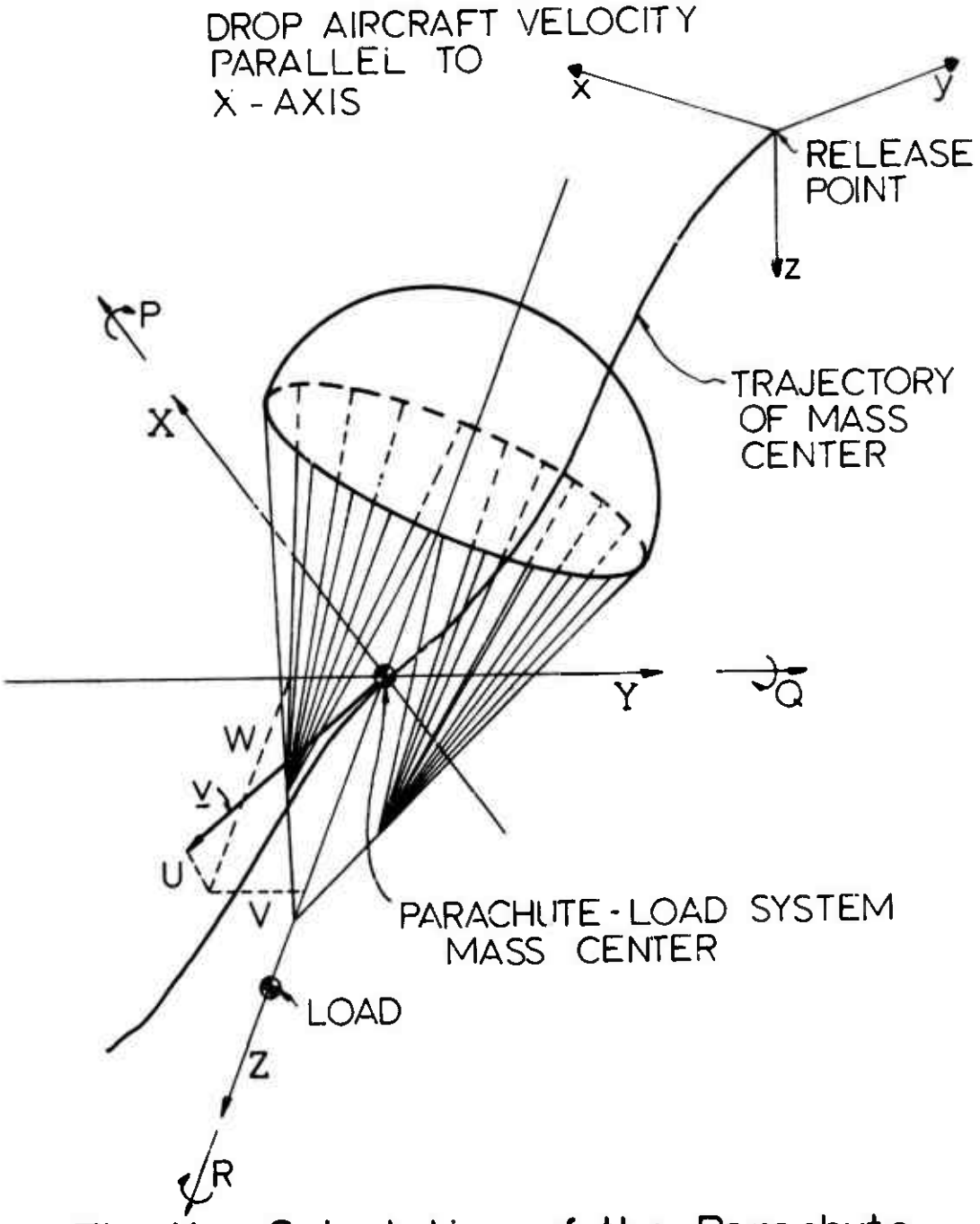

Fig 11a Orientation of the Parachute-Load System

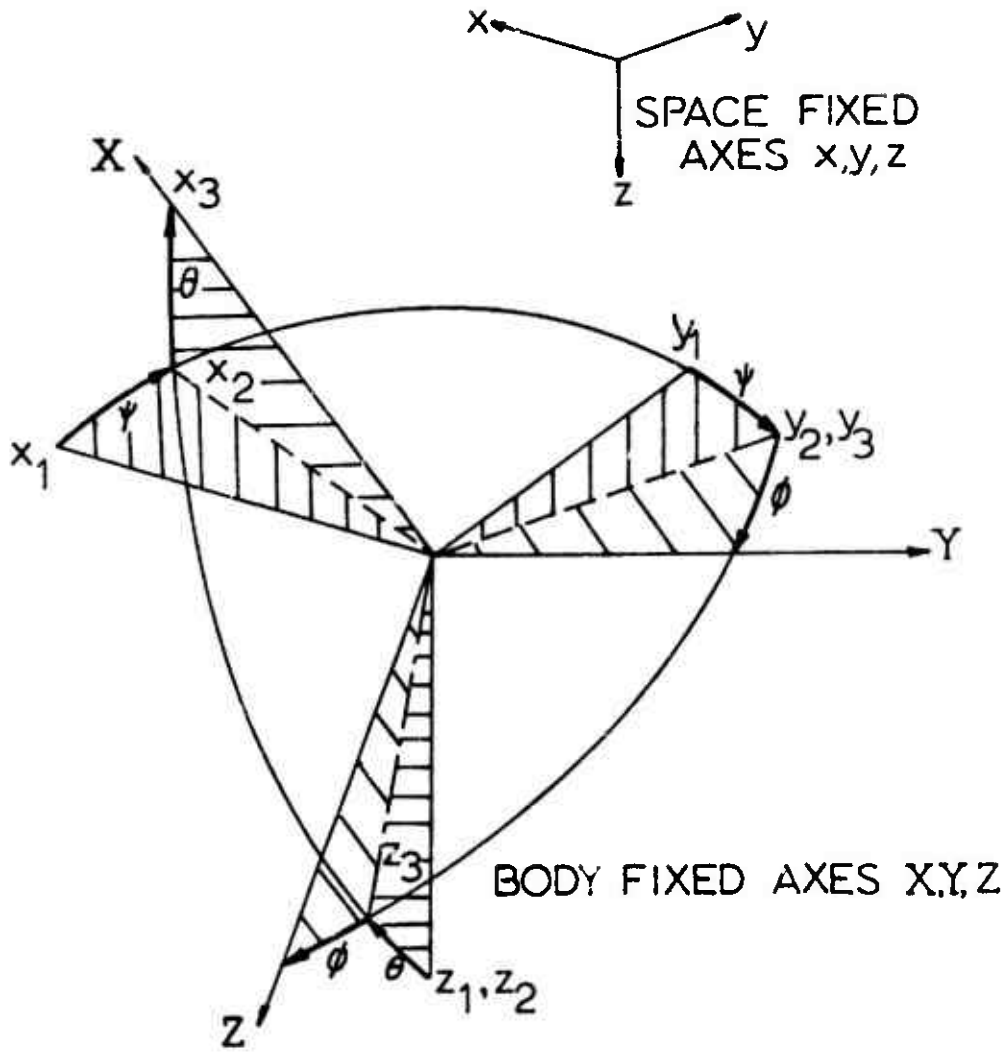

ALL DIRECTIONS INDICATED ARE POSITIVE

Fig 11b Euler Angles ψ, θ, ϕ

$$\underline{\underline{A}} = \begin{pmatrix} \cos\theta\cos\psi & \sin\varphi\sin\theta\cos\psi - \cos\varphi\sin\psi & \cos\varphi\sin\theta\cos\psi + \sin\varphi\sin\psi \\ \cos\theta\sin\psi & \sin\varphi\sin\theta\sin\psi + \cos\varphi\cos\psi & \cos\varphi\sin\theta\sin\psi - \sin\varphi\cos\psi \\ -\sin\theta & \sin\varphi\cos\theta & \cos\varphi\cos\theta \end{pmatrix} \tag{71}$$

Choosing the origin of the body-fixed coordinate system as the mass center of the parachute-load system allows the equations of motion in the body fixed system to be written as

$$\underline{F} = (m_l + m_{ss} + m_p)\frac{d\underline{V}}{dt} \tag{72}$$

$$\underline{M} = \frac{d}{dt}(\underline{H}) \tag{73}$$

Time derivatives of vectors in the rotating reference frame must be measured relative to the Newtonian reference frame. If the parachute, and thus the body-fixed coordinate system, rotates with an angular velocity $\underline{\omega}$, the time derivative of a vector $\underline{E}$ is given by Euler's equation,

$$\frac{d}{dt}(\underline{E}) = \left(\frac{d\underline{E}}{dt}\right)_{XYZ} + \underline{\omega} \times \underline{E} \tag{74}$$

Thus the equations of motion (73) and (74) can be expressed in scalar form as follows:

$$\Sigma F_X = (m_l + m_{ss} + m_p)\left[\dot{U} + QW - RV\right] \tag{75}$$

$$\Sigma F_Y = (m_\ell + m_{ss} + m_p)\left[\dot{V} + RU - PW\right] \tag{76}$$

$$\Sigma F_Z = (m_\ell + m_{ss} + m_p)\left[\dot{W} + PV - QU\right] \tag{77}$$

$$\begin{aligned}\Sigma L = {} & \dot{P} I_{XX} - \dot{Q} I_{XY} - \dot{R} I_{XZ} + QR(I_{ZZ} - I_{YY}) \\ & + (R^2 - Q^2) I_{YZ} + PR I_{XY} - PQ I_{XZ}\end{aligned} \tag{78}$$

$$\begin{aligned}\Sigma M = {} & \dot{Q} I_{YY} - \dot{R} I_{YZ} - \dot{P} I_{XY} + PR(I_{XX} - I_{ZZ}) \\ & + (P^2 - R^2) I_{XZ} + PQ I_{YZ} - QR I_{XY}\end{aligned} \tag{79}$$

$$\begin{aligned}\Sigma N = {} & \dot{R} I_{ZZ} - \dot{P} I_{XZ} - \dot{Q} I_{YZ} + PQ(I_{YY} - I_{XX}) \\ & + (P^2 - Q^2) I_{XY} + QR I_{XZ} - PR I_{YZ}\end{aligned} \tag{80}$$

where L, M, N are the body-fixed components of the moment $\underline{M}$, U, V, W are the body-fixed components of the center of mass velocity $\underline{v}$, and P, Q, R are the body-fixed components of the angular velocity $\underline{\omega}$. In terms of the angular velocity components, the Euler angles are found from the differential equations (Ref 8)

$$\dot{\theta} = Q\cos\varphi - R\sin\varphi \tag{81}$$

$$\dot{\varphi} = P + Q\sin\varphi\tan\theta + R\cos\varphi\tan\theta \tag{82}$$

$$\dot{\psi} = (Q\sin\varphi + R\cos\varphi)\sec\theta \tag{83}$$

The velocity of the mass center in space-fixed coordinates is related to the velocity in body-fixed coordinates by

$$\dot{x} = Ua_{11} + Va_{12} + Wa_{13} \tag{84}$$

$$\dot{y} = Ua_{21} + Va_{22} + Wa_{23} \tag{85}$$

$$\dot{z} = Ua_{31} + Va_{32} + Wa_{33} \tag{86}$$

Thus Eqns (75) through (86) represent a complete description of the system, and a solution to these twelve equations provides the necessary information for a three-dimensional trajectory simulation. Linearizing the equations as is usually done in dynamic stability analyses, for example airplane dynamic stability, is not an appropriate solution method for a trajectory simulation of a parachute-load system due to the large angle deflections which occur in parachute-load system trajectories. Thus the approach taken for this trajectory simulation is to solve the equations

numerically using the Runge-Kutta method. The remaining task which must first be accomplished is the formulation of the external forces and moments in the equations of motion (75) through (80).

a. Three Degrees of Freedom

When the trajectory simulation is restricted to three degrees of freedom, the quantities V, P, R, φ, ψ, and y are all constrained to zero. Figure 12 illustrates the orientation of the parachute-load system and the external forces and moments which act upon the parachute and the load for the three-degree-of-freedom-problem. The formulation of the equations of motion is simplified considerably by the restriction to three degrees of freedom, and the number of equations required for a complete description of the system is reduced from twelve to six. These equations are:

$$\Sigma F_x = (m_\ell + m_{ss} + m_p)\left[\dot{U} + QW\right] \tag{87}$$

$$\Sigma F_z = (m_\ell + m_{ss} + m_p)\left[\dot{W} - QU\right] \tag{88}$$

$$\Sigma M = \dot{Q} I_{YY} \tag{89}$$

$$\dot{\theta} = Q \tag{90}$$

$$\dot{x} = U\cos\theta + W\sin\theta \tag{91}$$

$$\dot{z} = -U\sin\theta + W\cos\theta \tag{92}$$

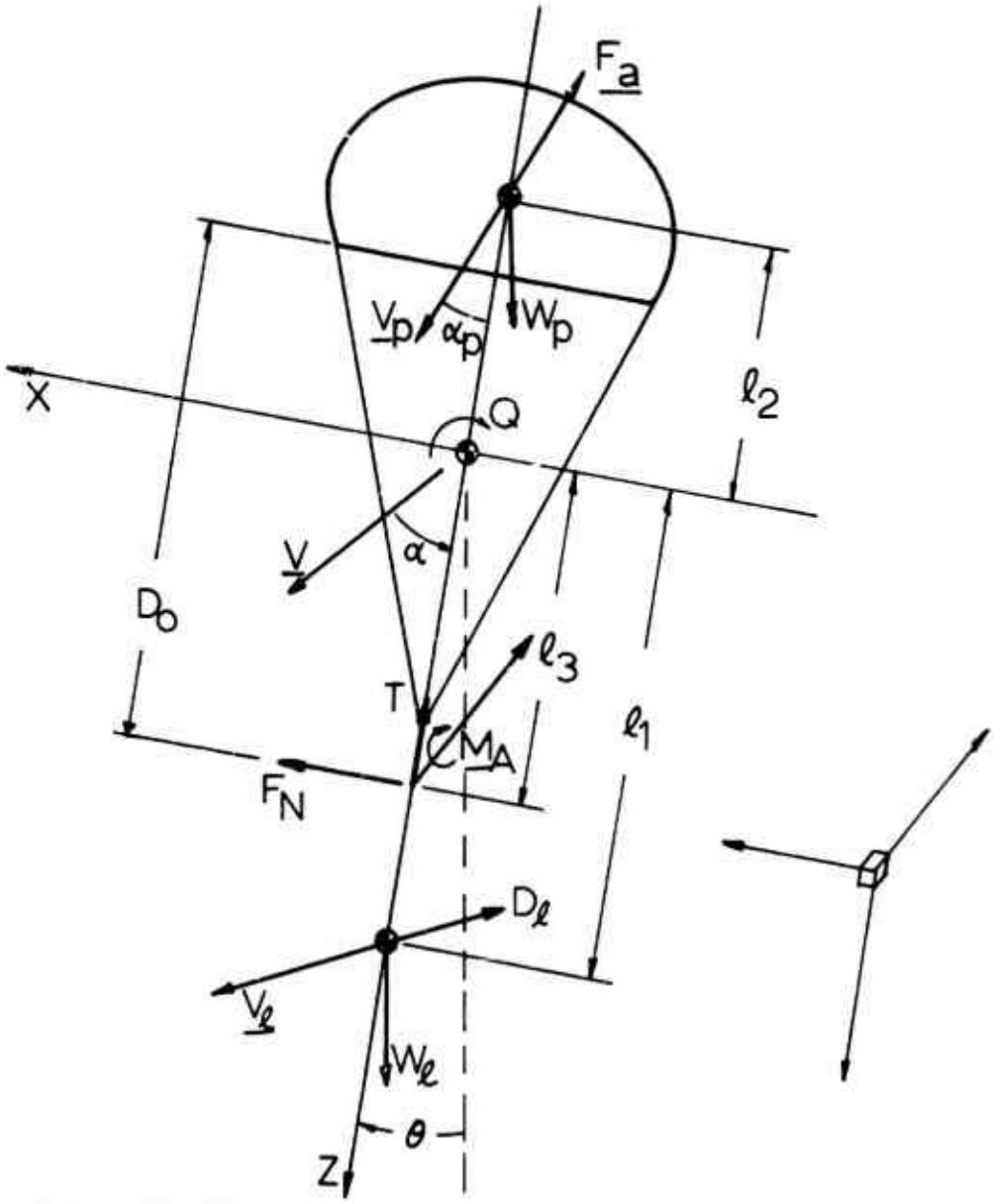

Fig 12 The Parachute-Load System Constrained to Three Degrees of Freedom

The external forces and moments which are considered in the trajectory simulation are due to the weights of the various components of the parachute-load system, the aerodynamic tangent and normal forces and aerodynamic moment due to the parachute, the aerodynamic drag force on the load, and the force due to the acceleration of the included mass and the effect of the apparent mass of the parachute. The lengths ℓ_1, ℓ_2, and ℓ_3 from the system mass center to the load, parachute center of volume, and moment center, respectively, are signed quantities, the positive direction coinciding with the positive Z-coordinate direction. These distances are functions of the air density, since the mass center position changes as the included mass changes. The aerodynamic normal force and the aerodynamic moment due to the parachute act at the moment center, which is defined as a point located a distance equal to D_o ahead of the canopy skirt. Thus the length ℓ_1 is always positive, ℓ_2 is always negative, and ℓ_3 can conceivably have either sign.

The force required to accelerate the included mass and the effect of the apparent mass are given by

$$\underline{F} = -(m_a + m_i)\frac{d}{dt}(\underline{v}_p) \tag{93}$$

assuming that the apparent mass has the same value in each of the coordinate directions. The acceleration of the parachute center of volume is given by

$$\frac{d}{dt}(\underline{v}_p) = \left(\frac{d\underline{v}_p}{dt}\right)_{XYZ} + \underline{\omega} \times \underline{v}_p \tag{94}$$

The components of the forces for the two-dimensional case can then be written as

$$\Sigma F_x = -(m_\ell + m_{ss} + m_p)\, g \sin\theta + F_N + D_\ell \sin\alpha_\ell - (m_i + m_a)\left[(\dot{U} + QW) + \dot{Q}\ell_2\right] \tag{95}$$

$$\Sigma F_z = (m_\ell + m_{ss} + m_p)\, g \cos\theta - T - D_\ell \cos\alpha_\ell - (m_i + m_a)\left[(\dot{W} - QU) - Q^2 \ell_2\right] \tag{96}$$

If the moment of inertia tensor is defined such that it includes the effect of the apparent and included mass, i.e.

$$\underline{\underline{I}} = \underline{\underline{I}}_a + \underline{\underline{I}}_{CM} \tag{97}$$

the moment due to the apparent force need not be considered. The moment in the two-dimensional case is then

$$\Sigma M = -(m_\ell \ell_1 + m_p \ell_2)\, g \sin\theta + D_\ell \sin\alpha_\ell\, \ell_1 + F_N \ell_3 + M_{AY} \tag{98}$$

The masses of the risers, suspension lines, bridle, etc., are neglected in the formulation of the moment (98).

Using the definition of total mass employed in the inflation analysis

$$m_T = m_\ell + m_{ss} + m_p + m_i + m_a \tag{99}$$

the equations of motion (87) through (89) can be written in terms of equations for the derivatives of the velocity and angular velocity components in the body-fixed coordinate system. This formulation is

$$\dot{U} = -\left(\frac{m_\ell + m_{ss} + m_p}{m_T}\right) g \sin\theta + \frac{F_N}{m_T} + \frac{D_\ell}{m_T} \sin\alpha_\ell - \left(\frac{m_i + m_a}{m_T}\right) \ell_2 \dot{Q} - QW \tag{100}$$

$$\dot{W} = \left(\frac{m_\ell + m_{ss} + m_p}{m_T}\right) g \cos\theta - \frac{T}{m_T} - \frac{D_\ell}{m_T}\cos\alpha_\ell \tag{101}$$

$$-\left(\frac{m_\ell + m_a}{m_T}\right) \ell_2 Q^2 + QU$$

$$\dot{Q} = \frac{(m_\ell \ell_1 + m_p \ell_2)\, g \sin\theta}{I_{YY}} + \frac{D_\ell \ell_1 \sin\alpha_\ell}{I_{YY}} \tag{102}$$

$$+ \frac{F_N \ell_3}{I_{YY}} + \frac{M_{AY}}{I_{YY}}$$

The six equations (100), (101), (102), (90), (91), and (92) then form a system of first order differential equations which completely describe the parachute-load system.

The aerodynamic forces and moments are given by

$$T = \tfrac{1}{2}\rho v_p^2 C_{T_0} S_0 \tag{103}$$

$$F_N = \tfrac{1}{2}\rho v_p^2 C_{N_0} S_0 \tag{104}$$

$$M_A = \tfrac{1}{2}\rho v_p^2 C_{M_0} S_0 D_0 \tag{105}$$

$$D_\ell = \tfrac{1}{2}\rho v_\ell^2 C_D S_\ell \tag{106}$$

The velocities of the load and parachute are found from

$$v_\ell^2 = W^2 + (U + Q\ell_1)^2 \tag{107}$$

$$V_p^2 = W^2 + (U + Q\,\ell_2)^2 \tag{108}$$

and the angles of attack of the parachute and load are

$$\alpha_\ell = \tan^{-1}\left[-\frac{U + Q\,\ell_1}{W}\right] \tag{109}$$

$$\alpha_p = \tan^{-1}\left[-\frac{U + Q\,\ell_2}{W}\right] \tag{110}$$

The angle α_p is required since the coefficients C_{T_o}, C_{N_o}, and C_{M_o} are dependent on the parachute angle of attack.

The lengths ℓ_1, ℓ_2, and ℓ_3 are found from the geometry of the parachute-load system. Figure 13 shows the profile of a parachute-load system in the XZ-plane, which is defined as the plane of symmetry for a general parachute-load system. The distances s_1, s_2, s_3, s_4, and s_5 are reference distances from the canopy skirt to the centers of mass of the suspension lines, risers, riser extensions, bridle, and load, respectively, and s_c is the distance to the parachute center of volume. If all these distances, as well as the volume V of the inflated parachute canopy and the masses of the suspension lines, risers, riser extensions, bridle, and load are known, the parachute-load system mass center location can be determined for any value of the air density. The distance of the mass center from the canopy skirt is then given by

$$\bar{s} = \frac{m_{L_s} s_1 + m_R s_2 + m_E s_3 + m_{Br} s_4 + m_\ell s_5 - m_p s_c - m_i s_c}{m_\ell + m_{ss} + m_p + m_i} \tag{111}$$

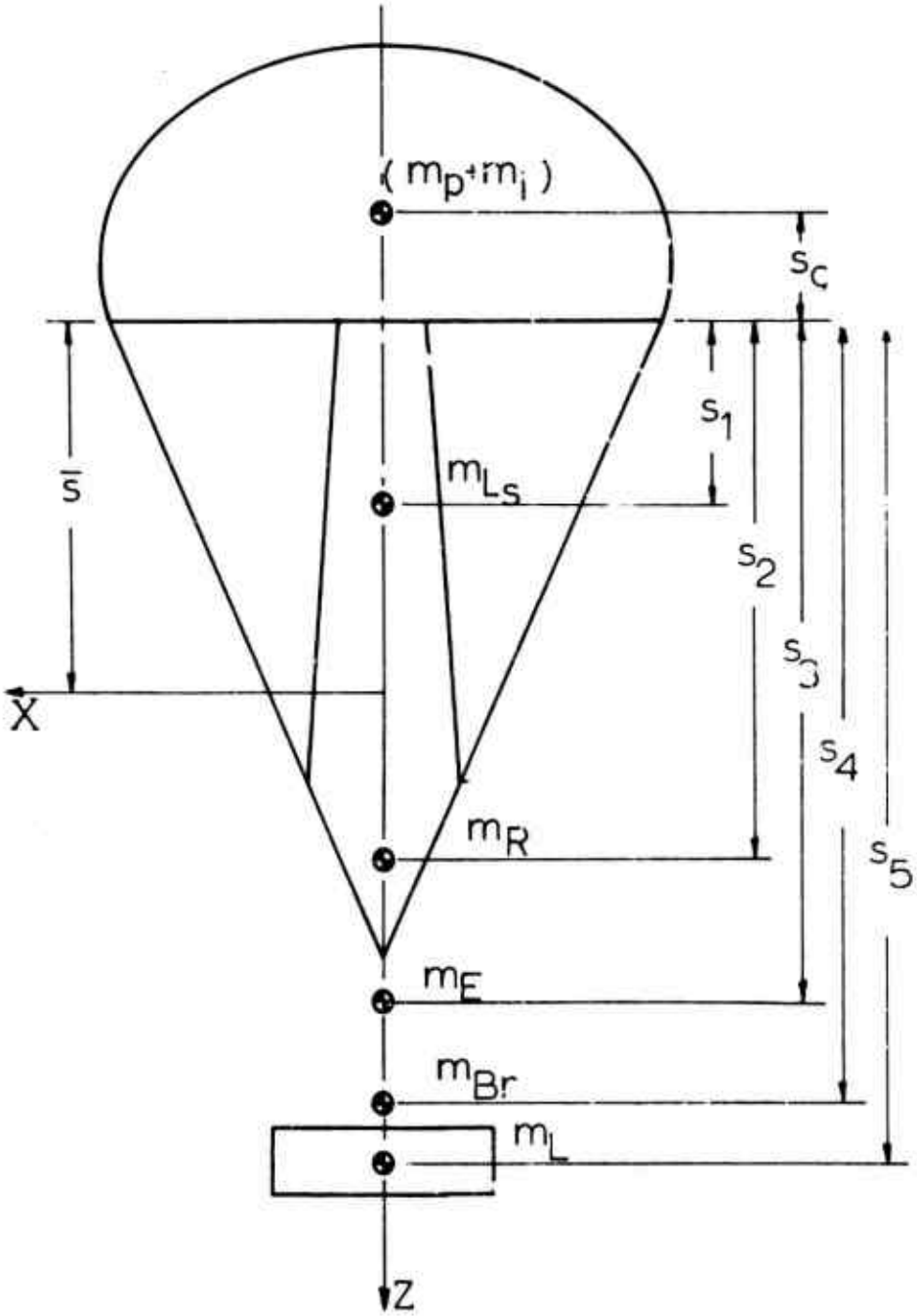

Fig 13 Profile View of Parachute Load System in the X-Z Plane

where

$$m_i = \rho V \tag{112}$$

It is assumed that the values of s_1, s_2, s_3, s_4, s_5, and s_c do not change during the free descent phase. Thus the lengths from the system mass center are

$$\ell_1 = (s_5 - \bar{s}) \tag{113}$$

$$\ell_2 = -\bar{s} - s_c \tag{114}$$

$$\ell_3 = D_o - \bar{s} \tag{115}$$

An approximation to the moment of inertia of the parachute-load system about the Y axis is

$$I_{YY} = I_Y + I_a \tag{116}$$

where

$$\begin{aligned} I_Y = {} & m_p \ell_2^2 + m_{L_s}(s_1 - \bar{s})^2 + m_R(s_2 - \bar{s})^2 \\ & + m_{\equiv}(s_3 - \bar{s})^2 + m_{Br}(s_4 - \bar{s})^2 + m_\ell \ell_1^2 \end{aligned} \tag{117}$$

and

$$I_a = (0.252)\frac{4\pi}{3}\rho\left(\frac{D_{p_{max}}}{2}\right)^3 \ell_2^2 \tag{118}$$

The relation (118) is based on Ref 11 with the coefficient 0.252 selected for a solid flat circular parachute. The apparent mass is assumed to be given by

$$m_a = \frac{3}{8} m_i \tag{119}$$

which results from Eqns (43) and (44) when $D_p = D_{P_{max}}$.

Thus all information is available for the solution of the equations governing the motion of the system during the free descent phase of the trajectory simulation. Once the equations are solved for U, W, Q, θ, x, and z, further information can be readily obtained. In particular, the position, velocity, and acceleration of the load relative to the space-fixed coordinate system are given by

$$r_{\ell_x} = x + \ell_1 \sin\theta \tag{120}$$

$$r_{\ell_z} = z + \ell_1 \cos\theta \tag{121}$$

$$v_{\ell_x} = (U + Q\ell_1)\cos\theta + W\sin\theta \tag{122}$$

$$v_{\ell_z} = -(U + Q\ell_1)\sin\theta + W\cos\theta \tag{123}$$

$$a_{\ell_x} = (\dot{U} + QW + \dot{Q}\ell_1)\cos\theta + (\dot{W} - QU - Q^2\ell_1)\sin\theta \tag{124}$$

$$a_{\ell_z} = -(\dot{U} + QW + \dot{Q}\ell_1)\sin\theta + (\dot{W} - QU - Q^2\ell_1)\cos\theta \tag{125}$$

b. Six Degrees of Freedom

For the general case, allowing six degrees of freedom for the parachute-load system during the free descent phase, the equations describing the system are far more complicated than those for three degrees of freedom. The external forces and moments are indicated in Fig 14.

In order to express the forces and moments in the body-fixed system it is convenient to define the following angles:

$$\alpha_\ell = \tan^{-1} - \left[\frac{U + Q\ell_1}{W}\right] \tag{126}$$

$$\beta_\ell = \tan^{-1}\left[\frac{V - P\ell_1}{W}\right] \tag{127}$$

$$\alpha_p = \tan^{-1}\left[-\frac{U + Q\ell_2}{W}\right] \tag{128}$$

$$\beta_p = \tan^{-1}\left[\frac{V - P\ell_2}{W}\right] \tag{129}$$

$$\gamma_\ell = \tan^{-1}\left\{\frac{V - P\ell_1}{\left[(U + Q\ell_1)^2 + W^2\right]^{1/2}}\right\} \tag{130}$$

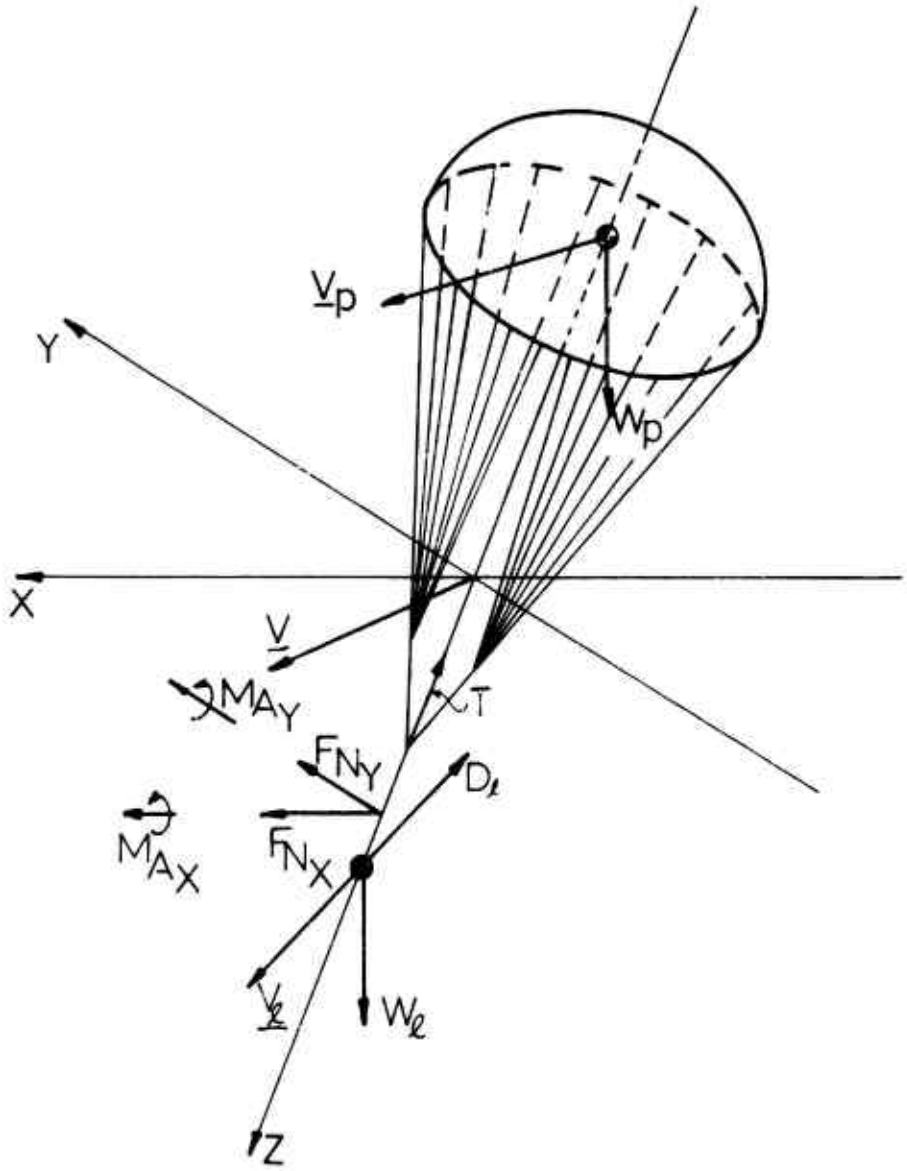

Fig 14 External Forces and Moments Acting on the Parachute - Load System

$$\delta_\ell = \tan^{-1}\left\{\frac{V + Q\ell_1}{\left[(V - P\ell_1)^2 + W^2\right]^{1/2}}\right\} \tag{131}$$

where the subscripts ℓ and p refer to the load and the parachute center of volume, respectively. The angles α_ℓ and α_p are the same angles of attack in the XZ-plane as discussed previously. The angles β_ℓ and β_p, analagously, are angles of attack in the YZ-plane. The angles γ_ℓ and δ_ℓ represent the angles between the load velocity and the XZ- and YZ-planes, respectively.

The force required to accelerate the included mass and the effect of the apparent mass are given by Eqn (93) and the forces and moments are

$$\begin{aligned}\Sigma F_X = {} & (m_\ell + m_{ss} + m_p)\, g\, a_{31} + F_{NX} \\ & + D_\ell \cos\gamma_\ell \sin\alpha_\ell - (m_i + m_a)\cdot \\ & \left[\dot{U} + QW - RV + \ell_2(\dot{Q} + PR)\right]\end{aligned} \tag{132}$$

$$\begin{aligned}\Sigma F_Y = {} & (m_\ell + m_{ss} + m_p)\, g\, a_{32} + F_{NY} \\ & - D_\ell \cos\delta_\ell \sin\beta_\ell - (m_i + m_a)\cdot \\ & \left[\dot{V} + RU - PW - \ell_2(\dot{P} - QR)\right]\end{aligned} \tag{133}$$

$$\begin{aligned}\Sigma F_Z = {} & (m_\ell + m_{ss} + m_p)\, g\, a_{33} - T - D_\ell \cos\gamma_\ell \cos\alpha_\ell \\ & - (m_i + m_a)\left[\dot{W} + PV - QU - \ell_2(P^2 + Q^2)\right]\end{aligned} \tag{134}$$

$$\Sigma L = -g\, a_{32}(m_p l_2 + m_l l_1) - F_{NY}\, l_3 + D_l\, l_1 \cos\delta_l \sin\beta_l + M_{AX} \tag{135}$$

$$\Sigma M = g\, a_{31}(m_p l_2 + m_l l_1) + F_{NX}\, l_3 + D_l\, l_1 \cos\gamma_l \sin\alpha_l + M_{AY} \tag{136}$$

$$\Sigma N = M_c \tag{137}$$

where M_c is a control or turning moment applied to the system. Arranging the equations of motion as equations for the time derivatives of U, V, W, P, Q, and R, we have

$$\dot{U} = \left(\frac{m_l + m_{ss} + m_p}{m_T}\right) g\, a_{31} + \frac{F_{NX}}{m_T} + \frac{D_l}{m_T} \cos\gamma_l \sin\alpha_l - \frac{m_i + m_a}{m_T}\, l_2 (\dot{Q} + PR) - QW + RV \tag{138}$$

$$\dot{V} = \left(\frac{m_l + m_{ss} + m_p}{m_T}\right) g\, a_{32} + \frac{F_{NY}}{m_T} - \frac{D_l}{m_T} \cos\delta_l \sin\beta_l + \frac{m_i + m_a}{m_T}\, l_2 (\dot{P} - QR) - RU + PW \tag{139}$$

$$\dot{W} = \frac{m_\ell + m_{33} + m_p}{m_T} g a_{33} - \frac{T}{m_T} - \frac{D_\ell}{m_T} \cos\gamma_\ell \cos\alpha_\ell$$

$$+ \frac{m_\ell + m_a}{m_T} \ell_2 (P^2 + Q^2) - PV + QU \tag{140}$$

$$\dot{P} = - \frac{g a_{32}(m_p \ell_2 + m_\ell \ell_1)}{I_{XX}} - \frac{F_{NY} \ell_3}{I_{XX}} + \frac{D_\ell \ell_1}{I_{XX}} \cdot$$

$$\cos\delta_\ell \sin\beta_\ell + \frac{M_{AX}}{I_{XX}} + \dot{R} \frac{I_{XZ}}{I_{XX}} - QR\left(\frac{I_{ZZ} - I_{YY}}{I_{XX}}\right) \tag{141}$$

$$+ PQ \frac{I_{XZ}}{I_{XX}}$$

$$\dot{Q} = \frac{g a_{31}(m_p \ell_2 + m_\ell \ell_1)}{I_{YY}} + \frac{F_{NX} \ell_3}{I_{YY}} + \frac{D_\ell \ell_1}{I_{YY}} \cos\gamma_\ell \cdot$$

$$\sin\alpha_\ell + \frac{M_{AY}}{I_{YY}} - PR\left(\frac{I_{XX} - I_{ZZ}}{I_{YY}}\right) - (P^2 - R^2) \frac{I_{XZ}}{I_{YY}} \tag{142}$$

$$\dot{R} = \frac{M_c}{I_{ZZ}} + \dot{P} \frac{I_{XZ}}{I_{ZZ}} - PQ \frac{I_{YY} - I_{XX}}{I_{ZZ}} - QR \frac{I_{XZ}}{I_{ZZ}} \tag{143}$$

making use of the fact that all parachutes are bilaterally symmetric and hence (choosing the XZ-plane as the plane of symmetry) $I_{XY} = I_{YZ} = 0$. For most parachutes, it is also true that the XYZ-axes are the principal axes, so that $I_{XZ} = 0$, and $I_{XX} = I_{YY}$. Equations (141) through (143) are left in the general form, however, and are thus applicable to any

parachute. Equations (137) through (142) and (81) through (86) then form a system of twelve differential equations which can be solved for U, V, W, P, Q, R, ψ, θ, φ, x, y, and z, thus completely describing the velocity and angular velocities as well as the Euler angles and location of the parachute-load system.

The parachute aerodynamic forces and moments and the drag of the load are given by

$$T = \frac{1}{2} \rho v_p^2 C_{T_0} S_0 \tag{144}$$

$$F_{NX} = \frac{1}{2} \rho v_p^2 C_{NX_0} S_0 \tag{145}$$

$$F_{NY} = \frac{1}{2} \rho v_p^2 C_{NY_0} S_0 \tag{146}$$

$$M_{AX} = \frac{1}{2} \rho v_p^2 C_{MX_0} S_0 \tag{147}$$

$$M_{AY} = \frac{1}{2} \rho v_p^2 C_{MY_0} S_0 \tag{148}$$

$$D_\ell = \frac{1}{2} \rho v_\ell^2 C_0 S_\ell \tag{149}$$

where

$$v_\ell^2 = (U + Q\ell_1)^2 + (V - P\ell_1)^2 + W^2 \tag{150}$$

$$v_p^2 = (U + Q\ell_2)^2 + (V - P\ell_2)^2 + W^2 \tag{151}$$

Again, the coefficients in Eqns (144) through (148) depend on the angles of attack α_p and β_p.

Since the XZ-plane is a plane of symmetry, the lengths ℓ_1, ℓ_2, ℓ_3, and the value of I_{YY} are found in the same manner as for three degrees of freedom, with Eqns (113) through (116). In general, the values of I_{XX}, I_{ZZ}, and I_{XZ} are not given by such a simple approximation, but depend on the particular parachute-load system. As discussed previously, it is often the case that $I_{XX} = I_{YY}$ and $I_{XZ} = 0$, but even in this case the value of I_{ZZ} must be formulated for the general six degree of freedom system.

Once the equations have been solved for U, V, W, P, Q, R, ψ, θ, φ, x, y, and z, which are related to the mass center, the position, velocity, and acceleration of the load are given by

$$r_{\ell_x} = x + \ell_1 a_{13} \tag{152}$$

$$r_{\ell_y} = y + \ell_1 a_{23} \tag{153}$$

$$r_{\ell_z} = z + \ell_1 a_{33} \tag{154}$$

$$v_{\ell_x} = (U + Q\ell_1)\, a_{11} + (V - P\ell_1)\, a_{12} + W a_{13} \tag{155}$$

$$v_{\ell_y} = (U + Q\ell_1)\, a_{21} + (V - P\ell_1)\, a_{22} + W a_{23} \tag{156}$$

$$v_{\ell_z} = (U + Q\ell_1)\, a_{31} + (V - P\ell_1)\, a_{32} + W a_{33} \tag{157}$$

$$\begin{aligned} a_{\ell_x} = {} & (\dot{U} + QW - RV + \dot{Q}\ell_1 + PR\ell_1)\, a_{11} + (\dot{V} + RU \\ & - PW - \dot{P}\ell_1 + QR\ell_1)\, a_{12} + [\dot{W} + PV - QU \\ & - (P^2 + Q^2)\ell_1]\, a_{13} \end{aligned} \tag{158}$$

$$a_{l_y} = (\dot{U} + QW - RV + \dot{Q}l_1 + PRl_1)\,a_{21} + (\dot{V} + RU - PW - \dot{P}l_1 + QRl_1)\,a_{22} + [\dot{W} + PV - QU - (P^2 + Q^2)l_1]\,a_{23} \tag{159}$$

$$a_{l_z} = (\dot{U} + QW - RV + \dot{Q}l_1 + PRl_1)\,a_{31} + (\dot{V} + RU - PW - \dot{P}l_1 + QRl_1)\,a_{32} + [\dot{W} + PV - QU - (P^2 + Q^2)l_1]\,a_{33} \tag{160}$$

The numerical solution of these equations then represent the desired information concerning the characteristics of the descent trajectory of the suspended load allowing six degrees of freedom of the parachute-load system.

2. Summary of Assumptions for the Free Descent Phase

In summary, the model for the free descent phase includes the following assumptions. (1) The parachute-load system can be described as a rigid body whose shape does not change as the center of mass location changes due to change in air density. (2) The aerodynamics of the parachute can be fully described by a tangent force and by normal forces and aerodynamic moments acting at the moment center. (3) The aerodynamics of the load are described sufficiently by the drag force. (4) The moments about the center of mass due to the suspension lines, risers, extensions, and bridle are negligible, although their masses are included in calculation of the center of mass position and the moment of inertia about the Y-axis. (5) The apparent moment of inertia can be sufficiently approximated with a coefficient measured for models of a solid flat circular parachute, and the apparent mass is the same in any direction.

IV. NUMERICAL TRAJECTORY CALCULATIONS OF SEVERAL PARACHUTE-LOAD SYSTEMS

In the preceding Sections II and III, various mechanical arrangements of different parachute systems and their functioning are described and the governing equations established. In view of the overall objective of this study a continuous computer program incorporating all phases of the functioning of the various parachute-load systems was developed. This program is based on the equations shown in Section III.

In order to check the functioning of this program and to obtain results which can be compared to a certain extent with field test observations, a number of total trajectory simulations were carried out. The results of these calculations and details of the systems for which the simulations were made will be shown later.

At this time it may be stated merely that the program works and that the results compare favorably with field test observations. However, before reviewing these total trajectory simulations it appears to be advisable to discuss the more general inputs to the governing equations.

A. Steady State Canopy Volume and Geometry

For the trajectory simulations, certain assumptions were made concerning the shape of the parachute canopy during the free descent phase. In accordance with Ref 11, the volume of a fully inflated solid flat circular parachute is

$$V = (0.0667)\, D_o^3 \tag{161}$$

whereas the projected diameter of a fully inflated solid flat circular parachute amounts to

$$D_{p_{max}} = (0.648)\, D_o \tag{162}$$

as indicated in Ref 6. Assuming that the shape of the parachute is semi-ellipsoidal and the volume and major axis are given by (161) and (162), the distance to the parachute center of volume from the canopy skirt amounts to

$$s_c = (0.129)\, D_o \tag{163}$$

These values of V, $D_{p_{max}}$, and s_c were used in the trajectory simulations when the solid flat circular parachutes G-13, G-12D, and G-11A were used.

For the extended skirt parachute, type T-10, it was assumed that (161) is valid, whereas measurements of photographs from Ref 13, combined with the assumption of a semi-ellipsoidal canopy give for the diameter and the mass center distance

$$D_{p_{max}} = (0.686)\, D_o \tag{164}$$

$$s_c = (0.133)\, D_o \tag{165}$$

The geometry of the parachute-load suspension system is defined by the value of $D_{p_{max}}$, the lengths of the suspension lines, risers, extensions and bridle, and the load dimensions. This allows the determination of the distances s_1 through s_5, and together with s_c and the masses of the components of each parachute-load system all data for determination of the various lengths ℓ_1, ℓ_2, ℓ_3, and the moment of inertia I_{YY} are known, provided that the free descent phase is constrained to three degrees of freedom. For the more general case of six

degrees of freedom, the only additional requirement is sufficient data to calculate the moment of inertia about the Z-axis, I_{ZZ}, since for the T-10 and solid flat circular parachutes the moment of inertia $I_{XX} = I_{YY}$ and the product of inertia I_{XZ} vanishes.

Further details of the calculation of inputs to the trajectory simulation program are discussed in Volume II of this report.

B. Aerodynamic Coefficients

The remaining information necessary for the trajectory simulation are the aerodynamic coefficients for the force and the moment for the T-10 and solid flat circular parachutes. Reference 14 presents in tables and graphs the results of recently conducted measurements, and these coefficients were used in the sample calculations.

The tangent force coefficient for the solid flat circular parachute, taken from Ref 14, can be approximated by the expression

$$\begin{aligned} C_{T_0} &= 0.647 - (1.2\times10^{-5})|\alpha_p| + (9.15\times10^{-4})|\alpha_p|^2 \\ &\quad - (7.13\times10^{-5})|\alpha_p|^3 + (1.33\times10^{-6})|\alpha_p|^4, \quad 0 \le |\alpha_p| < 30^\circ \\ C_{T_0} &= 0.620, \quad |\alpha_p| \ge 30^\circ \end{aligned} \tag{166}$$

Similarly, the tangent force coefficient for the T-10 parachute is approximately

$$\begin{aligned} C_{T_0} &= 0.570 - (2.48\times10^{-3})|\alpha_p| + (1.219\times10^{-3})|\alpha_p|^2 \\ &\quad - (7.687\times10^{-5})|\alpha_p|^3 + (1.2797\times10^{-6})|\alpha_p|^4, \\ &\qquad 0 \le |\alpha_p| < 30^\circ \\ C_{T_0} &= -.0032(|\alpha_p| - 30^\circ) + .553, \quad |\alpha_p| \ge 30^\circ \end{aligned} \tag{167}$$

The measured data points from Ref 14, and these approximate expressions are shown in Fig 15.

The aerodynamic moment coefficient for the solid flat circular parachute can be approximated by

$$C_{M_0} = (4.844 \times 10^{-3})\alpha_p - (3.94 \times 10^{-4})\alpha_p^2 + (1.043 \times 10^{-5})\alpha_p^3 - (1.32 \times 10^{-7})\alpha_p^4 \quad , \quad 0 \le \alpha_p < 30^\circ$$

$$C_{M_0} = -.0044\,(\alpha_p - 30^\circ) - .034, \quad \alpha_p \ge 30^\circ \tag{168}$$

and for the T-10 parachute by

$$C_{M_0} = (1.845 \times 10^{-2})\alpha_p - (1.929 \times 10^{-3})\alpha_p^2 - (6.78 \times 10^{-5})\alpha_p^3 - (8.709 \times 10^{-7})\alpha_p^4, \quad 0 \le \alpha_p < 30^\circ$$

$$C_{M_0} = -.0060\,(\alpha_p - 30^\circ) - .056, \quad \alpha_p \ge 30^\circ \tag{169}$$

Moment coefficient data points, Ref 14, and their approximations are shown in Fig 16.

Finally, the normal force coefficients for the solid flat circular parachute can be approximated by

$$C_{N_0} = -(6.74 \times 10^{-3})\alpha_p + (5.57 \times 10^{-4})\alpha_p^2 - (1.53 \times 10^{-5})\alpha_p^3 + (1.9 \times 10^{-7})\alpha_p^4 \quad , \quad 0 \le \alpha_p < 30^\circ$$

$$C_{N_0} = .0056\,(\alpha_p - 30^\circ) + .040, \quad \alpha_p \ge 30^\circ \tag{170}$$

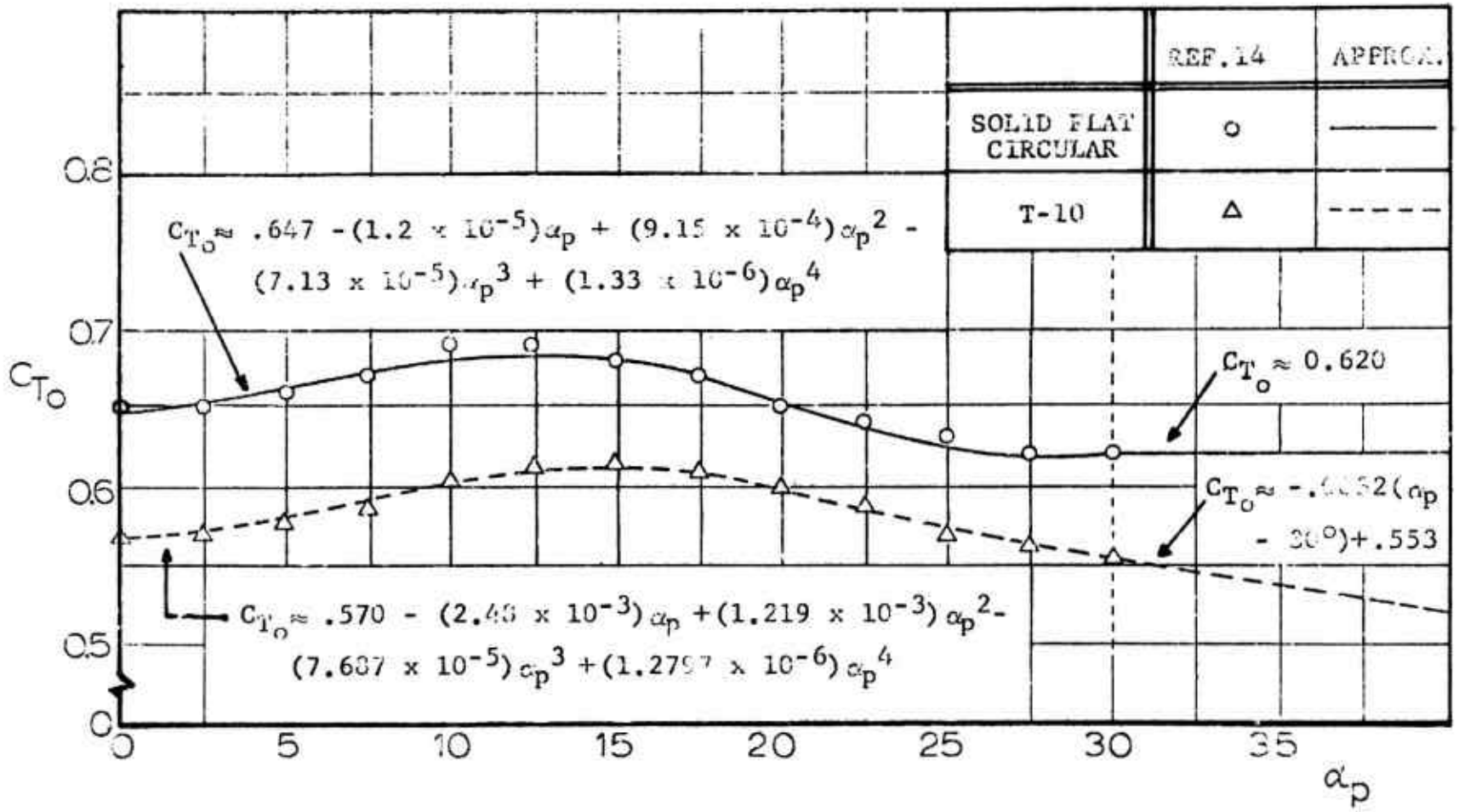

Fig 15 Tangent Force Coefficient vs Parachute Angle of Attack; Solid Flat Circular and T-10 Parachutes

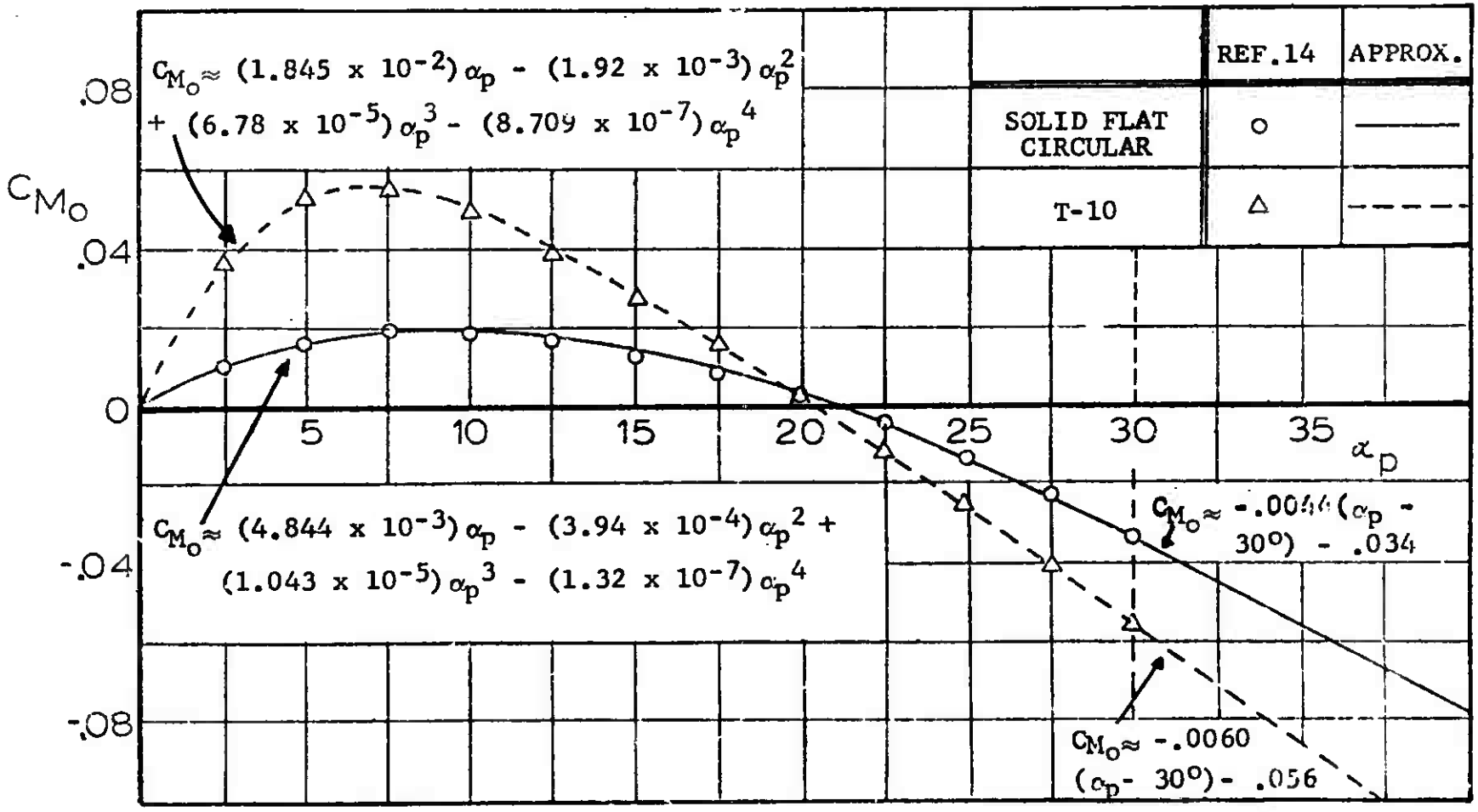

Fig 16 Moment Coefficient vs Parachute Angle of Attack; Solid Flat Circular and T-10 Parachutes

and for the T-10 parachute by

$$C_{N_o} = -(2.508 \times 10^{-2})\alpha_p + (1.95 \times 10^{-3})\alpha_p^2 - (6.022 \times 10^{-5})\alpha_p^3 + (6.827 \times 10^{-7})\alpha_p^4 \quad , \quad 0 \le \alpha_p < 30^\circ$$

$$C_{N_o} = .0072\ (\alpha_p - 30^\circ) + .064, \alpha_p \ge 30^\circ \tag{171}$$

Again, data points from Ref 14 and expressions (170) and (171) are shown in Fig 17. Because of the parachute symmetry, the signs of the coefficients of C_{N_o} and C_{M_o} are reversed for negative angles of attack.

It should be noted that the signs for the normal forces, Fig 12, and coefficients, Fig 16, are reversed from those shown in Refs 14 and 15 in order to arrange them in a standard right-hand coordinate system. This was done because it was necessary that in this trajectory simulation, all forces, moments, and angles follow a sign convention consistent with a right-hand coordinate system.

C. Examples of Total Trajectory Simulations

Once the governing equations had been formulated and the computer programming completed, several sets of input data were selected to provide a basis for debugging the program, demonstrating that all of the calculation methods function as intended, and, of course, to see if the results agreed reasonably well with field test experience. Five parachute-load systems were used with various release velocities, release altitudes, suspended loads, and main parachute reefings to give inputs for a data production run of 21 total trajectory

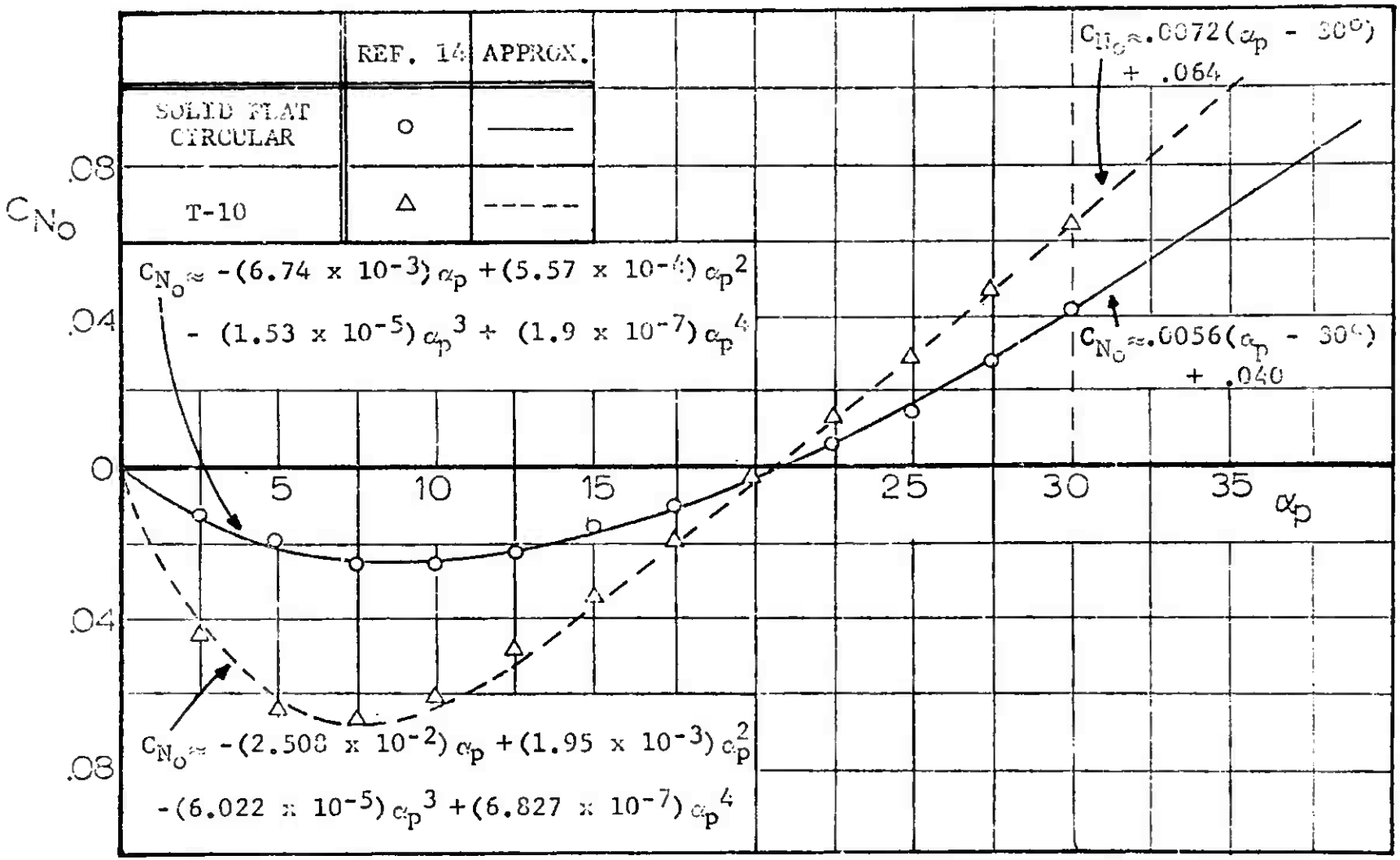

Fig 17 Normal Force Coefficient vs Parachute Angle of Attack; Solid Flat Circular and T-10 Parachutes

simulations specified by the procuring agency. The input data for these 21 cases is presented in detail in the Appendix. The data was not intended to provide the extensive parametric variations which would be needed to judge the accuracy of the calculations.

All of the sample calculations presented were constrained to three degrees of freedom, since no measurements of aerodynamic coefficients for a system allowing six degrees of freedom exist. However, one sample calculation was accomplished with six degrees of freedom using the same aerodynamic coefficients in the XZ- and YZ-planes. These functions were the same as those used with three degrees of freedom. Since no disturbance in the YZ-plane was introduced, the calculation gave results which remained two-dimensional and were exactly the same as for the calculation allowing only three degrees of freedom. This indicates that the total trajectory simulation with six degrees of freedom functions properly.

In the following, graphical and numerical results are presented for calculations for four separation-deployment methods, including one case with disreefing of the main parachute. Also, some results for the remainder of the 21 sample calculations are tabulated.

1. T-10 Parachute with Static Line System

The physical data for this calculation were from a T-10 personnel parachute, D_0 = 35 ft, with a suspended load of 250 lb. In this case it was released from an altitude of 6,000 ft at a speed of 220 ft/sec. The physical processes which occur throughout the airdrop for the static line system, followed by the particular Subsection or Part of this

report in which the modeling equations were developed, are: load falling away from aircraft, IIIC2, deployment of main parachute, IIID1, main parachute inflation, IIIE, and free descent, IIIF.

The trajectory variables of altitude loss, z, system angle, θ, horizontal velocity, and vertical velocity are plotted versus time in Figs 18 and 19. These show a system oscillation with a period of about 6 sec, which has to be expected since the T-10 is unstable at $\alpha_p = 0^o$. The small discontinuity in the curves at 3.2 sec is the result of changing from data at the mass center to data at the load center after full inflation. This discontinuity occurs in all cases, and becomes larger as the parachute-load system lengths increase. For this T-10 static line system there is no snatch force calculation, the unreefed filling time was 1.65 sec, and the maximum opening force was 1868 lb.

2. G-12D Cargo Parachute with Static Line Deployed Pilot Chute System.

The parachute-load system that provided the physical data for this calculation was a G-12D parachute with a suspended load of 2200 lb. The G-12D is a solid flat circular parachute, $D_o = 64$ ft, also unstable at $\alpha_p = 0^o$. The release conditions were again $h_o = 6{,}000$ ft, $v_o = 220$ ft/sec. The physical processes and modeling equations were : load falling away from aircraft, IIIC2, suspension system deployment, IIID2a, snatch force, IIID2b, main parachute unfolding, IIID2c, main parachute inflation, IIIE, free descent, IIIF.

The trajectory variables calculated for this case are shown in Figs 20 and 21. Again a damped oscillation is calculated, but with a system larger than the T-10 system, the period is about 8 sec. The figures show that this system is

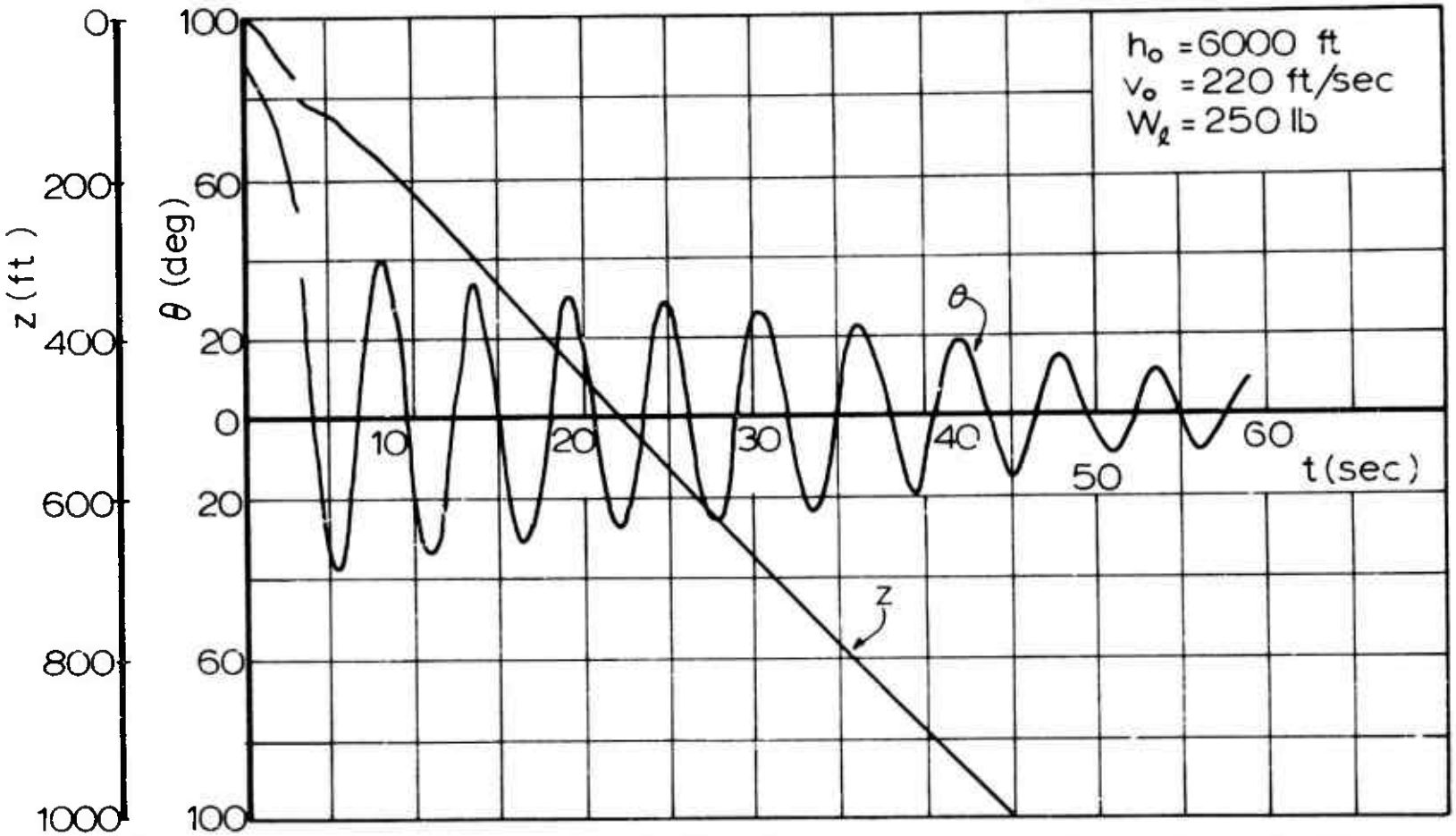

Fig 18 Altitude Loss and System Angle for the T-10 Parachute with Static Line System

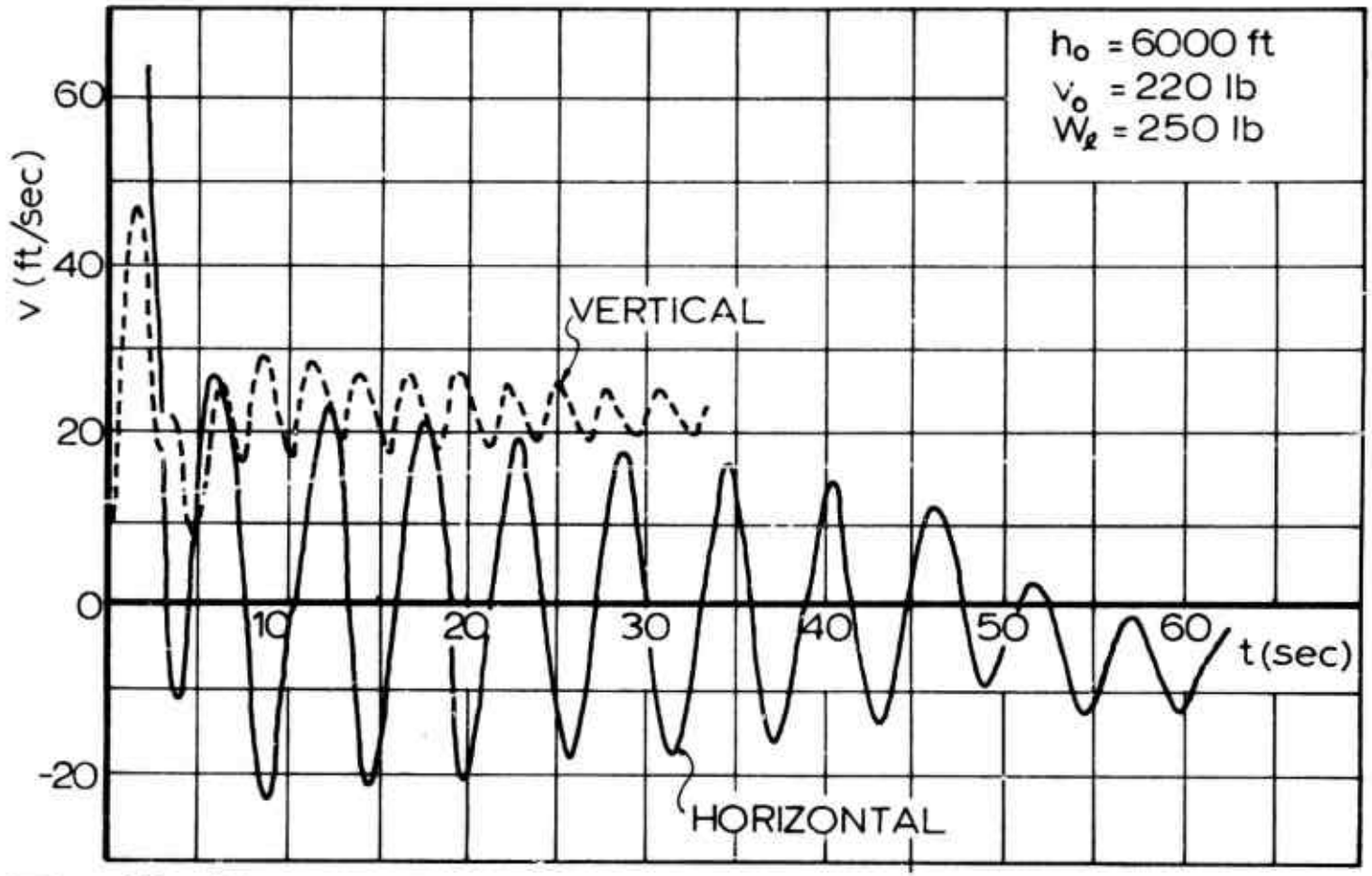

Fig 19 Horizontal and Vertical Velocities for the T-10 Parachute with Static Line System

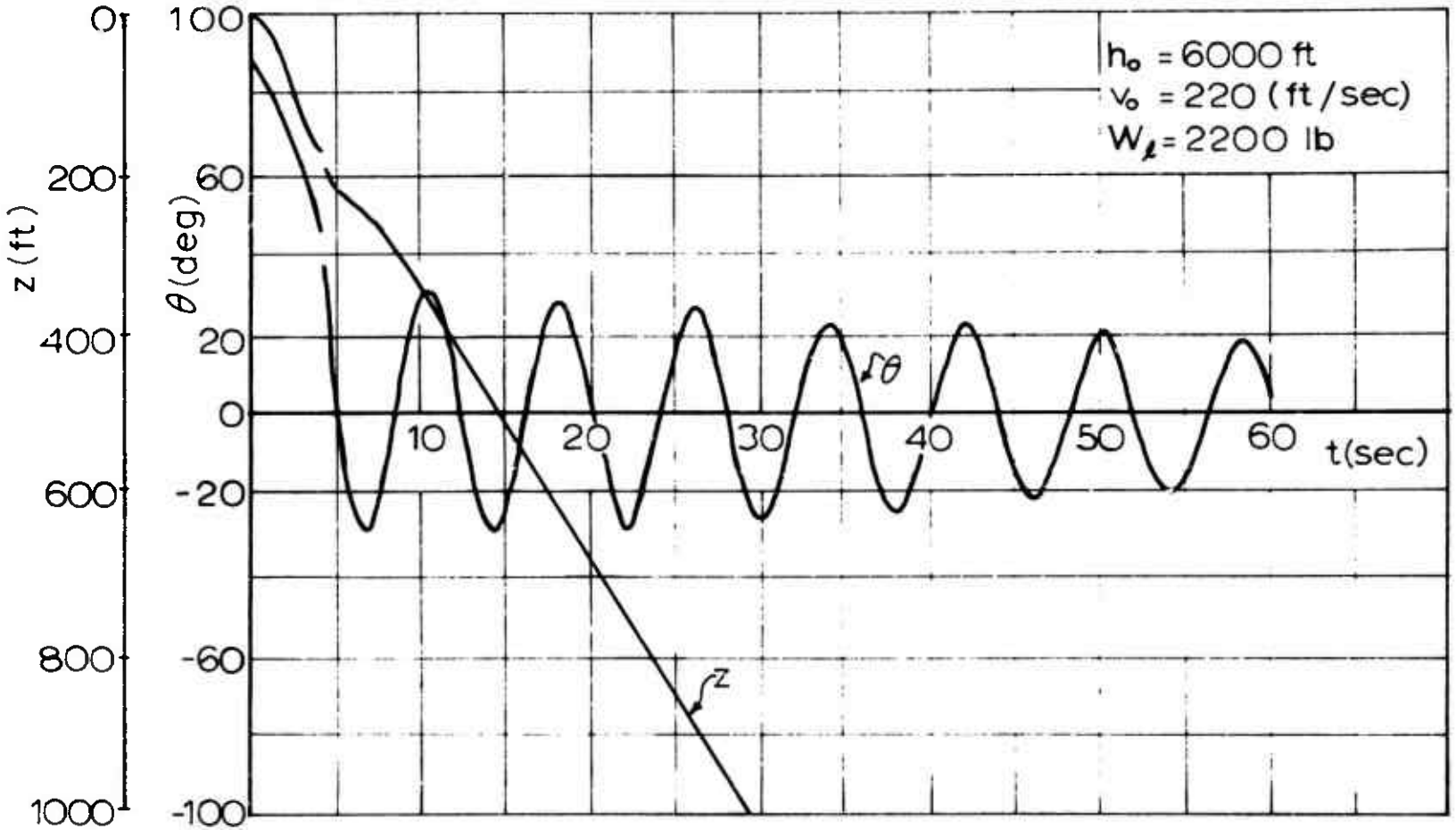

Fig 20 Altitude Loss and System Angle for the G-12D Cargo Parachute with Static Line Deployed Pilot Chute System

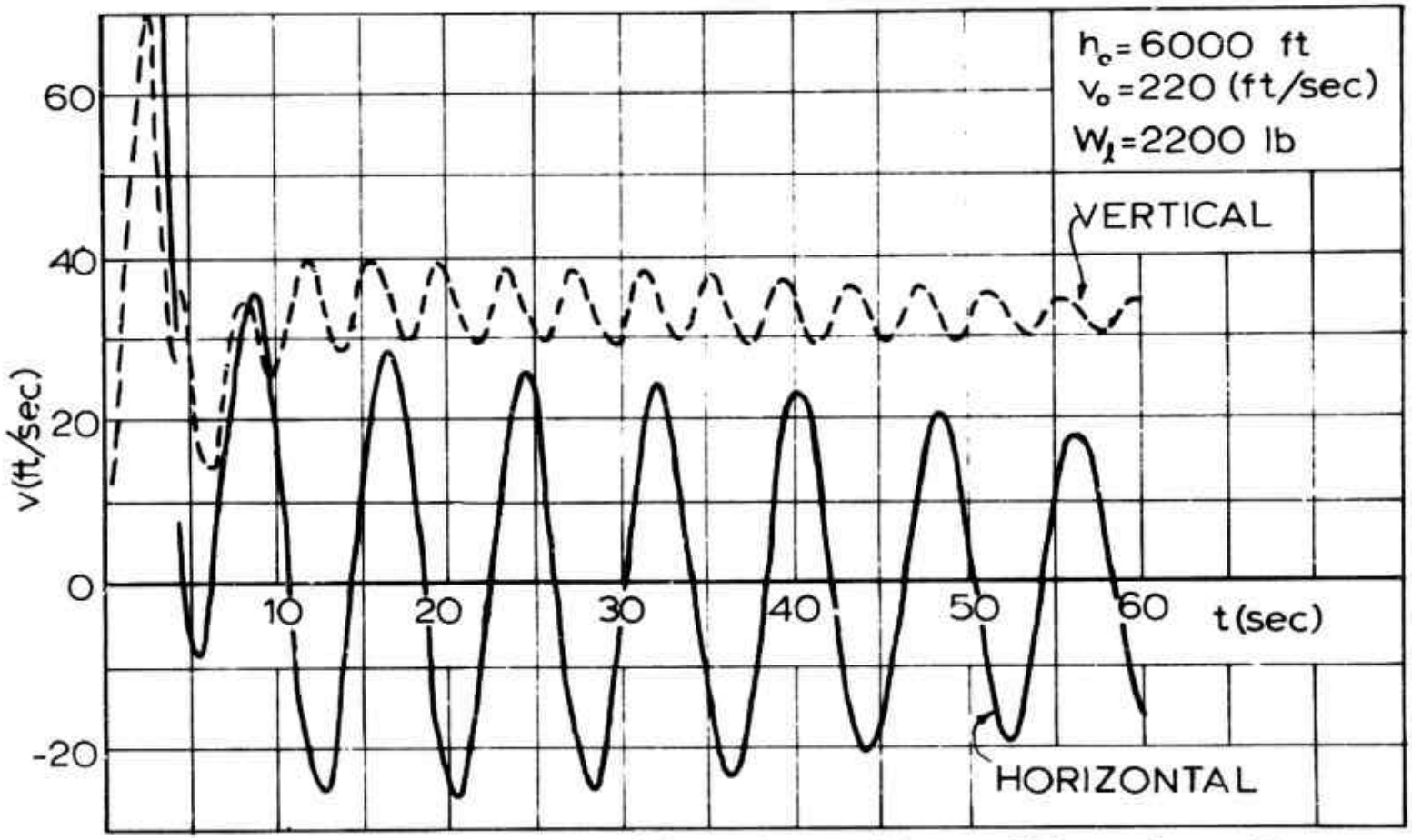

Fig 21 Horizontal and Vertical Velocities for the G-12D Cargo Parachute with Static Line Deployed Pilot Chute System

approaching a steady glide related to the parachute's stable angle of attack, as all systems did when given enough altitude. The snatch force was 8293 lb at a velocity of 197 ft/sec, the unreefed filling time was 1.65 secs, with a maximum opening force of 11,847 lb.

3. G-11A Cargo Parachute with Extraction Parachute System.

a. Unreefed Main Parachute Inflation

Data for this case was obtained from a G-11A parachute, D_o = 100 ft with a 3500 lb suspended load. The extraction parachute used was a 15 ft reefed ringslot parachute. The release conditions were h_o = 2,000 ft, v_o = 220 ft/sec. The physical processes and modeling equations were: extraction of load from aircraft, IIIC1, suspension system deployment, IIID2a, snatch force, IIID2b, main parachute unfolding, IIID2c, main parachute inflation, IIIE, and free descent, IIIF.

The trajectory variables, Figs 22 and 23, again show a damped oscillation with a period of 11 secs. The calculated snatch force was 2,357 lb at a velocity of 160 ft/sec, and the maximum opening force was 9,331 lb for an unreefed filling time of 5.41 sec.

b. Reefed Main Parachute Inflation

This calculation was made to demonstrate that reefed inflations could be modeled. The case presented here uses the same separation-deployment system and parachute-load system as discussed in the previous item. The release conditions were h_o = 2,000 ft, v_o = 169 ft/sec. This sample case represents a three stage reefed inflation with reefing

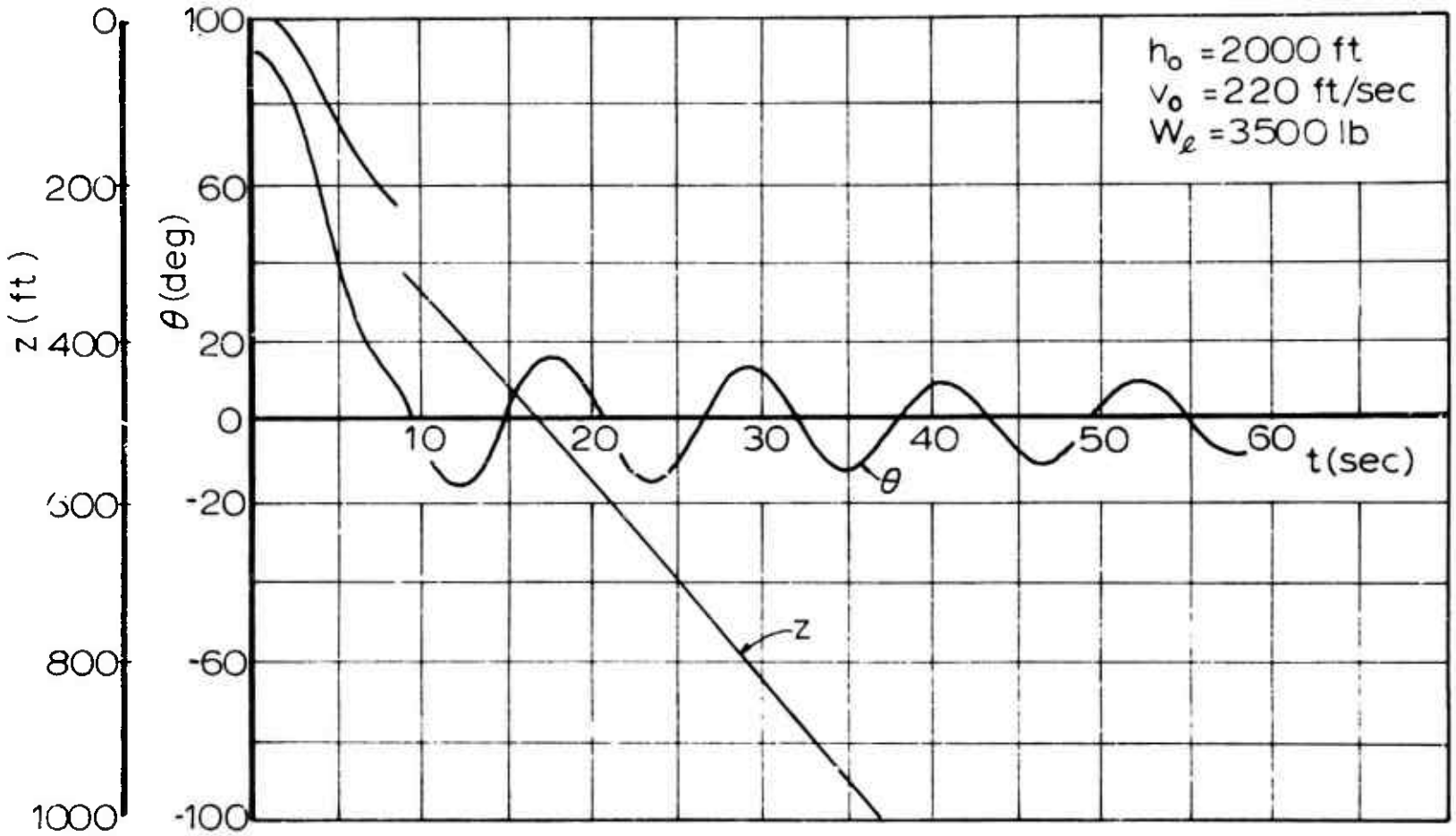

Fig 22 Altitude Loss and System Angle for the Unreefed G-11A Cargo Parachute with Extraction Parachute System

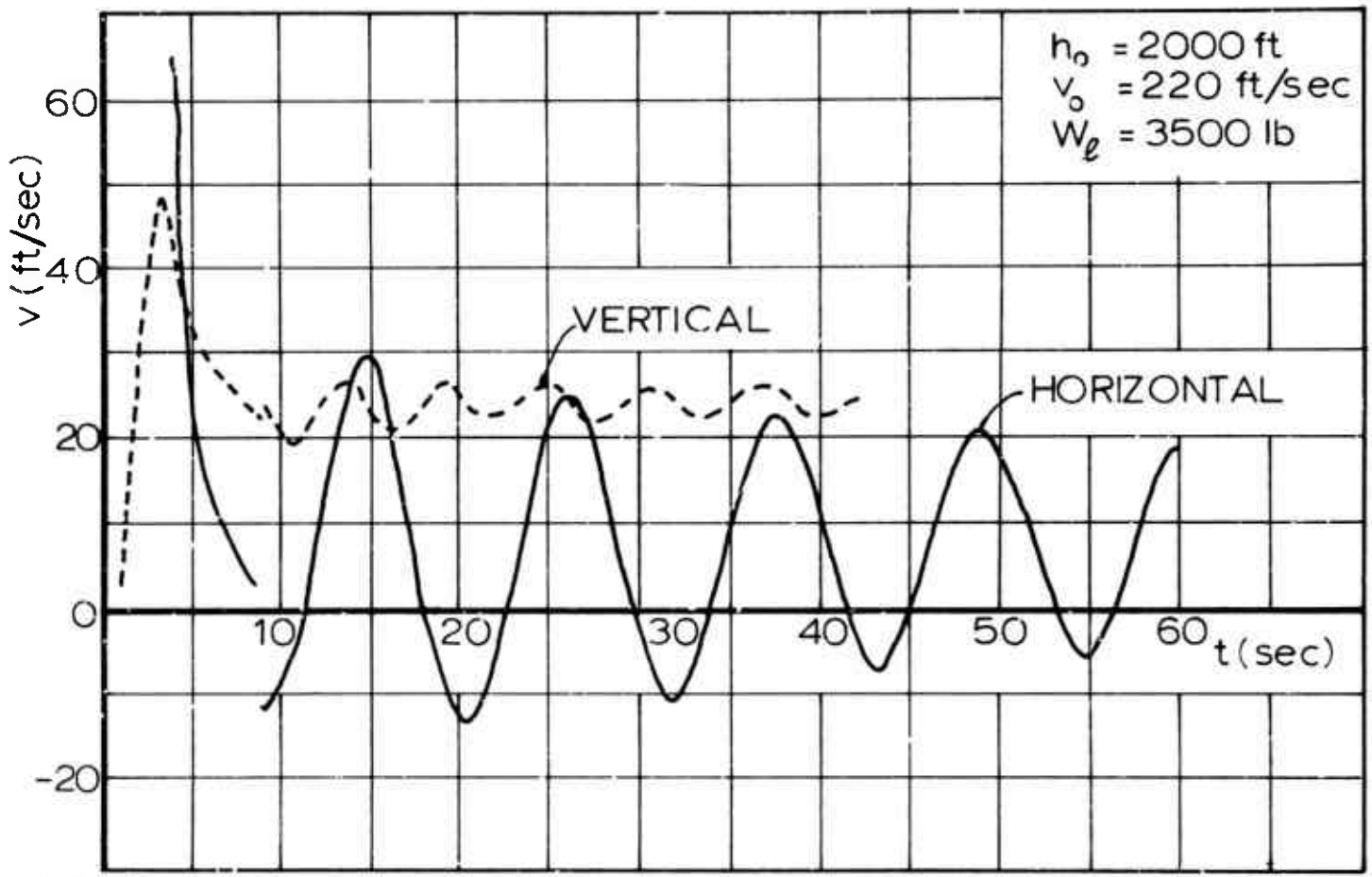

Fig 23 Horizontal and Vertical Velocities for the Unreefed G-11A Cargo Parachute with Extraction Parachute System

cutter delay times of 2 sec, 4 sec, and 6 sec after snatch force. The equations of subsection IIIB were used for the coasting periods of constant drag area between inflation stages.

Figures 24 and 25 present the trajectory variables, and again show a damped oscillation with an 11 sec period. It is interesting that the amplitude of the oscillations was considerably smaller than the unreefed G-11A. The snatch force was 2078 lb at a velocity of 130 ft/sec; the reefed inflation times, excluding cutter delays, were 1.68, 0.96, 0.72, and 4.01 sec with corresponding maximum forces of 3,062 lb, 5,667 lb, 6,032 lb, and 5,828 lb.

4. G-11A Cargo Parachute with Reefed Main Parachute Extraction System.

The physical data for this system came from a G-11A parachute with a 20-ft reefing line and a 3500 lb extracted and suspended load. The reefing line was cut 4 sec after the load was released in the aircraft. The release conditions were h_o = 2,000 ft, v_o = 220 ft/sec. This sample case has the following physical processes and modeling equations: extraction from aircraft, IIIC1, main parachute inflation, IIIE, and free descent IIIF.

The trajectory variables are presented in Figs 26 and 27 and were very similar to the other G-11A systems. The maximum opening force was 8,348 lb for a reefed inflation time of 5.12 sec.

5. Additional Calculations.

Tables I and II show numerical results for all of the 21 total trajectory calculations made, including those just discussed. Graphs like those presented previously were made

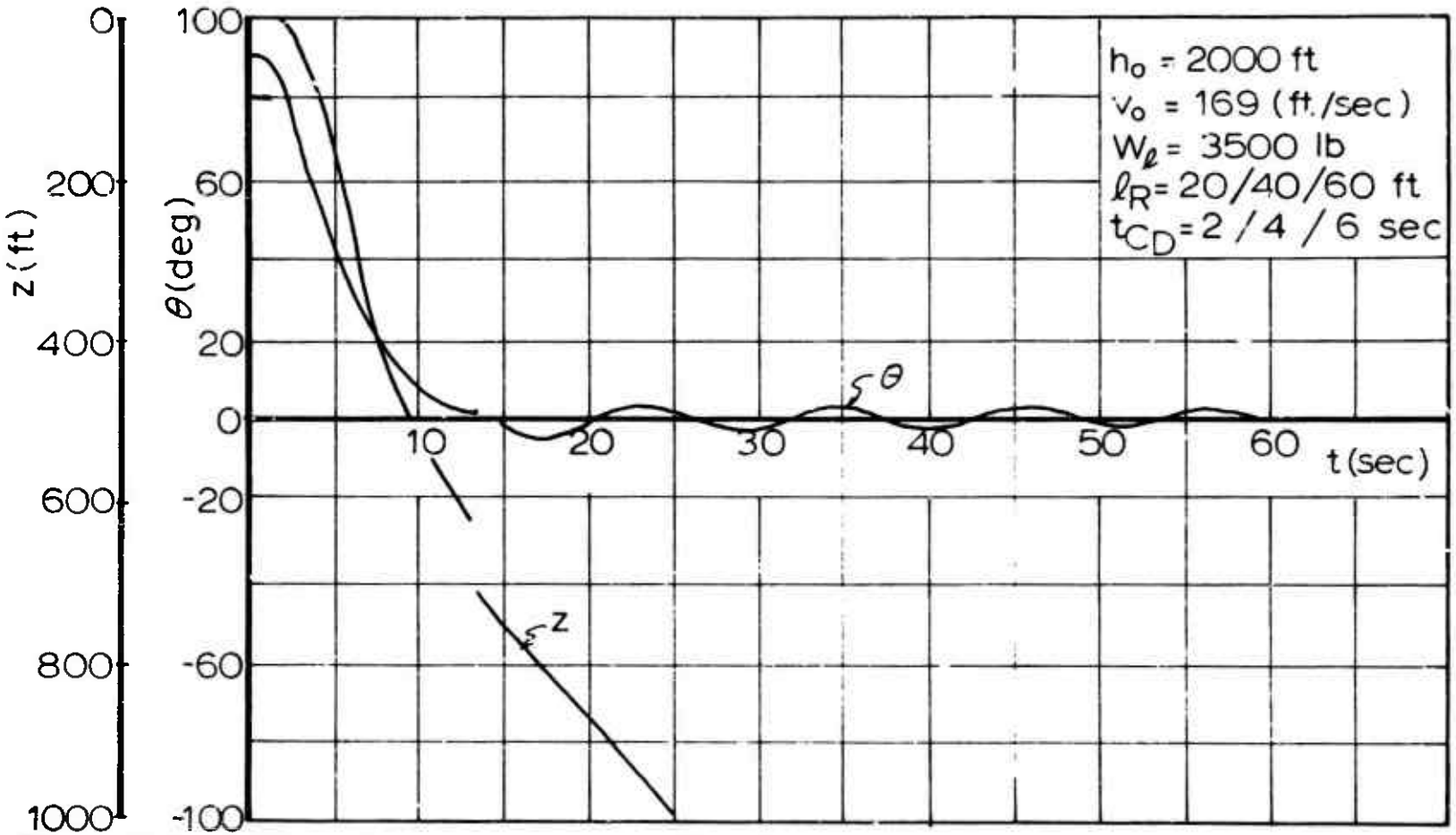

Fig 24 Altitude Loss and System Angle for the Reefed G-11 A Cargo Parachute with Extraction Parachute System

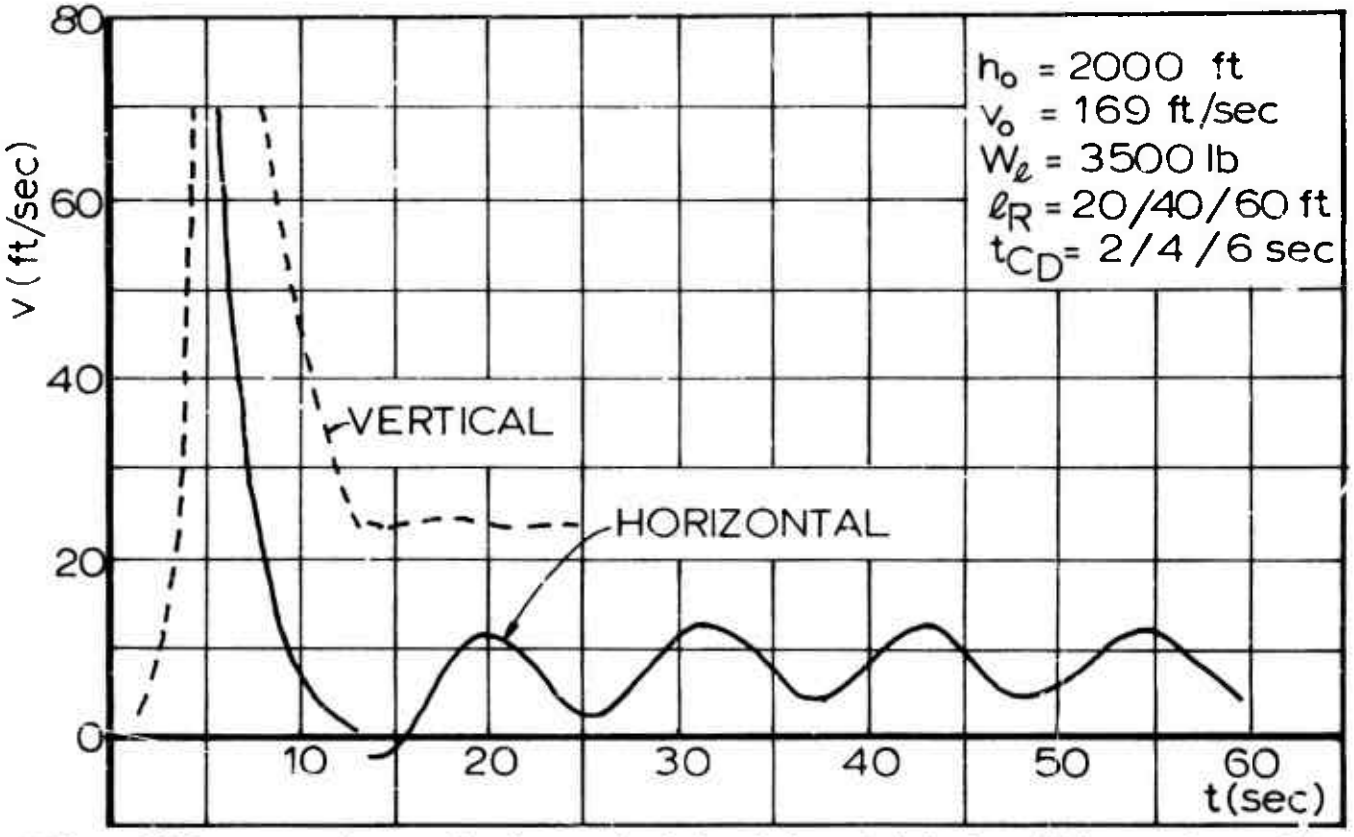

Fig 25 Horizontal and Vertical Velocities for the Reefed G-11A Cargo Parachute with Extraction Parachute System

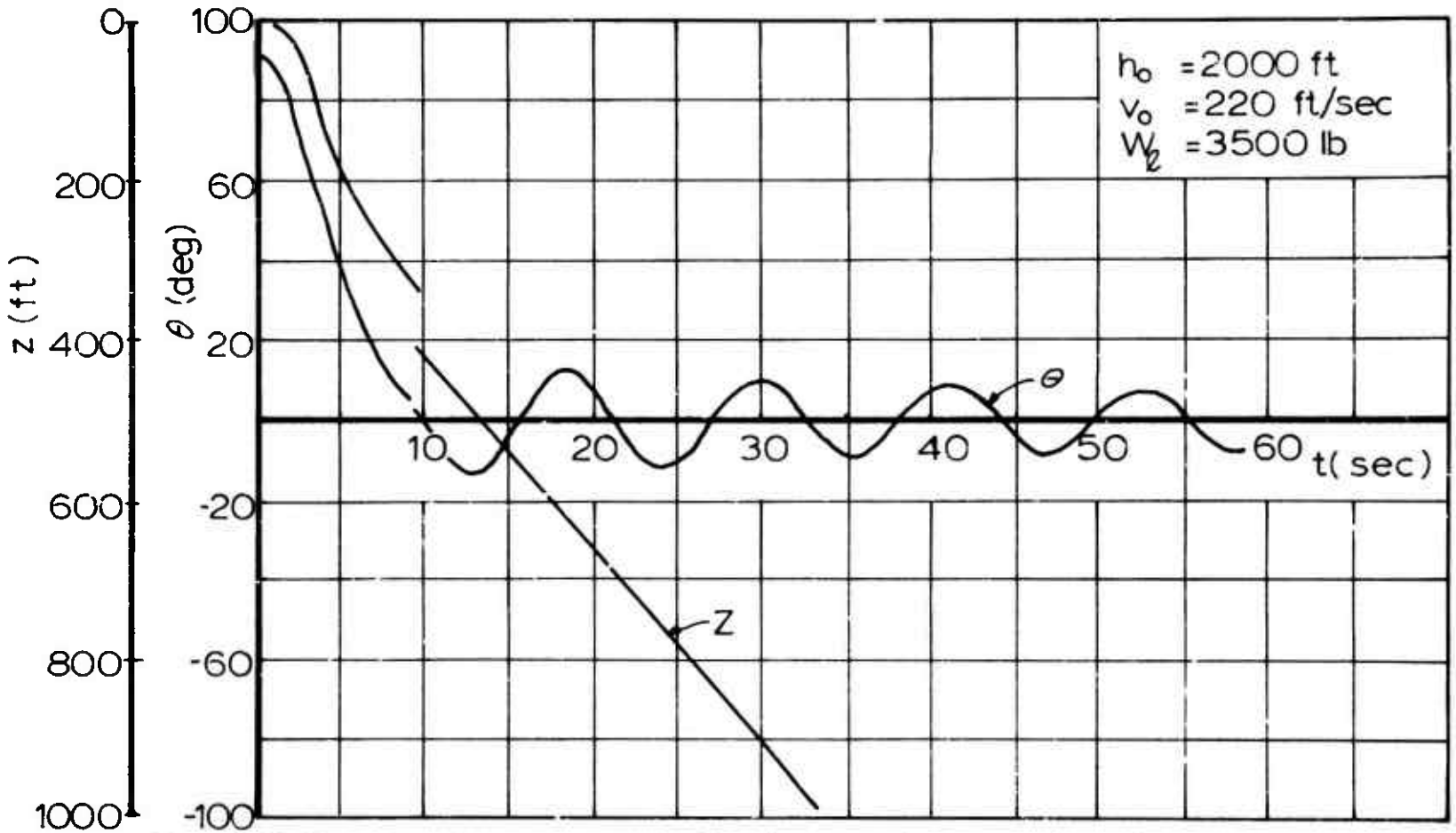

Fig 26 Altitude Loss and System Angle for the G-11A Cargo Parachute with Reefed Main Parachute Extraction System

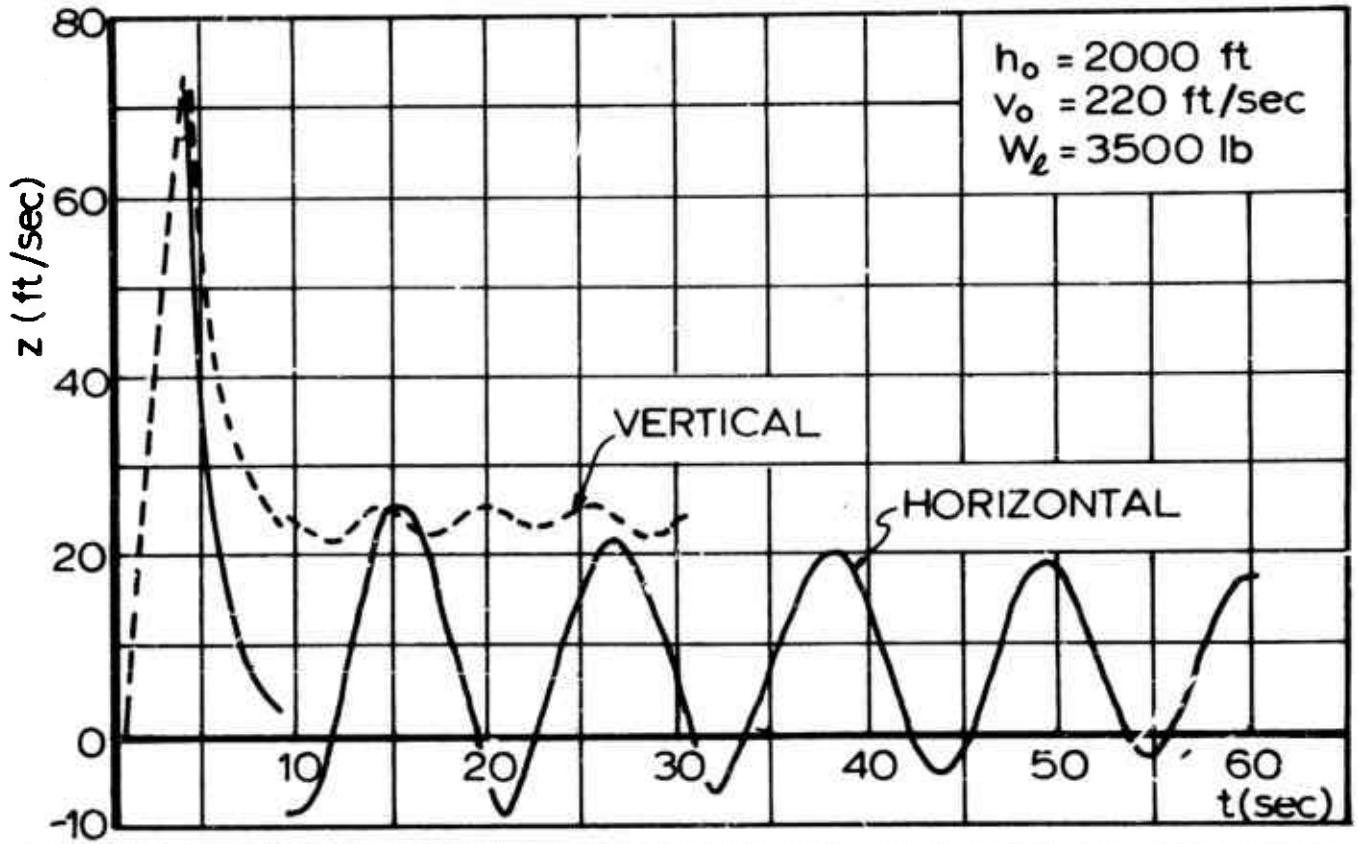

Fig 27 Horizontal and Vertical Velocities for the G-11A Cargo Parachute with Reefed Main Parachute Extraction System

TABLE I
PARACHUTE - LOAD SYSTEMS AND INITIAL CONDITIONS FOR THE TOTAL TRAJECTORY SIMULATION CALCULATIONS

CALCULATION	PARACHUTE	SEPARATION-DEPLOYMENT SYSTEM	W_ℓ (lb)	ℓ_R (ft)	t_{CD} (sec)	h_o (ft)	v_o (ft/sec)
1	T-10	Static Line	250	-	-	500	220
2*	T-10	Static Line	250	-	-	6,000	220
3	G-15	Static Line	500	-	-	500	169
4	G-15	Static Line	500	-	-	500	220
5	G-13	Static Line	500	-	-	500	254
6	G-12B	Static Line Deployed Pilot Chute	2,200	-	-	500	220
7*	G-12B	Static Line Deployed Pilot Chute	2,200	-	-	6,000	220
8	G-12B	Extraction Parachute	2,200	-	-	500	220
9*	G-11A	Extraction Parachute	3,500	-	-	2,000	220
10	G-11A	Extraction Parachute	3,000	-	-	2,000	220
11	G-11A	Extraction Parachute	3,500	20	2	2,000	220
12	G-11A	Extraction Parachute	3,500	20	2	10,000	220
13	G-11A	Extraction Parachute	3,500	20	4	2,000	220
14	G-11A	Extraction Parachute	3,500	20	4	10,000	220
15	G-11A	Extraction Parachute	5,000	20	2	2,000	220
16	G-11A	Extraction Parachute	5,000	20	2	10,000	220
17	G-11A	Extraction Parachute	5,000	20	4	2,000	220
18	G-11A	Extraction Parachute	5,000	20	4	10,000	220
19*	G-11A	Extraction Parachute	3,500	20/40/60	2/4/6	2,000	169
20*	G-11A	Reefed Main Parachute Extraction	3,500	20	4	2,000	220
21	G-11A	Reefed Main Parachute Extraction	3,500	20	6	2,000	220

*Graphical Results Presented.

TABLE II

RESULTS OF THE TRAJECTORY SIMULATION CALCULATIONS

CALCULATION	V_s (ft/sec)	P_{max} (lb)	P_{max} (lb)	$t_{ff} + t_{f_R}$ (sec)	IMPACT V_{f_x} (ft/sec)	IMPACT V_{f_z} (ft/sec)	IMPACT TRAJECTORY ANGLE (Deg)
1	-	-	1784	1.99	20.19	22.69	-7.22
2*	-	-	1868	1.65	-6.76	18.39	-20.18
3	-	-	3421	0.73	10.56	26.97	21.36
4	-	-	4972	0.61	12.25	27.17	24.26
5	-	-	6186	0.55	13.81	27.53	26.64
6	193	8364	11,435	1.92	22.49	38.49	30.29
7*	197	8293	11,847	1.65	-10.74	28.51	-20.64
8	154	5871	7004	2.52	17.40	27.83	32.01
9*	160	2365	9331	5.41	5.04	23.19	12.21
10	173	2511	14,833	4.22	5.86	27.92	11.85
11	160	2365	3311/9371	1.56/5.02	6.01	22.81	14.74
12	168	2514	3202/10,034	1.40/4.17	8.81	23.03	20.95
13	160	2365	3311/9460	1.56/4.92	3.53	22.92	8.76
14	168	2514	3202/10,175	1.40/4.07	8.61	22.99	20.53
15	173	2511	4550/14,622	1.35/3.93	-3.63	27.62	-7.49
16	180	2663	4258/15,595	1.23/3.21	10.39	27.28	20.84
17	173	2511	4550/14,783	1.35/3.82	21.42	27.87	37.55
18	180	2663	4258/16,033	1.23/3.12	9.99	27.25	20.13
19*	130	2084	3062/5667/6032/5828	1.68/0.96/0.72/4.01	8.49	22.83	20.40
20*	-	-	8348	5.12	1.36	23.03	3.38
21	-	-	9157	4.94	6.45	23.20	15.52

*Graphical Results Presented.

for all cases, but they have not been reproduced because they were essentially the same as those presented. They showed differences in oscillation period and terminal velocity, but this would be expected from systems with various sizes and loadings. The accuracy of the results cannot be judged at this time, but obtaining all of these results from a single submission of the computer program certainly shows that the total trajectory simulation functions satisfactorily with any pertinent inputs.

V. SUMMARY

The functioning of an airdrop or recovery system by means of parachutes was organized in phases covering the main events. These were the separation of the load from an aircraft, the deployment of the parachute system, the dynamic and aerodynamic forces during the parachute snatch and parachute inflation processes, and the movement of the parachute-load system after the inflation of the main parachute. The phases indicated above included considerations related to the various methods required by the differing arrangements of the parachute systems. For example, consideration was given to the inflation of the main parachute in an unrestrained single process as well as in steps accomplished by different reefing line arrangements.

For all phases, the basic equations were taken from existing literature, when available, or they were established, as, for example, the equations of motion of the fully inflated and descending parachute allowing six degrees of freedom.

A continuous computer program was developed which allowed the total trajectory simulation of any parachute-load system whose arrangement fits any one of the cases discussed in this study. The program was designed in such a way that different subroutines relating to mechanical, aerodynamic, and dynamic methods can be introduced, removed, or exchanged.

After completion of the computer program a number of numerical total trajectory calculations was carried out and the results were indicated in tables and graphical presentations. A study of the calculated results showed that they fell well within the broad ranges one would expect based upon a familiarity with existing field test results. All

calculated results follow the known basic parachute performance characteristics very well. Statements about the accuracy of the calculated results cannot be made without having more complete field test data. Also, the calculation of the movement of the parachute-load system after full inflation of the main parachute had to be restricted to movement in one plane because aerodynamic coefficients of parachutes at composite angles of attack were not available.

The computer program has been laid out and calculations have been made which consider the known non-linearities of the aerodynamic coefficients versus their angle of attack. The calculations do prove that the complete single computer program is capable of predicting the dynamics of the entire aerial delivery process. In particular it has been shown that the movements of the parachute-load system in two orthogonal planes can be predicted provided that the aerodynamic inputs are available.

It appears that the program is ready to be used for predicting parachute performance and that intensive comparisons between calculated and observed performance characteristics are highly desirable.

VI. REFERENCES

1. Haak, Eugene L. and Hovland, Richard V.: Calculated Values of Transient and Steady State Performance Characteristics of Men-Carrying, Cargo, and Extraction Parachutes, USAF Report No. AFFDL-TR-66-103, July 1966.

2. U.S. Standard Atmosphere, 1962, prepared under sponsorship of National Aeronautics and Space Administration, United States Air Force, United States Weather Bureau, U. S. Government Printing Office, Washington, D. C.

3. Heinrich, H. G.: "Parachute Snatch Force Theory Incorporating Line Disengagement Impulses," presented at the AIAA Aerodynamic Deceleration Systems Conference, May 1973, Palm Springs, California.

4. Haak, E. L. and Thompson, R. E.: Analytical and Empirical Investigation of the Drag Area of Deployment Bags, Cargo Platforms and Containers, and Parachutists, USAF Report No. AFFDL-TR-67-166, July 1968.

5. Heinrich, H. G.: "A Linearised Theory of Parachute Opening Dynamics," The Aeronautical Journal, The Royal Aeronautical Society, London, Vol. 76, No. 744, December 1972, pp. 723-731.

6. Berndt, R. J.: "Experimental Determination of Parameters for the Calculation of Parachute Filling Times," Jahrbuch des Wissenschaftlichen Gesellschaft fuer Luft- und Raumfahrt E.V. (WGLR), 1964, pp. 299-316.

7. Neustadt, M, Erickson, R. E., Guiteras, J. J., and Larrivee, J. A.: "A Parachute Recovery System Dynamic Analysis," AIAA Paper No. 66-25, 3rd Aerospace Science Meeting, Jan. 24-26, 1966.

8. Gionfriddo, Maurice P.: Two-Body Trajectory Analysis of a Parachute-Cargo Airdrop System, U.S. Army Natick Laboratories Technical Report 69-80-AD, April 1969.

9. Etkin, Bernard: Dynamics of Flight: Stability and Control, John Wiley and Sons, Inc., New York, 1959.

10. Greenwood, Donald T.: Principles of Dynamics, Prentice-Hall, Inc., Englewood Cliffs, N. J., 1965.

11. Ibrahim, Shukry K.: Experimental Determination of the Apparent Moment of Inertia of Parachutes, USAF Technical Documentary Report FDL-TDR-64-153, April 1965.

12. Heinrich, H. G., Noreen, R. A., and Hedtke, J. C.: Analysis of the Opening Dynamics of Solid Flat and Ringslot Parachutes with Supporting Wind Tunnel Experiments, USAF Report No. AFFDL-TR-71-95, February 1972.

13. Heinrich, H. G., and Hektner, T. R.: Opening Dynamics of a T-10 Parachute with Inflation Aids, USAF Report No. AFFDL-TR-69-112, March 1970.

14. Heinrich, H. G., and Noreen, R. A.: Wind Tunnel Drag and Stability of Solid Flat Circular, T-10, and Ringslot Parachute Models with Centerlines, USAF Report No. AFFDL-TR-73-17, December 1972.

15. Performance of and Design Criteria for Deployable Aerodynamic Decelerators, USAF Report No. ASD-TR-61-579, December 1963.

APPENDIX

The numerical data for the 21 sample trajectory calculations discussed in Section IV were based on five parachute-load systems frequently used by the United States Army. The parachutes used in these five systems are the T-10 personnel parachute and the G-13, G-12D, and G-11A cargo parachutes. The four separation-deployment systems discussed in Section II correspond to these systems as follows: the static line system (System 1) is used for the T-10 and G-13 parachutes, the static line deployed pilot chute system (System 2) is used for the G-12D parachute, the extraction parachute system (System 3) is used with the G-11A and G-12D parachutes, and the reefed main parachute extraction system (System 4) is used with the G-11A parachute. All physical details of these five parachute-load systems as used with the four separation-deployment methods are indicated schematically and described in Figs 28 through 32. The various masses, lengths, volumes, etc. which were used as inputs to the total trajectory simulation were determined from Figs 28 through 32 and are listed in Tables III through VII. The drag coefficient C_{D_p} is given by

$$C_{D_p} = \frac{C_{D_0}}{(D_{p_{max}} / D_0)^2}$$

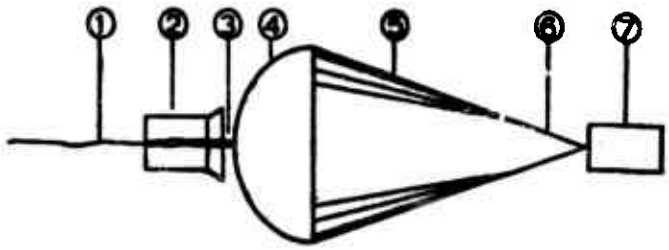

T-10 Personnel Parachute

1) Static line, L_{static} = 15 ft, material = MIL-W-4088, Type VIII nylon.

2) Deployment bag, dimensions length = 22 in, width = 12 in, height = 3 in, (C_DS) = 0.33 ft^2, weight = 3.3 lb.

3) Break cord, material = Type I, ¼ webbing, cotton, finished length = 3 in, weight = 0.11 oz.

4) D_o = 35 ft, 10% flat extended skirt canopy. Canopy material, nylon cloth MIL-C-7020, Type I, 1.1 oz/yd^2, nominal porosity = 72 - 132 ft^3/ft^2-min (assume 100 ft^3/ft^2-min). W_c = 11.7 lb, W_p = 14.13 lb, C_{D_o} = 0.70.

5) 30 suspension lines, MIL-C-5040, Type II, 375 lb, ϵ_{max} = 32%, L_s = 25.3 ft, weight = 2.42 lb.

6) 4 risers, material = MIL-W-4088, Type XIII nylon, ϵ_{max} = 30% (est), L_R = 30 in, weight = 1.0 lb.

7) Payload W_l = 250 lb, $(C_DS)_l$ = 6.0 ft^2.

Fig 28. T-10 Parachute with Static Line System

TABLE III

TOTAL TRAJECTORY SIMULATION INPUTS
FOR T-10 PARACHUTE WITH STATIC LINE SYSTEM

Dimensions and Lengths

$D_o = 35$ ft	$D_{p_{max}} = (0.686)D_o$	$s_1 = 11.52$ ft
$L_s = 25$ ft	$s_c = (0.133)D_o$	$s_2 = 24.17$ ft
$L_R = 2.5$ ft	$L_{static} = 15$ ft	$s_5 = 27.8$ ft

Masses

$m_p = 0.364$ slug	$m_R = 0.031$ slug	$m_{r_s} = 8.343$ slug
$m_{L_s} = 0.075$ slug	$m_\ell = 7.77$ slug	

Drag Areas, Drag Coefficient

$C_D S_\ell = 6$ ft^2	$C_D S_B = 0.33$ ft^2	$C_{D_p} = 1.487$

Main Parachute Canopy Volume

$V = 3317.5$ ft^3

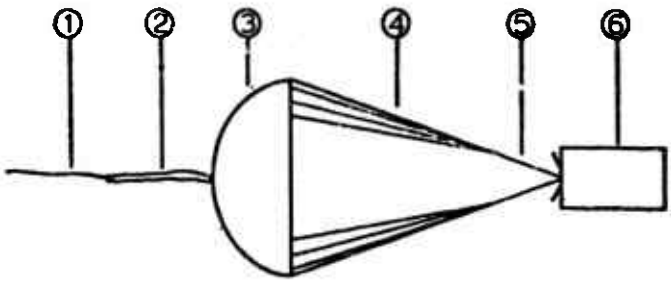

C-13 Cargo Parachute

1) Static line, L_{static} = 15 ft 6.0 in, material = MIL-W-5665, Type VIII cotton web, 2900 lb or. str. min.

2) Break cord, material = Type I ¼ inch cotton webbing, 80 lb, finished length = 6 in, weight = 0.17 oz.

3) D_o = 32 ft hemispherical canopy, canopy material, cotton muslin, 4.25 oz/yd^2 MIL-C-4279, Type II, nominal porosity = 153 - 253 ft^3/ft^2-min, W_c = 23.89, W_p = 33.89, C_{D_o} = 0.75.

4) 20 suspension lines, MIL-C-4232 Type I, 400 lb, ϵ_{max} = 17%, L_s = 30 ft, weight = 4.8 lb.

5) Risers, material = MIL-W-5665, Type VIII cotton webbing 2900 lb (min), ϵ_{max} = 8 - 10% (est), L_R = 30 in, weight ≈ 1.2 lb.

6) Cargo container, length = 30 in, width = 30 in, height = 20 in, type A-21, $(C_DS)_1$ = 7.125 ft^2, W_1 = 500 lb.

Fig 29. G-13 Cargo Parachute with Static Line System

TABLE IV

TOTAL TRAJECTORY SIMULATION INPUTS FOR G-13
CARGO PARACHUTE WITH STATIC LINE SYSTEM

Dimensions and Lengths

$D_o = 32$ ft	$D_{p_{max}} = (0.648)D_o$	$s_1 = 14.215$ ft
$L_s = 30$ ft	$s_c = (0.129)D_o$	$s_2 = 29.615$ ft
$L_R = 2.5$ ft	$L_{static} = 15$ ft	$s_5 = 31.635$ ft

Masses

$m_p = 0.743$ slug	$m_R = 0.037$ slug	$m_{rs} = 16.471$ slug
$m_{L_s} = 0.149$ slug	$m_\ell = 15.542$ slug	

Drag Area and Drag Coefficient

$C_D S_\ell = 7.125$ ft^2 $\qquad$ $C_{D_p} = 1.786$

Main Parachute Canopy Volume

$V = 2185.62$ ft^3

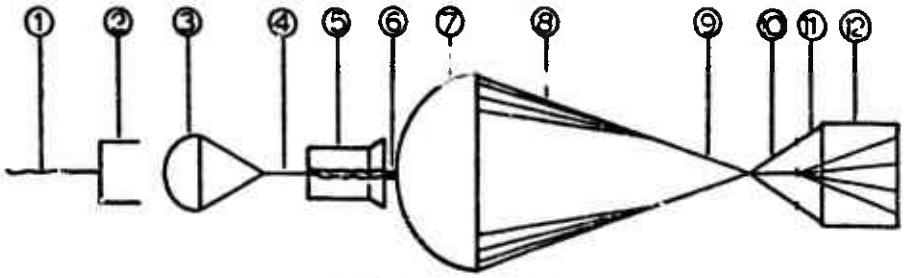

G-12D Cargo Parachute

1) Static line, L_{static} = 15 ft, material = Type VIII cotton webbing, rolled MIL-W-5665.

2) Pilot Parachute Pack, weight = 0.5 lb, $(C_DS) = 0.5$ ft^2.

3) Pilot Parachute, D_n = 5.66 ft, octagonal canopy, 8 suspension lines, L_s = 5.5 ft, MIL-C-7515, Type II, C_{D_n} = 0.75, weight = 1.75 lb.

4) Deployment line and bridle, material = Type VIII nylon webbing, ϵ_{max} = 30% (est), length = 14 ft, weight ≈ 2.0 lb w/clevis.

5) Deployment bag, dimensions, length = 36 in, width = 24.5 in, height = 10 in, (C_DS) = 2.78 ft^2, weight = 6 lb.

6) Break cord, material = Type III 550 lb nylon cord MIL-C-5040, finished length = 6 in, weight = 0.005 lb.

7) D_n = 64 ft circular flat canopy, canopy material, nylon, 2.25 oz/yd^2 MIL-C-7350, Type I, nominal porosity = 90 - 165 ft^3/ft^2-min, W_c = 76.79 lb, W_p = 109.5 lb.

8) 64 suspension lines, MIL-C-7515, Type IV, 1,000 lb. ϵ_{max} = 20%, L_s = 51 ft, weight = 27.9 lb.

9) 8 risers, MIL-W-27265, Type X, Class R, ϵ_{max} = 25%, 8700 lb, L_R = 5 ft 5 in, weight = 4.75 lb.

10) 4 Suspension Slings, MIL-W-27265 Type VII nylon web, 5500 lb, ϵ_{max} = 30%, length = 28 in, weight ≈ 2 lb.

11) 16 A-22 Suspension Slings, MIL-W-5665 Type VIII cotton web, 2900 lb, ϵ_{max} = 18%, length = 5 ft, weight = 7 lb (shown on front side of container; typical of all four sides).

12) A-22 Cargo container, length = 52 in, width = 43 in, height = 50 in, $(C_DS)_f$ = 18.9 ft^2, W_f = 2,200 lb (with cargo)

Fig 30. G-12D Cargo Parachute with Static Line Deployed Pilot Chute System

TABLE V

TOTAL TRAJECTORY SIMULATION INPUTS FOR G-12D CARGO PARACHUTE WITH STATIC LINE DEPLOYED PILOT CHUTE SYSTEM

Dimensions and Lengths

$D_o = 54$ ft	$D_{p_{max}} = (0.648)D_o$	$s_1 = 23.75$ ft
$L_s = 51$ ft	$s_c = (0.129)D_o$	$s_2 = 50.00$ ft
$L_R = 5.42$ ft	$L_{static} = 15$ ft	$s_4 = 56.23$ ft
$L_{Br} = 8$ ft	$D_{o)pilot} = 5.66$ ft	$s_5 = 57.21$ ft
	$(L_s + L_{Br})_{pilot} = 14.75$ ft	

Masses

$m_p = 2.383$ slug	$m_{Br} = 0.280$ slug	$m_{pb} = 0.303$ slug
$m_{L_s} = 0.867$ slug	$m_\ell = 68.386$ slug	$m_{rs} = 72.870$ slug
$m_R = 0.147$ slug		

Drag Areas and Drag Coefficient

$C_D S_\ell = 18.9$ ft^2	$C_D S_{II} = 26.016$ ft^2	$C_{D_p} = 1.786$

Main Parachute Canopy Volume

$V = 17{,}301.5$ ft^3

Suspension System Spring Constant

$1/A = 4777$ lb/ft

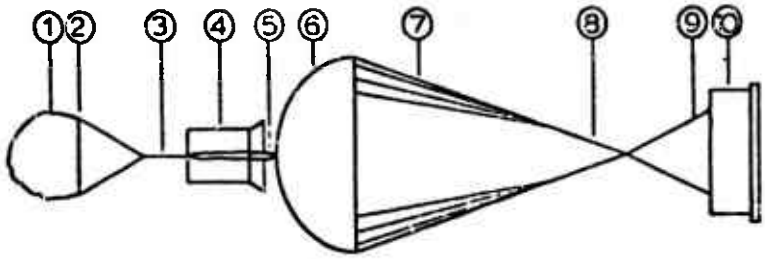

G-12D Cargo Parachute

1) 15 ft ringslot parachute - reefed to $D_{o_{eff}}$ = 12 ft, canopy material, nylon cloth MIL-C-7350, Type I, 2.25 oz/yd^2, nominal porosity = 90 - 165 ft^3/ft^2-min, C_{D_o} = 0.55, W_c = 6.06 lb, W_p = 8.06 lb, $(C_DS)_{reefed}$ = 62.2 ft^2.

2) Reefing line, length = 260 in.

3) Extraction parachute bridle; material = MIL-W-27265, nylon, Type X, 8700 lb br. st. (min), ϵ_{max} = 30% (est), length = 60 ft, 1 loop, weight = 10 lb.

4) Deployment bag, dimensions, length = 36 in, width = 24.5, height = 10 in, (C_DS) = 1.78 ft^2, weight = 6 lb.

5) Break cord, material = Type III 550 lb nylon cord MIL-C-5040, finished length = 6 in, weight = 0.005 lb.

6) D_o = 64 ft circular flat canopy, canopy material, nylon, 2.25 oz/yd^2 MIL-C-7350, Type I, nominal porosity = 90 - 165 ft^3/ft^2-min, W_c = 76.79 lb, W_p = 109.5 lb.

7) 64 suspension lines, MIL-C-7515, Type IV, 1,000 lb, ϵ_{max} = 20%, L_e = 51 ft, weight = 27.9 lb.

8) 8 risers, MIL-W-27265, Type X, Class R, ϵ_{max} = 28%, 8700 lb, L_R = 5 ft 5 in, weight = 4.75 lb.

9) Platform bridle, material = MIL-W-27265, nylon webbing, Type X, 8700 lb br. str. (min), ϵ_{max} = 30% (est), length = 9 ft (4 each 2 loop) weight = 11.0 lbs.

10) Cargo platform, length = 8 ft, width = 8 ft, $(C_DS)_f$ = 76.8 ft^2, W_f = 2,200 lb (with cargo).

Fig 31. G-12D Cargo Parachute with Extraction Parachute System

TABLE VI

TOTAL TRAJECTORY SIMULATION INPUTS FOR G-12D CARGO PARACHUTE WITH EXTRACTION PARACHUTE SYSTEM

Dimensions and Lengths

$D_o = 64$ ft	$L_{Br} = 8$ ft	$s_1 = 23.75$ ft
$L_s = 51$ ft	$D_{p_{max}} = (0.648)D_o$	$s_2 = 50.00$ ft
$L_R = 5.42$ ft	$s_c = (0.129)D_o$	$s_4 = 56.50$ ft
		$s_5 = 62.50$ ft

Masses

$m_p = 2.383$ slug	$m_{Br} = 0.341$ slug	$m_{pb} = 0.746$ slug
$m_{L_s} = 0.867$ slug	$m_\ell = 68.386$ slug	$m_{rs} = 72.8$[illegible]
$m_R = 0.147$ slug		

Drag Areas and Drag Coefficient

$C_D S_\ell = 76.8$ ft^2	$C_D S_{II} = 63.98$ ft^2	$C_{D_p} = 1.786$

Main Parachute Canopy Volume

$V = 17,301.5$ ft^3

Suspension System Spring Constant

$1/A = 4777$ lb/ft

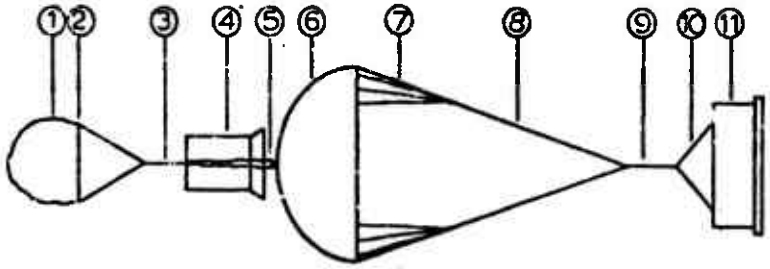

G-11A Cargo Parachute

1) 15 ft ringslot parachute - reefed to $D_{o_{eff}}$ = 12.0 ft, canopy material, nylon cloth MIL-C-7350, Type I, 2.25 oz/yd^2, nominal porosity = 90 - 165 ft^3/ft^2-min, C_{D_o} = 0.55, W_c = 6.06 lb, W_p = 8.06 lb, $(C_DS)_{reefed}$ = 62.2 ft^2.

2) Reefing line, length = 260 in.

3) Extraction parachute bridle; material = MIL-W-27265 nylon, Type X, 8700 lb br. str. (min), ϵ_{max} = 30% (est), length = 60 ft (one loop), weight = 10 lbs.

4) Deployment bag, dimensions, length = 48 in, width = 35 in, height = 12 in, (C_DS) = 2.33 ft^2, weight = 28 lb..

5) Break cord, material = Type III 550 lb nylon cord MIL-C-5040, finished length = 6 in, weight = 0.005 lb.

6) D_o = 100 ft circular flat canopy, canopy material, nylon, 1.6 oz/yd^2 -MIL-C-7020, Type II, nominal porosity = 70 - 176 ft^3/ft^2-min, W_c = 133.7 lb, W_p = 193 lb.

7) 120 suspension lines, MIL-C-5040, Type III, 550 lb, ϵ_{max} = 35%, L_s = 35 ft, weight = 20.7 lb.

8) 12 risers, MIL-W-27265, Type XVIII, 6,000 lb, ϵ_{max} = 21%, L_R = 60 ft, weight = 33.6 lb.

9) Load attachment risers, material = MIL-W-27265 nylon, Type X, 8700 lb br. str. (min), ϵ_{max} = 30% (est), L_R = 20 ft (one loop), weight = 4 lb.

10) Platform bridle, material = MIL-W-27265 nylon, Type X, 8700 lb br. str. (min), ϵ_{max} = 30% (est), length = 9 ft, weight = 11.0 lb.

11) Cargo platform, length = 5 ft, width = 8 ft, $(C_DS)_1$ = 76.8 ft^2, W_1 = 3500 lb or 5000 lb (with cargo).

Fig 32. G-11A Cargo Parachute with Extraction Parachute System

TABLE VII

TOTAL TRAJECTORY SIMULATION INPUTS FOR G-11A CARGO PARACHUTE WITH EXTRACTION PARACHUTE SYSTEM OR REEFED MAIN PARACHUTE EXTRACTION SYSTEM

Dimensions and Lengths

D_o = 100 ft	L_{Br} = 8 ft	s_1 = 16.45 ft
L_s = 35 ft	$D_{p_{max}} = (0.648)D_o$	s_2 = 61.10 ft
L_R = 60 ft	$s_c = (0.129)D_o$	s_3 = 99.30 ft
		s_4 = 113.30 ft
		s_5 = 119.30 ft

Masses

m_p = 4.156 slug	m_{Br} = 0.342 slug	m_{pb} = 1.432 slug
m_{L_s} = 0.643 slug	m_ℓ = 108.8 slug or 155.4 slug	m_{rs} = 116.697 slug or 163.324 slug
m_E = 0.124 slug		

Drag Areas and Drag Coefficient

$C_D S_\ell$ = 76.8 ft^2	$C_D S_{II}$ = 64.53 ft^2	C_{D_p} = 1.786

Main Parachute Canopy Volume

$V = 66{,}700\ ft^3$

Suspension System Spring Constant

$1/A = 910.7$ lb/ft